INTERLOCKED ARCHITECTURES BASED ON A BIS-CALIX[4]PYRROLE MACROCYCLE FOR ION-PAIR RECOGNITION

Jose Ramon Romero Lopez

UNIVERSITAT ROVIRA i VIRGILI

Interlocked architectures based on a bis-calix[4]pyrrole macrocycle for ion-pair recognition

J. Ramón Romero López

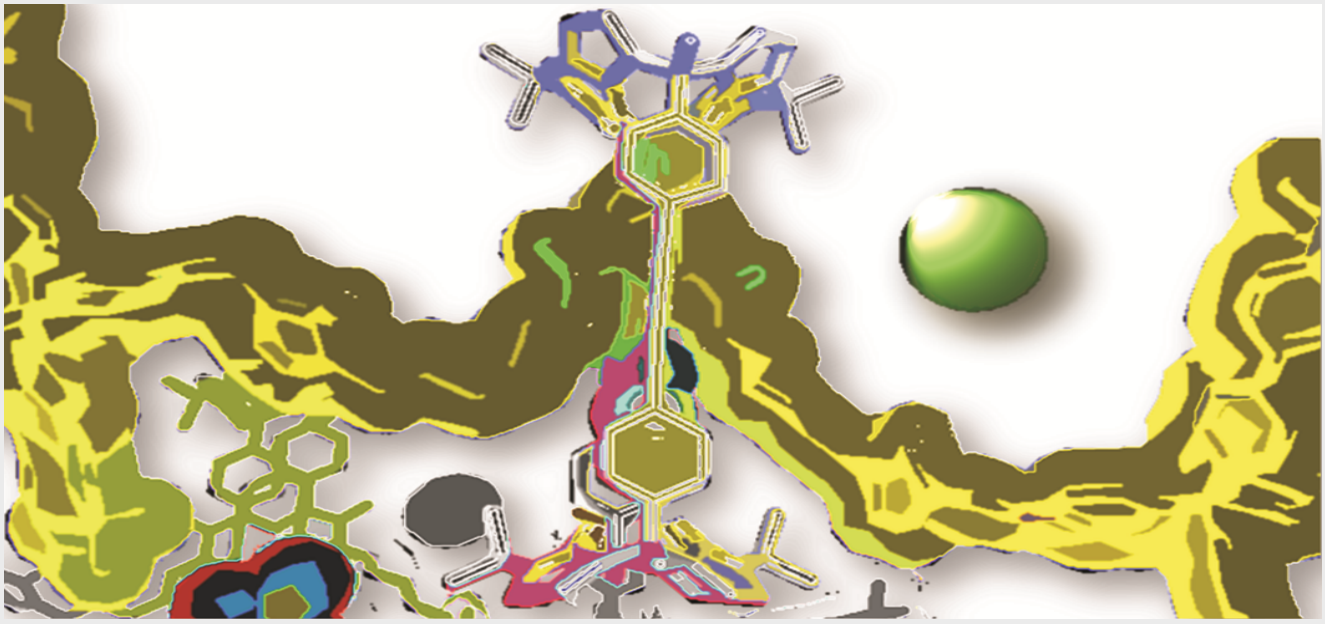

DOCTORAL THESIS

2017

UNIVERSITAT ROVIRA I VIRGILI
INTERLOCKED ARCHITECTURES BASED ON A BIS-CALIX[4]PYRROLE MACROCYCLE FOR ION-PAIR RECOGNITION
Jose Ramon Romero Lopez

UNIVERSITAT ROVIRA I VIRGILI
INTERLOCKED ARCHITECTURES BASED ON A BIS-CALIX[4]PYRROLE MACROCYCLE FOR ION-PAIR RECOGNITION
Jose Ramon Romero Lopez

PhD Thesis

INTERLOCKED ARCHITECTURES BASED ON A BIS-CALIX[4]PYRROLE MACROCYCLE FOR ION-PAIR RECOGNITION

J. Ramón Romero López

Supervised by Prof. Dr. Pablo Ballester

Tarragona

March 2017

UNIVERSITAT ROVIRA I VIRGILI

ICIQ
Institut Català d'Investigació Química

UNIVERSITAT ROVIRA I VIRGILI
INTERLOCKED ARCHITECTURES BASED ON A BIS-CALIX[4]PYRROLE MACROCYCLE FOR ION-PAIR RECOGNITION
Jose Ramon Romero Lopez

ICIQ
Institut Català d'Investigació Química

UNIVERSITAT ROVIRA I VIRGILI
DEPARTAMENT DE QUIMICA ANALITICA I QUIMICA ORGANICA
C/ Marcel.lí Domingo s/n
Campus Sescelades
43007 Tarragona
Tel. 34 977 55 97 69
Fax 34 977 55 84 46
e-mail: secqaqo@urv.net

Av. Països Catalans,16
43007, Tarragona, Spain
Tel +34 977920200 (Ext. 316)
Fax +34 977920221

Prof. Pablo Ballester, Group Leader of the Institute of Chemical Research of Catalonia (ICIQ) and Research Professor of the Catalan Institution for Research and Advanced Studies (ICREA).

CERTIFIES that the research work entitled "Interlocked architectures based on a bis-calix[4]pyrrole macrocycle for ion-pair recognition" that José Ramón Romero López presents to obtain the PhD degree in Chemistry, has been carried out under my supervision in the ICIQ and fulfils all the requirements to be awarded with the "Doctor Europaeus" Mention.

Tarragona, March 2017

PhD Thesis Supervisor
Prof. Pablo Ballester

UNIVERSITAT ROVIRA I VIRGILI
INTERLOCKED ARCHITECTURES BASED ON A BIS-CALIX[4]PYRROLE MACROCYCLE FOR ION-PAIR RECOGNITION
Jose Ramon Romero Lopez

Acknowledgements

En primer lugar agradecer a mi supervisor **Prof. Pablo Ballester** por haberme permitido realizar esta tesis doctoral en su grupo de investigación. Gracias por darme la oportunidad de conocer el mundo de la química supramolecular, por la ayuda y por todo lo aprendido en este tiempo.

Muchas gracias **Gemma** por todo lo que has hecho por mí, por haberme ayudado tantísimo, porque entender estas moléculas muchas veces ha sido una locura y me has guiado para juntos poder ver algo de luz, gracias por tu paciencia, porque a pesar de que en muchas ocasiones ha sido difícil no me has dejado sólo y juntos lo hemos sacado adelante. Gracias por confiar en mí, por haberme apoyado, por creer en mí, por tus ánimos y por todo lo que me has enseñado. Te echaré mucho de menos.

Gracias **Leti** por todo os momentos compartidos. Pola túa amistad xa desde antes de vir e polo tempo xuntos nestos anos. Para min foi unha gran sorte poder coindicir aquí contigo, que estivesemos xuntos, ter alguén en quen confiar, con quen contar e con quen divertirse. Terche aquí non solo é un apoio, supón moito mais, eres unha constante diaria do único que teño de Galicia. Xa boto de menos moitas cousas, pero cando esto termine sei que a nostalxia será maior. Gracias **Albano** por escuchar mis dramas, por tu ayuda en el laboratorio pero sobre todo por los momentos que hemos compartido. A lo largo de los años coincides con muchas personas pero sólo muy pocas terminan siendo importantes, tú te has quedado formando parte de mi día a día y estoy muy contento de tenerte como amigo. Tarragona no volvió a ser lo mismo sin ti. Gracias **Martina** por lo bien que te has portado conmigo, por comprenderme, por las charlas entre reacciones y columnas en la vitrina. Ha sido muy divertido trabajar contigo todo este tiempo y me alegro de poder seguir contando contigo. Gracias **Dani** por haberme ayudado siempre que te lo he pedido, por escucharme y por no solo aguantar las ralladas que doy y mis monólogos sino también por entenderme. Gracias por tu apoyo en los momentos de histeria y porque sin ti esta última etapa no hubiese sido lo mismo.

Quiero agradecer al resto de los actuales miembros del grupo, a **Jordi** por todos sus ánimos y los odios compartidos. Extender mi agradecimiento al resto de personas **Luís**,

Acknowledgements

Giulia, **Guillem**, **Rajesh**, **Ricardo**, cada uno de ellos siempre dispuestos a ayudar. Gracias **Bea**, porque con tu trabajo lo haces todo más fácil. Gracias a todos los miembros que han formado parte del grupo en algún momento porque en cierto modo han contribuido en la realización de esta tesis, ya bien aportando ayuda o con sus consejos. Especialmente a **Nelson**, **Frank**, **Louis**, **Alejandro**, **Sasha**. Agradecer también a todos los visitantes del grupo porque ha sido un placer trabajar con ellos: **Shanon**, **Rio**, **Giorgio**, **Aina**, **Kaisa**. Gracias **Virginia** y **Mónica**, me habéis recibido con los brazos abiertos y me habéis facilitado mi primera etapa en el grupo y en Tarragona. Ha sido un placer haber coincidido y poder seguir contando con vosotras.

Agradecer al **Prof. David Leigh** por aceptarme en su grupo para realizar una estancia. Gracias a todos los miembros de su grupo porque han sido muy amables conmigo, especialmente a **Guzman**, **Matt** y **Vanesa**. Muchas gracias Vanesa por todo lo que me has ayudado incluso después de la estancia.

Gracias a todas la unidades de soporte a la investigación del ICIQ, especialmente a la unidad de RMN, la unidad de masas y la unidad de cromatografía por su ayuda e implicación.

Quero agradecer ó resto de persoas que ainda que non contribuiron directamente na realización desta tesis, sí o fixeron de forma indirecta co seu apoio. Ós meus amigos Cris, Sara, Tania, Marcos, sempre estades a pesares da distancia. Rocío e María José, porque compartimos o medo e a incertidumbre de cando viña e ó final xa se termina. Gracias Bea por estar sempre pendiente de min e axudarme en todo. Vero, Belén e Marga, déchedesme a vida en Santiago e estou moi contento de seguir téndovos. Gracias Luís por tu comprensión y paciencia en esta última etapa.

Finalmente, gracias ás personas máis importantes, ós meus pais e meus irmans, por respetarme en cada elección que tomo na miña vida.

El trabajo recogido en esta tesis doctoral ha sido posible gracias a la financiación del Ministerio de economía industria y competitividad (FPI:BES-2012-052958), Generalitat de Catalunya y Fundación ICIQ.

"Airiños, airiños aires,
airiños da miña terra;
airiños, airiños aires,
airiños levaime a ela"
Rosalía de Castro

UNIVERSITAT ROVIRA I VIRGILI
INTERLOCKED ARCHITECTURES BASED ON A BIS-CALIX[4]PYRROLE MACROCYCLE FOR ION-PAIR RECOGNITION
Jose Ramon Romero Lopez

Table of Contents

Table of contents

Chapter 1

Introduction

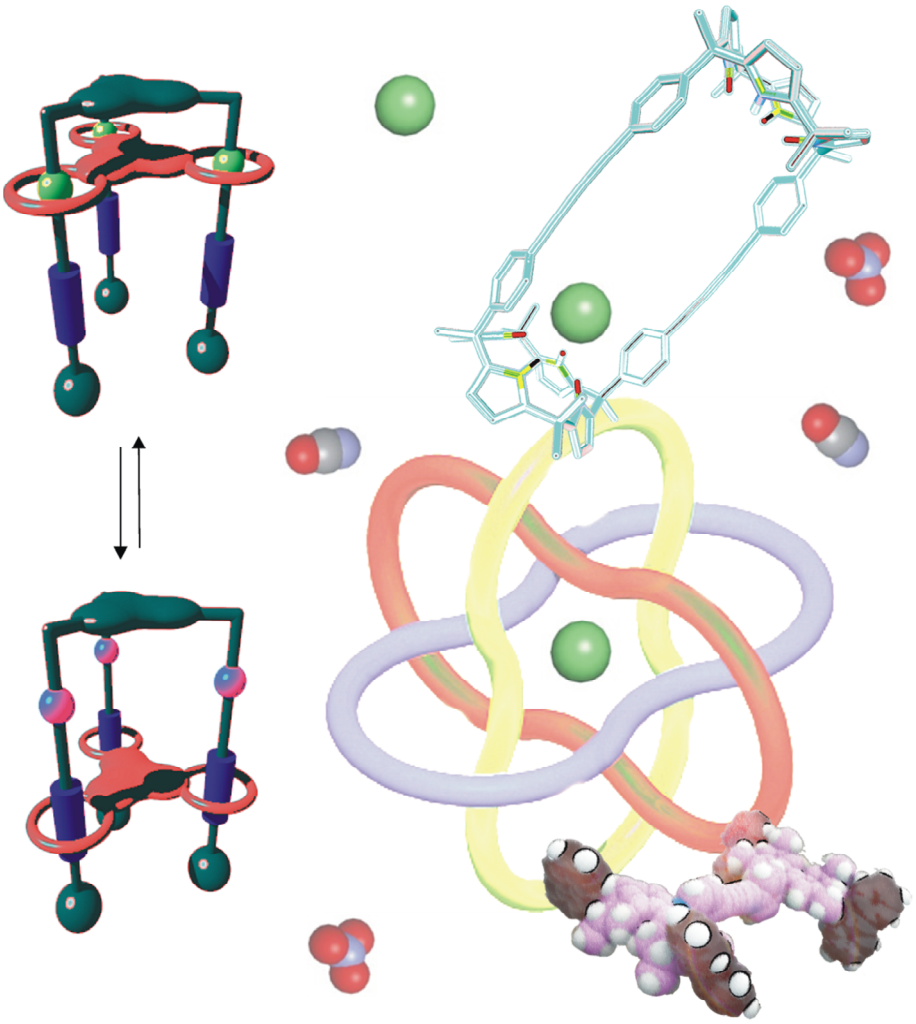

UNIVERSITAT ROVIRA I VIRGILI
INTERLOCKED ARCHITECTURES BASED ON A BIS-CALIX[4]PYRROLE MACROCYCLE FOR ION-PAIR RECOGNITION
Jose Ramon Romero Lopez

1.1 General Introduction

1.1.1 Interlocked molecules

Mechanically interlocked structures, namely [n]catenanes and [n]rotaxanes (where [n] denotes the total number of components in the interlocked assembly), are molecules in which their components are maintained together as a consequence of their topology.[1] The constituents of an interlocked molecule are connected by the so-called mechanical bond and cannot be separated without breaking a covalent bond. Figure 1. 1 shows the typical graphs used for the schematic representations of [2]catenanes, [2]rotaxanes and [2]pseudorotaxanes. A [2]catenane is composed of two interlocked rings while a [2]rotaxane contains a macrocyclic component threaded by a lineal axle with two attached terminal bulky stoppers that prevent the dethreading of the components from each other. Often, the key intermediate for the synthesis of [2]catenane and [2]rotaxane structures are [2]pseudorotaxane assemblies. In a [2]pseudorotaxane, the axle threading the macrocycle does not have bulky stoppers. Thus, their assembly is a reversible process.[2]

Figure 1. 1. Schematic representation of a catenane, a rotaxane and a pseudorotaxane assembly.

The chemical processes taking place in Nature are still far away from total comprehension for the chemistry community. The complexity and variety of the reactions occurring in biological systems is still a deep source from which chemist take inspiration. Nature has been using mechanical bonds long time before their synthetic analogues were obtained. Since this discovery, the development of interlocked molecules has generated even more interest. It was found that biological systems such as DNA or enzymes display catenane and rotaxane like structures during their active processes in Nature. For example, catenanes[3] and knots[4] are intermediate structures in DNA recombination and replication processes mediated by various enzymes.[5] It was

possible to image this natural topological DNA structures by electron microscopy[6] and also to resolve the crystal structure of mitochondria enzyme with catenane structure.[7] Other topologies like pseudorotaxane structures are found in some enzymes[8,9] during their biological operations. Some researchers have started to mimic these processes in more simple and early synthetic catalysts.[10,11,12,13,14] These findings in biological systems may indicate that the mechanical bond plays a vital functional role in Natural systems since they are present in different processes at molecular level presumably adding stability to spatial organization of proteins and nucleic acids.

The first preparation of an interlocked molecule was reported by Wasserman in 1960.[15] He successfully synthesized a [2]catenane based on a statistical threading approach. This statistical approach relies on the random nature of the threading process giving the final products in low yields. Later on in 1967, Harrison and Harrison reported the first example of a [2]rotaxane synthesis using the statistical approach.[16]

During the same decade the concept of templation at molecular scale emerged.[17] A molecular template interacts reversibly with the reactive components without altering the intrinsic chemistry of the system. The interactions between the template and reagents are generally non-covalent interactions such as coordinate bonds, electrostatic (ion-ion or ion-dipole) interactions or hydrogen bonding interactions. This offers the possibility to easily remove the template from the final assembly.[18,19]

The use of templates to generate interlocked molecules was introduced by Sauvage in the 1980´s using the orthogonal arrangement of bidentate phenanthroline ligands around a copper (I) center to template the synthesis of [2]catenane **1** (Figure 1. 2). This approach greatly facilitated the formation of interlocked molecules, their accessibility and applicability.[20,21] By using this template strategy, Sauvage and coworkers reported the isolation of the [2]catenane in much greater yields than those obtained using the statistical approach. They developed two parallel templation strategies. In one hand, they described a simultaneous macrocyclisation of two phenantroline ligands (Figure 1. 2A) to afford [2]catenane **1**. On the other hand, They reported an improved alternative by ring closure of a pseudorotaxane intermediate (Figure 1. 2B) that afforded the [2]catenane **1** even with a higher yield.

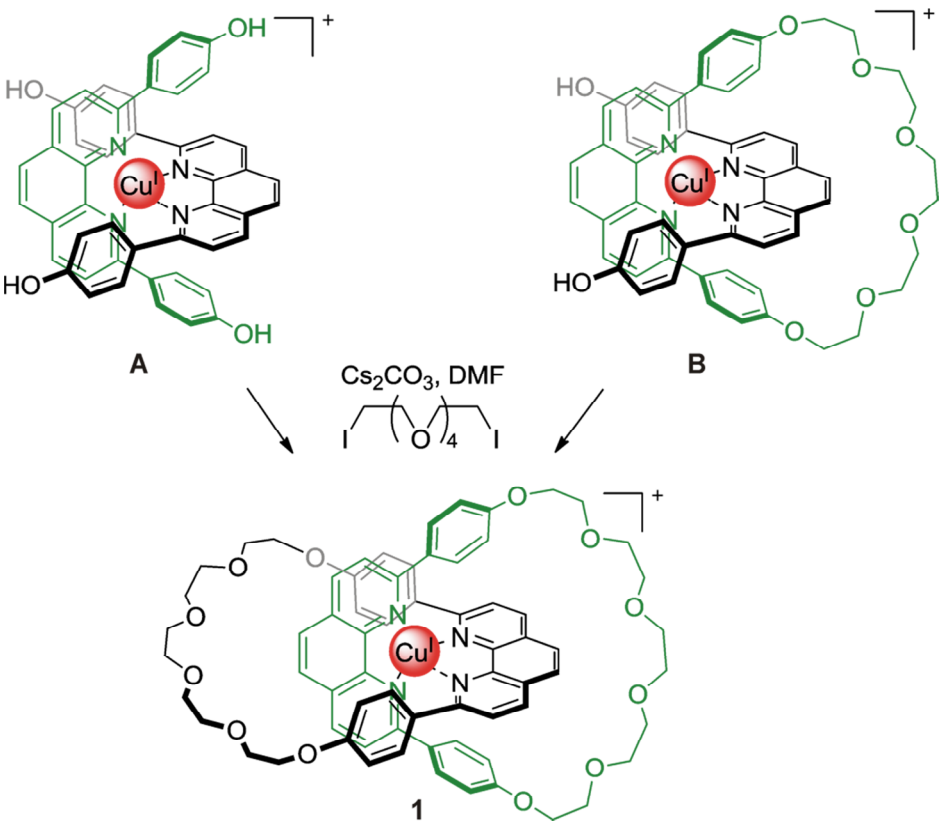

Figure 1. 2.Reaction scheme of the first cation-template synthesis of a [2]catenane reported by Sauvage et al.[20]

The discovery of the potential of the template strategy in the construction of complex interlocked architectures prompted the scientists working in the field to design and synthesize precursor molecules bearing mutual recognition motifs in their structures that could act as a motion force for their self-recognition, thus enhancing the yield of the interlocked structure. In this vein, the [2]catenane **4** was synthesized for the first time using hydrogen bonding templation by Hunter,[22] (Figure 1. 3). The macrocyclization reaction between the diamine **2** and iso-phthaloyl chloride **3** at high dilution concentration unexpectedly yielded [2]catenane **4** in 34% yield. In each macrocycle of catenane **4**, one iso-phthaloyl subunit has its amide groups in *cis* disposition forming hydrogen bonds with the carbonyl oxygen of the other macrocycle. However, the other iso-phthaloyl subunits adopt a *trans* conformation.[23] This approach introduced by

Hunter, was further used by others such as Vogtle[24,25] and Leigh[26] for the synthesis of interlocked molecules.

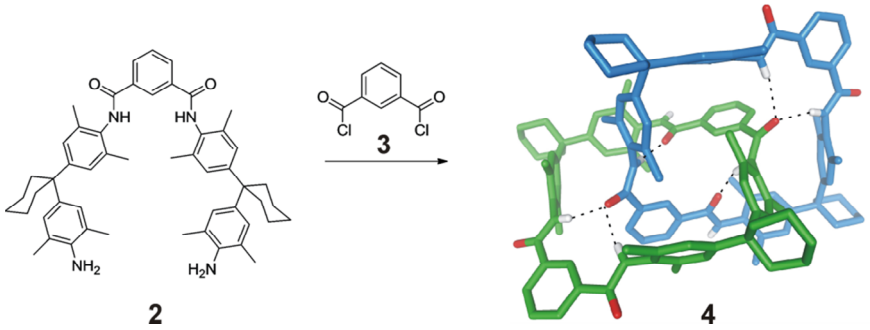

Figure 1. 3. Reaction scheme of the synthesis of hydrogen bond templated [2]catenane described by Hunter. X-ray structure of catenane **4** was extracted from the Cambridge Crystallographic Data Centre.[23] Non-polar hydrogen atoms were omitted for clarity. [2]catenane **4** is shown as stick representation.

Other non-covalent interactions such as hydrophobic[27,28] forces or π-π stacking have also been used in the design of template approaches.[29,30] (Figure 1. 4).Commonly in these approaches there is no external template that needs to be removed from the interlocked architecture, the non-covalent forces that drive the self-assembly of the two components function as template.

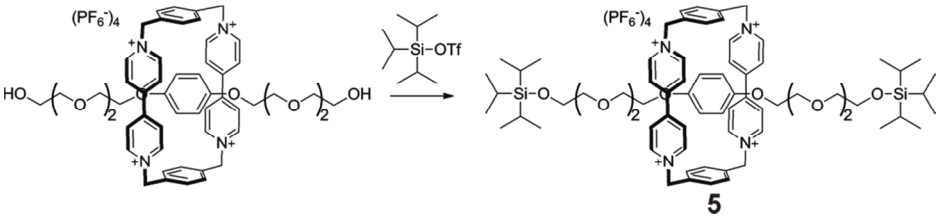

Figure 1. 4. Reaction scheme of the synthesis of Stoddart´s templated [2]rotaxane **5** by π-stacking template approach.

The use of anions as templates is far less common. This could be attributed to the anion intrinsic properties such as pH sensitivity or their relatively high energies of solvation. Vogtle et al. were the firsts reporting the synthesis of a [2]rotaxane based on anion templation between the components of the interlocked structure, (Figure 1. 5).[31] In this example, the macrocycle is hydrogen bonded to a bulky phenoxide anion that reacted

with a suitably aligned electrophile to afford the [2]-rotaxane **6**. Smith[32] and co-workers have further exploited this methodology as well as the Schalley´s group.[33]

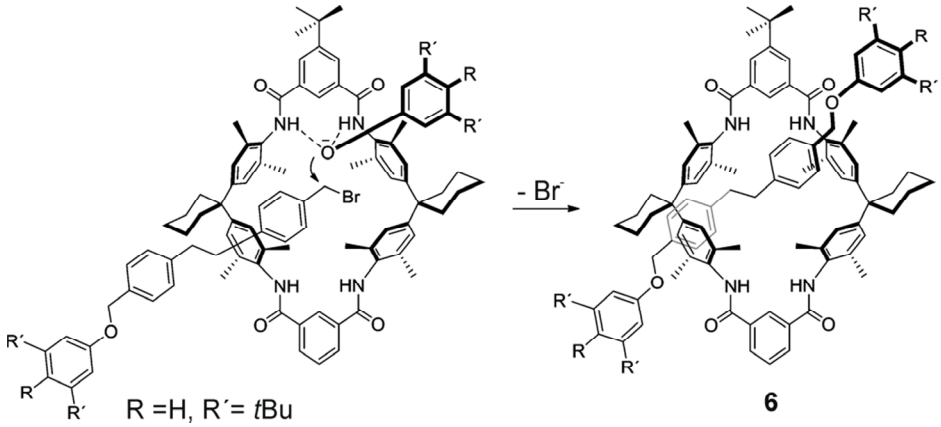

Figure 1. 5. Reaction scheme of [2]rotaxane **6** using anion template approach reported by Vogtle et al.

In this first part of the introduction, we have just described the early synthetic strategies used in the synthesis of interlocked molecules, most of them featuring [2]catenane topology. However, in the last decades the interest in [2]rotaxanes has significantly increased in comparison to [2]catenanes. Most likely, this change in the trend of the topology interest is related to the applications of interlocked molecules in the field of molecular machines where [2]rotaxanes showed to be more versatile. Taking this consideration into account, the present doctoral thesis is focused in the synthesis and study of interlocked architectures featuring [2]rotaxane topology. Consequently, the rest of the introduction will be directed exclusively to gain a deeper knowledge about [2]rotaxane architectures, their synthesis and applications.

1.1.2 Synthetic strategies of [2]rotaxane structures

As briefly explained in the first part of the introduction, [2]rotaxanes can be synthesized following different synthetic methodologies.[2] The selection of one or another approach depends on the synthetic limitations of the final reaction used to form the mechanical bond between the components of the assembly and also on the thermodynamic stability of the assembly under the used reaction conditions. The design of the interlocked

molecule should take into account these synthetic considerations in order to be successful for the isolation of the desired molecule. Figure 1. 6 shows a schematic representation of the most common synthetic strategies used for [2]rotaxane synthesis. Some of these strategies involve the previous formation of a [2]pseudorotaxane complex. On the one hand, the stoppering strategy consists on the attachment of bulky groups at both extremes of the previously threaded axle. The bulky stoppers must be large enough to avoid slippage of the axle from the macrocycle. A different strategy is the clipping method that affords the desired [2]rotaxane by a final ring closing reaction of an acyclic component in a previously formed assembly with a dumbbell-shaped linear component.

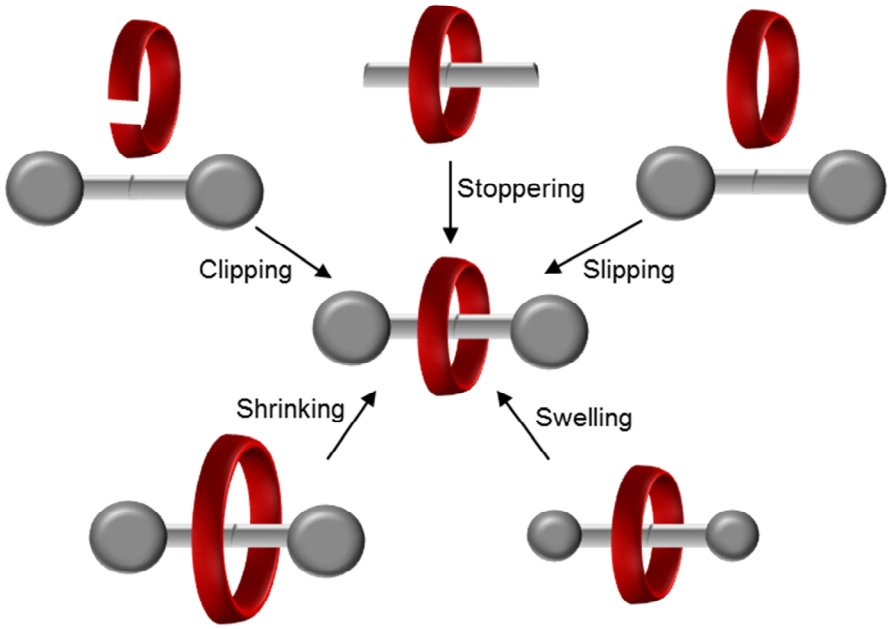

Figure 1. 6. Schematic representation of the different approaches for rotaxane synthesis.

The slipping method exploits the size complementarity between the ring and the stoppers. The ring can pass through the stoppers when enough energy is applied (heat or pressure) forming the kinetically trapped rotaxane at ambient conditions. More recently, other procedures were developed for the synthesis of rotaxanes. The swelling approach developed by Chiu and coworkers,[34,35] consists on the use of a dumbbell assembly

already featuring stoppers at its lineal axle. The small size of the stoppers allows slippage of the ring until a final reaction increases their size and locks the assembly. Alternatively, the same effect can be achieved by using a reaction that reduces the effective size of the ring´s cavity. This is the procedure that involves the shrinking method.[36,37]

In 2006, a new strategy was introduced by Leigh[38] and coworkers, the so-called active metal template approach (Figure 1. 7). This strategy is inspired on the copper template synthesis developed by Sauvage that was described in the first part of this introduction. In the Leigh´s strategy, Cu(I) plays two different roles: it acts as template but also as catalyst to promote the formation of the covalent bond leading to the mechanical lock.

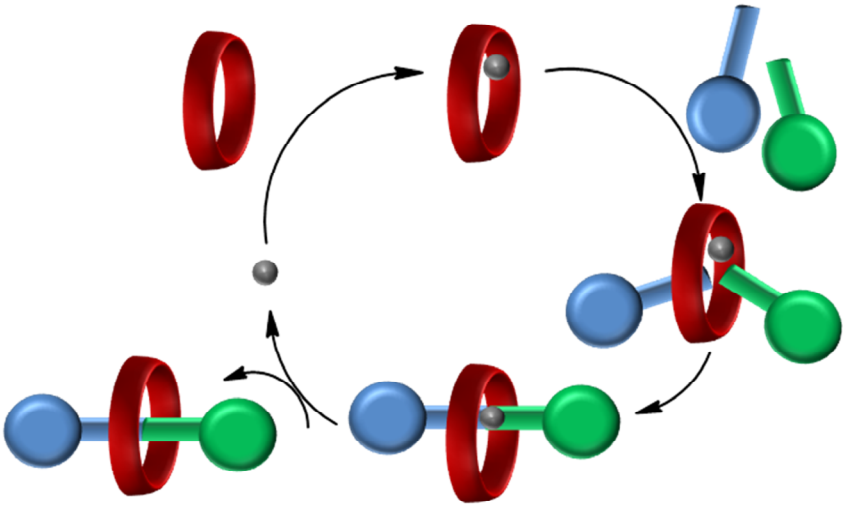

Figure 1. 7. Schematic representation of the catalytic cycle during the active metal template approach for the synthesis of rotaxanes.

The macrocycle included a coordinating ligand unit in its backbone that coordinates the copper catalyst. The later also holds the two fragments of the lineal component in the right disposition to catalyze the reaction between them leading to the desired interlocked product.

The synthetic strategies described up to now, required the use of stoichiometric amounts of the template to pre-organize the components of the assembly. Conversely, some

advantages of Leigh's approach are the catalytic amount of template required, which also facilitates the purification and template removal steps.

1.1.3 [2]Rotaxane structures for the recognition of anions and ion-pairs

Cationic and anionic species are involved in a wide range of important chemical processes in biological systems. Chloride anion is the most abundant anion in physiological media together with bicarbonate and phosphate. The ion concentration creates a gradient between the cell and the extracellular matrix that is regulated by the action of transport proteins integrated in the membranes. These chemical gradients act as energy sources for metabolic processes. Thus, the interest on developing synthetic ion transporters has increased. In addition, anions are also an important environmental problem related for example with the eutrophication of water derived from the overuse of fertilizers in agriculture, which release nitrate and phosphate anions that proliferate the formation of vegetation in aquatic systems.[39,40] Thus, the design of effective ion receptors that can be used in sensing, extraction procedures and also for industrial issues is of great interest.

Interlocked molecules featuring [2]rotaxane topology have been scarcely explored for anion recognition. This is strange taking into account the experimental evidence that confirm their superior binding affinity compared to their non-interlocked components.

In this field, Beer´s group reported the synthesis of [2]catenanes and [2]rotaxanes for anion recognition. The synthesis was based on an anion template strategy.[41,42] (Figure 1. 8). Beer and co-workers synthesized the macrocyclic unit **7** containing three different binding moieties: (i) a polyether unit, (ii) a hydroquinone unit and (iii) an isophthalamide unit. The linear component **8** consisted of a pyridinium unit functionalized with two amide groups. The anion template approach was based on the recognition of the chloride-pyridinium ion-pair **8·Cl** by the heteroditopic macrocycle **7** producing the interwoven assembly **9**.

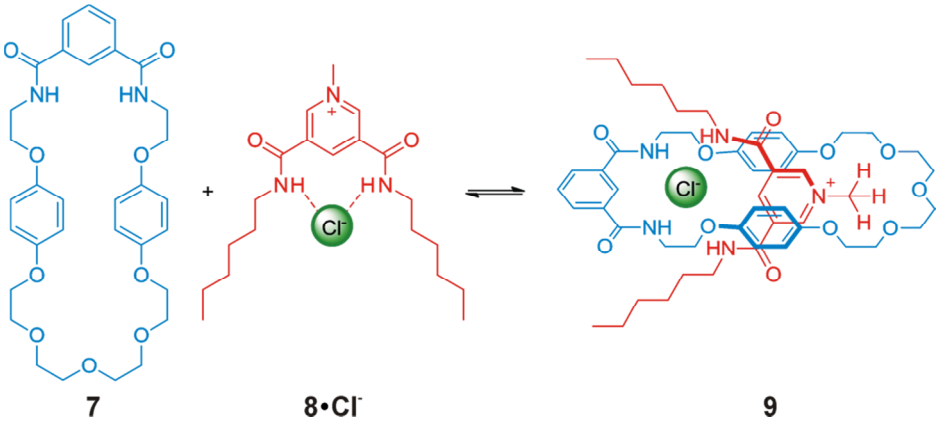

Figure 1. 8. Self-assembly of pseudorotaxane **9** by orthogonal coordination of ion-pairing species **8●Cl** with macrocycle **7**.

The authors envisaged that after a stoppering reaction of the axle with suitable blocking groups followed by template removal (anion metathesis), this synthetic strategy would afford a unique anion binding cavity. They state that the high degree of preorganization encoded in the cavity of the interlocked receptors will lead to strong association constant with anions of similar size and geometry to the used template, thus providing a highly selective host for anions. The use of anions as templates was also applied for the synthesis of other charged [2]rotaxanes and extended to the synthesis of neutral [2]rotaxanes.[43,44,45]

Following this anion template strategy, Beer and coworkers also synthesized the [2]rotaxane **10** by clipping procedure, using the ring-closing metathesis reaction to obtain the cyclic component (Figure 1. 9). The authors reported the binding studies of [2]rotaxane **10** with chloride anion in $CDCl_3$:CD_3OD (1:1 mixture). They demonstrated that the interlocked structure dramatically enhanced the selectivity for chloride binding compared to the free non-interlocked dumbbell-shaped pyridinium cation.[46] These initial results reported by Beer, contributed significantly to the development of other interlocked receptors that incorporate different anionic, cationic[44] and neutral[45] components, resulting in the preparation of a plethora of [2]rotaxane hosts featuring different selectivity for the binding of multiple species.

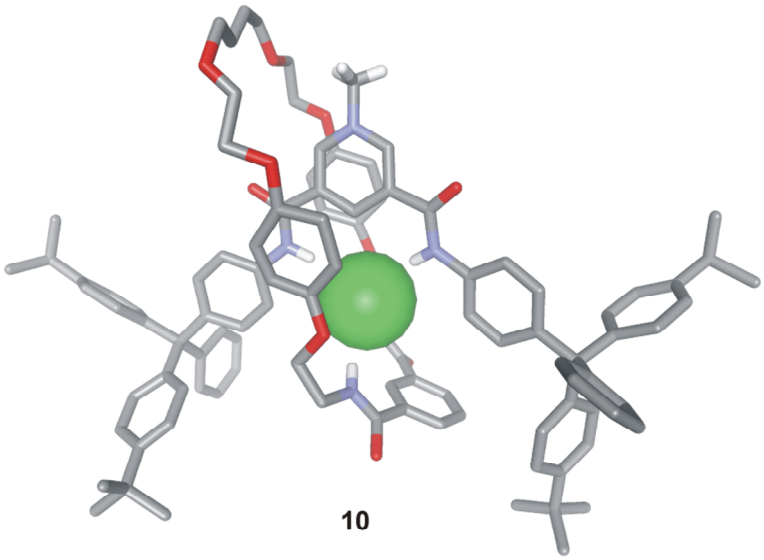

Figure 1. 9. [2]rotaxane **10** obtained by anion-templated strategy reported by Beer. X-ray structure of [2]rotaxane **10** was extracted from the Cambridge Crystallographic Data Centre. Non-polar hydrogen atoms were omitted for clarity. Bound chloride is shown as CPK model and the whole complex in stick representation.

The examples described so far in this introduction have been based on monotopic receptors, able to bind only the anion.[47,48] However, recognition of individual ions in non-polar solvents must overcome the energetic cost associated with the separation of the cation or anion from its counter ion, the so-called coulombic penalty. Heteroditopic receptors for the recognition of ion-pairs were designed in order to overcome this energetic cost. These receptors show an increase in the binding affinity towards ion-pairs compared to the discreet ions. Most likely, this is due to the existence of favorable electrostatic interactions between the co-bound ions and also to allosteric[49] and cooperative effects in the binding process.[50,51] Heteroditopic receptors have shown significant advantages in the development of membrane transport carriers, salt extraction and salt solubilization agents, as well as sensors in comparison to their monotopic counterparts.[52,53,54]

For example, Smith and coworkers demonstrated the advantage of using simple heteroditopic receptors over monotopic analogues (Figure 1. 10).[55] The presence of metal cations inhibited the anion binding affinity of the urea-based receptor **11** in

[D_6]DMSO solution. This inhibition effect was attributed to the competing ion-pairing outside the receptor. The incorporation of a crown ether in receptor **12** able to bind the cation dramatically enhanced the binding affinity for the ion-pair.

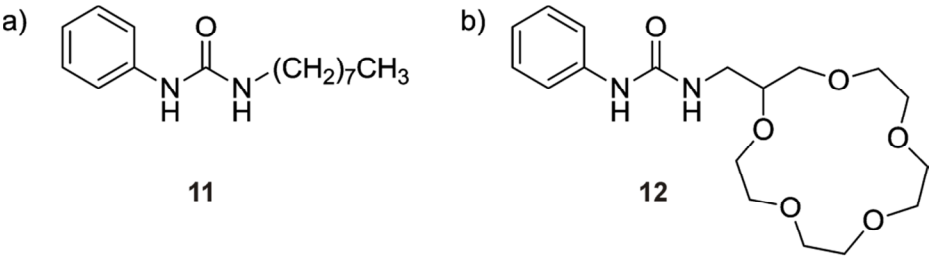

Figure 1. 10. a) Anion receptor reported by Smith. b) The incorporation of a crown ether to the previous receptor for binding the counter cation of the ion-pair, proved to enhance its binding affinity towards ion-pairs in comparison to discreet ions.

Even though considering the advantages offered by heteroditopic receptors, the number of examples of [2]rotaxane architectures that function as heteroditopic receptors for the recognition of ion-pairs is scarce.

Within the field of heteroditopic receptors, our group and others have demonstrated the potential of the calix[4]pyrrole scaffolds in ion-pair recognition. The calix[4]pyrrole core can bind anions by establishing four convergent hydrogen bonds with the four NH pyrrole protons. The binding of an anion induces a conformational change in the calix[4]pyrrole core, from alternate conformation to cone conformation, that results in the generation of a bowl-shaped and electron rich cavity opposite to the bound anion. This shallow cavity is ideal to complex certain cations of the ion-pairs such as alkylammonium cations that are bound by a combination of cation-π, CH- π, charge-charge and charge-dipole interactions, (Figure 1. 11).

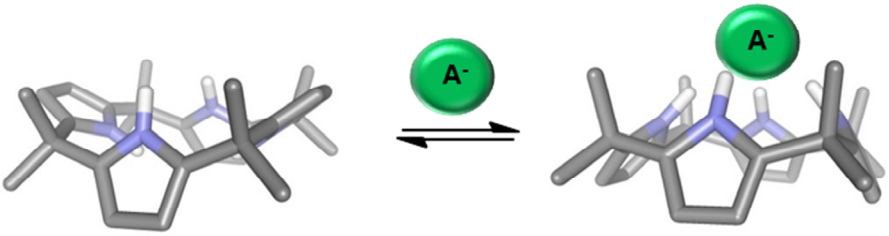

Figure 1. 11. Schematic representation of anion binding by a calix[4]pyrrole receptor. In a non-polar solvent, the 1,3-alternate conformation is preferred, upon anion binding the calix[4]pyrrole changes to a cone conformation that defines a shallow cavity opposite to the bound anion and is suitable for the recognition of cationic guests.

With this knowledge, we envisaged that the synthesis of an interlocked structure based on a calix[4]pyrrole macrocycle would lead to an efficient receptor for ion-pairs.

It is worthy to note that the binding of ion-pairs exerted by heteroditopic receptors results in different spatial arrangements of the two bound ions, (Figure 1. 12). These include: close-contact, solvent-separated and receptor-separated binding geometries.

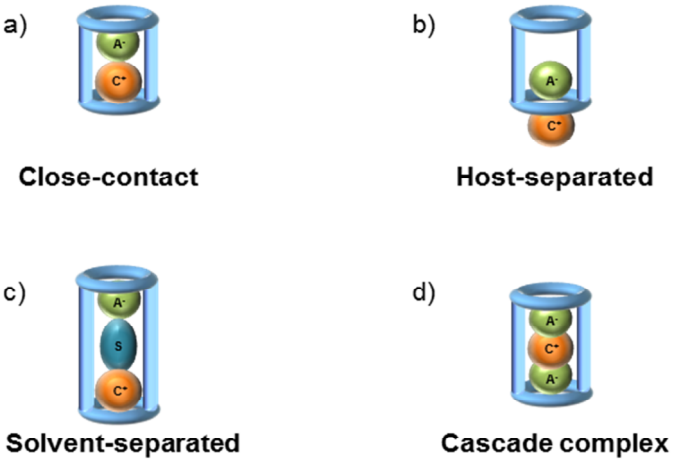

Figure 1. 12. Host-guest binding geometries for the complexes of heteroditopic receptors with ion-pairs: close-contact (a), host-separated ion-pair (b), solvent-separated ion-pair (c), cascade complex (d). A^-: anion, C^+: cation, S: solvent.

In a close contact binding geometry, the anion and the cation are in direct contact. In contrast in a solvent separated binding geometry solvent molecules fill the space between the ions of the ion-pair. Finally, the anion and the cation can be separated by

the receptor's framework producing a host-separated binding geometry for the complex. The binding of two ion-pairs might produce complexes with cascade binding geometry. That is, one of the bound ions is sandwiched between two counter-ions producing a net binding of an ion-triplet featuring close contact binding mode.[56]

1.1.4 Molecular shuttles

One of the aims of scientists working with interlocked molecules is their application as primitive molecular switches and machines. The control of the unidirectional rotational or translational motion of one of the components in an interlocked molecule with respect to the other, using an external physical or chemical stimulus, constitutes the basic unit of a molecular machine.

The first example of a synthetic molecular switch based on a [2]rotaxane architecture was reported by Stoddart et al.[57] The authors desymmetrized the rotaxane's thread by including in it two different binding sites. They were able to control the position of the ring and its switching along the molecular axle, (Figure 1. 13).

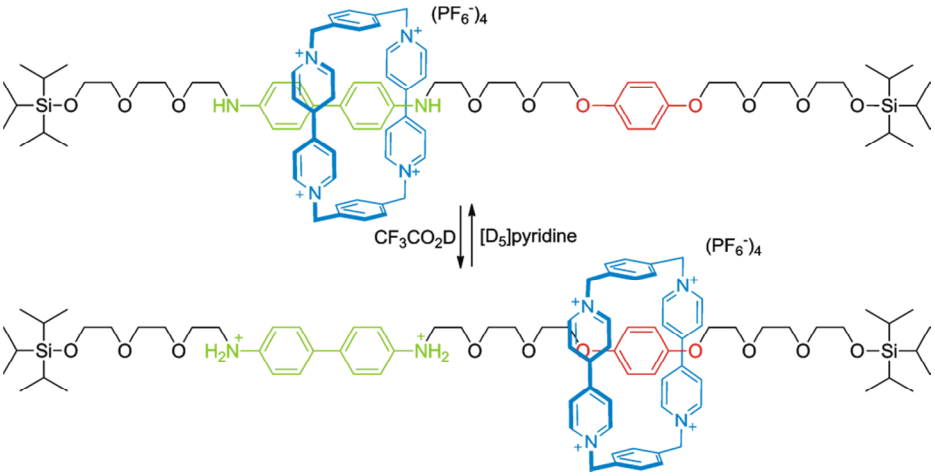

Figure 1. 13. Molecular shuttle reported by Stoddart. The axle component contains a biphenol and a benzidine unit as pi electron donors. Treatment of [2]rotaxane with trifluoroacetic acid protonates the benzidine nitrogen atoms and the macrocyle moves to the biphenol station in response to repulsive electrostatic interactions.

On the other hand, Sauvage and co-workers investigated the rotational switching of a [2]catenane by incorporating two coordination sites in one of the two macrocycles,[58] (Figure 1. 14).

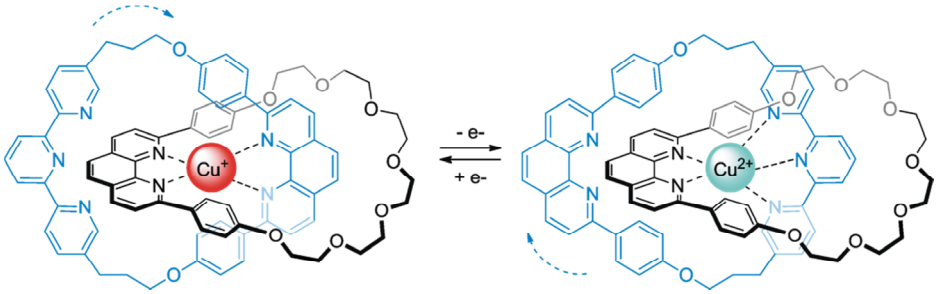

Figure 1. 14. [2]Catenane switch reported by Sauvage. The macrocycle depicted in blue color contains two coordinating units, a phenanthroline and terpyridine entities that rotate to coordinate the Cu cation in two different oxidation states that are electrochemically promoted.

Both works demonstrated externally controlled translational and rotational switching in mechanically interlocked molecules. These findings induced many other groups to investigate different ways to switch the position of the components in rotaxanes and catenanes architectures using various external stimuli (light, electrochemistry, pH value, polarity of the environment, cation binding, anion binding, allosteric effects, temperature, reversible covalent-bond formation, etc).[59] It is not surprising that all these efforts to investigate and synthesize these smart molecules, has contributed to develop more elaborated and sophisticated supramolecular systems. It is worth noting, that the importance of this research area has been recently acknowledged by awarding the Nobel Prize in Chemistry 2016 to Profs. Jean-Pierre Sauvage, Sir James Fraser Stoddart and Bernard L. Feringa “for the design and synthesis of molecular machines”.

It is also important to mention that the shuttling motions described above are considered the first examples of molecular machines. More recently, similar motions occurring on a unidirectional and cyclic manner have been reported in more complex interlocked architectures, which are synthetic examples of very primitive molecular motors. However, examples of molecular switching induced by the binding of anions or ion-pairs are still scarce. Leigh and co-workers described the first example of the use of anions for molecular shuttling. They demonstrated the macrocycle switching between

two stations integrated in the axle component of a [2]rotaxane structure, (Figure 1. 15).[60] Addition of $AgPF_6$ to the rotaxane **14●Cl** smoothly precipitated AgCl and afforded the quantitative formation of rotaxane **14●PF_6**. Conversely, the treatment of rotaxane **14●PF_6** with tetrabutylammonium chloride reverses this process to give the original rotaxane **14●Cl**.

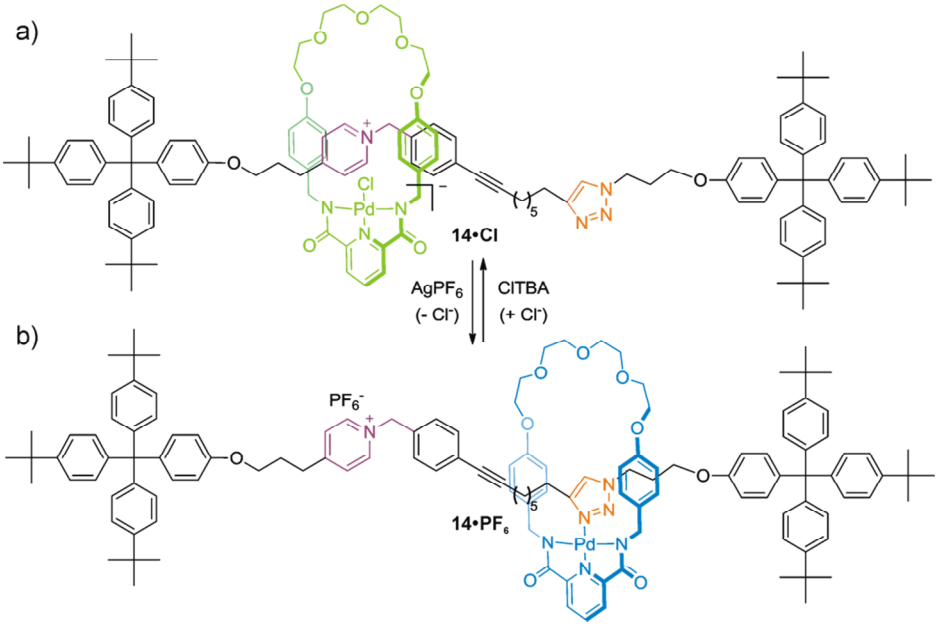

Figure 1. 15. Line-drawing structure of the [2]rotaxane reported by Leigh. The macrocycle component shuttle from one binding station to another by ion-pairing interactions after adding chloride and returns back to the previous station by removing the chloride anion using $AgPF_6$.

Later on, Beer et al. reported the synthesis of an anion induced shuttle based on a bis-imidazolium rotaxane,[61] followed by the more recent works exploiting the anion recognition with more sophisticated molecular shuttles[62,63] (Figure 1. 16).

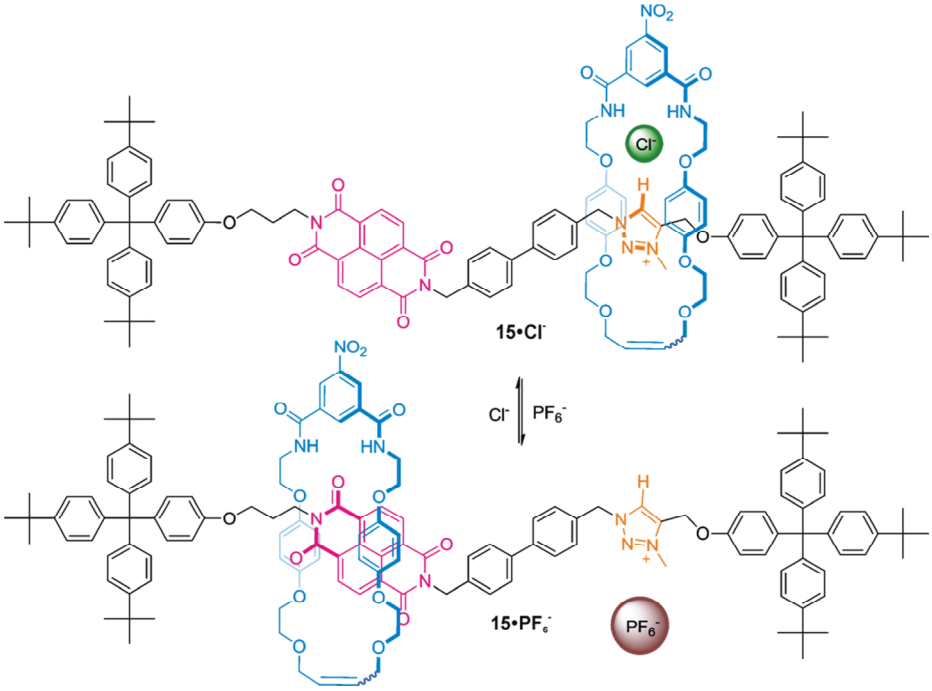

Figure 1. 16. Two station rotaxane **15** reported by Beer. Changing the coordinating anion (Cl^-) to a non-coordinating anion (PF_6^-) through column anion exchange, the macrocycle shuttled from triazolium station to the electron-deficient naphthalene diimide moiety by stablishing donor-acceptor interactions with its electron-rich hydroquinone groups.

The interest in controlling molecular motions resides in the design of molecules that could execute different tasks or have different properties. The idea is to couple the molecular function with the change in position of the components. Some works in this field have afforded the so-called molecular muscles,[64,65] molecular elevator,[66] nano-containers for controlled release of guest molecules,[67] storage devices[68] etc.

1.2 Aims of the thesis

The main objective of this PhD Thesis is the synthesis of interlocked molecules featuring [2]rotaxane topology. The designed molecules possess a pre-organized polar cavity, able to bind charged species (i.e. anions) or other small polar guest mainly using hydrogen bonding interactions. In particular, the work undertaken in this doctoral thesis relates to the design and synthesis of a [2]rotaxane based on a *bis*-calix[4]pyrrole macrocyclic component and a linear component containing a 3,5-*bis*-amidepyridyl-*N*-oxide unit. The targeted interlocked architecture is expected to function as a heteroditopic receptor for the complexation of ion-pairs in polar and non-polar solvents.

In line with this overarching aim, we outline below specific goals of the work undertaken during the development of the thesis:

O.1) **Design and synthesis of a [2]rotaxane based on a *bis*(calix[4]pyrrole) macrocycle and a 3,5-*bis*-amidepyridil-*N*-oxide axle.** We selected calix[4]pyrrole units as main binding scaffolds in the macrocyclic component of the assembly owing to their well-known anion and ion-pair binding properties. Previous work in the group suggested that the use of polyatomic anions as templates for the assembly of the [2]pseudorotaxane required as synthetic intermediate of interlocked molecules should favor the synthesis of the [2]rotaxane architecture.

O.2) **Explore the binding capability of the [2]rotaxanes as heteroditopic receptors for ion-pairs in different solvents.** Our purpose is the assessment of the thermodynamic properties of the synthesized [2]rotaxanes as heteroditopic receptors of ion-pairs in a non-polar solvent i.e. chloroform. We were interested in comparing the binding abilities of the [2]rotaxanes with those of its [2]pseudorotaxane counterparts. We also plan to evaluate the molecular recognition properties of the prepared [2]rotaxanes in more polar solvents (i.e. acetone). This study will constitute the starting point for the potential transfer of the designed [2]rotaxane structures as ion-pair receptors in aqueous media.

O.3) **Study the influence of the stopper's size in the synthesis of the [2]rotaxanes**. The selection of the stopper's size plays a key role on the final topology featured by the interwoven assemblies, as well as on their kinetic stability. Consequently, we considered that the study of several stoppers featuring different sizes as terminal

blocking groups for the [2]rotaxane architectures is mandatory. The stopper's size is an important factor to be evaluated in our assemblies because there are not previous reports in literature of [2]rotaxane architectures based on the macrocyclic component used in this work.

1.3 Outline of the thesis

In Chapter 2, we report the synthetic strategies investigated to obtain the calix[4]pyrrole based [2]rotaxane. We also disclose our findings on the use of ion-pairs as templates in the preparation of this interlocked structure.

In Chapter 3 we describe the results obtained in the binding studies of the synthesized [2]rotaxane with a series of tetraalkylammonium salts containing hydrogen-bonding anions (i.e. chloride, nitrate and cyanate), by means of ^{1}H NMR spectroscopy and Isothermal Calorimetry Titration (ITC) experiments. We discuss the influence of the anion size and shape in the determined binding constants. We also include and compare the results of the binding experiments performed in two different solvents: a non-polar non-protic solvent such as chloroform, and a polar non-protic solvent such as acetone.

Finally, in Chapter 4, we disclose our investigations on the effect of the stopper's size. We replace the large tris(biphenyl) stoppers for the smaller terphenyl stoppers in the synthesis of the interlocked structure. Most part of the last chapter reports our multiple and unsuccessful attempts to obtain the [2]rotaxane structure with the smaller terphenyl stoppers. The final part of the chapter includes a full set of characterization studies performed to figure out the structure of a new and unexpected isolated compound bearing the smaller terphenyl stoppers.

1.4 References and notes

[1] Frisch, H. L.; Wasserman, E., *J. Am. Chem. Soc.* **1961,** *83* (18), 3789-3795.
[2] Bruns C. J., Stoddart J. F. *The nature of the mechanical bond*, Wiley,Hoboken, **2017**.
[3] Hudson, B.; Vinograd, J., *Nature* **1967,** *216* (5116), 647-652.
[4] Krasnow, M. A.; Stasiak, A.; Spengler, S. J.; Dean, F.; Koller, T.; Cozzarelli, N. R., *Nature* **1983,** *304* (5926), 559-560.
[5] Wasserman, S. A.; Cozzarelli, N. R., *Science* **1986,** *232* (4753), 951-960.
[6] Kreuzer, K. N.; Cozzarelli, N. R., *Cell* **1980,** *20* (1), 245-254.
[7] Cao, Z. B.; Roszak, A. W.; Gourlay, L. J.; Lindsay, J. G.; Isaacs, N. W., *Structure* **2005,** *13* (11), 1661-1664.
[8] Subramanian, K.; Rutvisuttinunt, W.; Scott, W.; Myers, R. S., *Nucleic Acids Res.* **2003,** *31* (6), 1585-1596.
[9] Kovall, R.; Matthews, B. W., *Science* **1997,** *277* (5333), 1824-1827.
[10] Rowan, A. E.; Thordarson, P.; Coumans, R. G. E.; Bijsterveld, E.; Nolte, R. J. M., *Abstr. Pap. Am. Chem. Soc.* **2003,** *225*, 915-918.
[11] Coumans, R. G. E.; Elemans, J. A. A. W.; Nolte, R. J. M.; Rowan, A. E., *Proc. Natl. Acad. Sci. U. S. A.* **2006,** *103* (52), 19647-19651.
[12] Monnereau, C.; Ramos, P. H.; Deutman, A. B. C.; Elemans, J. A. A. W.; Nolte, R. J. M.; Rowan, A. E., *J. Am. Chem. Soc.* **2010,** *132* (5), 1529-1531.
[13] Blanco, V.; Leigh, D. A.; Marcos, V.; Morales-Serna, J. A.; Nussbaumer, A. L., *J. Am. Chem. Soc.* **2014,** *136* (13), 4905-4908.
[14] Blanco, V.; Leigh, D. A.; Lewandowska, U.; Lewandowsld, B.; Marcos, V., *J. Am. Chem. Soc.* **2014,** *136* (44), 15775-15780.
[15] Wasserman, E., *J. Am. Chem. Soc.* **1960,** *82* (16), 4433-4434.
[16] Harrison, I. T.; Harrison, S., *J. Am. Chem. Soc.* **1967,** *89* (22), 5723-5724.
[17] Thompson, M. C.; Busch, D. H., *J. Am. Chem. Soc.* **1964,** *86* (18), 3651-3656.
[18] Hubin, T. J.; Busch, D. H., *Coord. Chem. Rev.* **2000,** *200*, 5-52.
[19] Anderson, R. D., *Ann. Plast. Surg.* **1993,** *31* (5), 385-391.
[20] Dietrichbuchecker, C. O.; Sauvage, J. P.; Kintzinger, J. P., *Tetrahedron Lett.* **1983,** *24* (46), 5095-5098.
[21] Dietrichbuchecker, C. O.; Sauvage, J. P., *Tetrahedron Lett.* **1983,** *24* (46), 5091-5094.
[22] Hunter, C. A., *J. Am. Chem. Soc.* **1992,** *114* (13), 5303-5311.
[23] Adams, H.; Carver, F. J.; Hunter, C. A., *J. Chem. Soc., Chem. Commun.* **1995,** (8), 809-810.
[24] Ottenshildebrandt, S.; Meier, S.; Schmidt, W.; Vogtle, F., *Angew. Chem., Int. Ed. Engl.* **1994,** *33* (17), 1767-1770.
[25] Vogtle, F.; Dunnwald, T.; Handel, M.; Jager, R.; Meier, S.; Harder, G., *Chem. Eur. J.* **1996,** *2* (6), 640-643.
[26] Johnston, A. G.; Leigh, D. A.; Nezhat, L.; Smart, J. P.; Deegan, M. D., *Angew. Chem., Int. Ed. Engl.* **1995,** *34* (11), 1212-1216.
[27] Harada, A.; Li, J.; Kamachi, M., *Nature* **1992,** *356* (6367), 325-327.
[28] Craig, M. R.; Claridge, T. D. W.; Hutchings, M. G.; Anderson, H. L., *Chem. Commun.* **1999,** (16), 1537-1538.
[29] Anelli, P. L.; Ashton, P. R.; Ballardini, R.; Balzani, V.; Delgado, M.; Gandolfi, M. T.; Goodnow, T. T.; Kaifer, A. E.; Philp, D.; Pietraszkiewicz, M.; Prodi, L.; Reddington, M. V.; Slawin, A. M. Z.; Spencer, N.; Stoddart, J. F.; Vicent, C.; Williams, D. J., *J. Am. Chem. Soc.* **1992,** *114* (1), 193-218.
[30] Amabilino, D. B.; Ashton, P. R.; Reder, A. S.; Spencer, N.; Stoddart, J. F., *Angew. Chem., Int. Ed. Engl.* **1994,** *33* (12), 1286-1290.
[31] Hubner, G. M.; Glaser, J.; Seel, C.; Vogtle, F., *Angew. Chem., Int. Ed.* **1999,** *38* (3), 383-386.
[32] Mahoney, J. M.; Shukla, R.; Marshall, R. A.; Beatty, A. M.; Zajicek, J.; Smith, B. D., *J. Org. Chem.* **2002,** *67* (5), 1436-1440.

[33] Ghosh, P.; Mermagen, O.; Schalley, C. A., *Chem. Commun.* **2002,** (22), 2628-2629.
[34] Chiu, C. W.; Lai, C. C.; Chiu, S. H., *J. Am. Chem. Soc.* **2007,** *129* (12), 3500-3501.
[35] Ko, J. L.; Ueng, S. H.; Chiu, C. W.; Lai, C. C.; Liu, Y. H.; Peng, S. M.; Chin, S. H., *Chem. Eur. J.* **2010,** *16* (23), 6950-6960.
[36] Yoon, I.; Narita, M.; Shimizu, T.; Asakawa, M., *J. Am. Chem. Soc.* **2004,** *126* (51), 16740-16741.
[37] Hsueh, S. Y.; Ko, J. L.; Lai, C. C.; Liu, Y. H.; Peng, S. M.; Chiu, S. H., *Angew. Chem., Int. Ed.* **2011,** *50* (29), 6643-6646.
[38] Aucagne, V.; Hanni, K. D.; Leigh, D. A.; Lusby, P. J.; Walker, D. B., *J. Am. Chem. Soc.* **2006,** *128* (7), 2186-2187.
[39] Davis, A. P.; Sheppard, D. N.; Smith, B. D., *Chem. Soc. Rev.* **2007,** *36* (2), 348-357.
[40] Ko, S. K.; Kim, S. K.; Share, A.; Lynch, V. M.; Park, J.; Namkung, W.; Van Rosso, W.; Busschaert, N.; Gale, P. A.; Sessler, J. L.; Shin, I., *Nature Chem.* **2014,** *6* (10), 885-892.
[41] Wisner, J. A.; Beer, P. D.; Drew, M. G. B., *Angew. Chem., Int. Ed.* **2001,** *40* (19), 3606-3609.
[42] Sambrook, M. R.; Beer, P. D.; Wisner, J. A.; Paul, R. L.; Cowley, A. R.; Szemes, F.; Drew, M. G. B., *J. Am. Chem. Soc.* **2005,** *127* (7), 2292-2302.
[43] Mercurio, J. M.; Tyrrell, F.; Cookson, J.; Beer, P. D., *Chem. Commun.* **2013,** *49* (92), 10793-10795.
[44] Zapata, F.; Blackburn, O. A.; Langton, M. J.; Faulkner, S.; Beer, P. D., *Chem. Commun.* **2013,** *49* (74), 8157-8159.
[45] Knighton, R. C.; Beer, P. D., *Chem. Commun.* **2014,** *50* (13), 1540-1542.
[46] Wisner, J. A.; Beer, P. D.; Drew, M. G. B.; Sambrook, M. R., *J. Am. Chem. Soc.* **2002,** *124* (42), 12469-12476.
[47] Haynes, C. J. E.; Gale, P. A., *Chem. Commun.* **2011,** *47* (29), 8203-8209.
[48] Hussain, S.; Brotherhood, P. R.; Judd, L. W.; Davis, A. P., *J. Am. Chem. Soc.* **2011,** *133* (6), 1614-1617.
[49] Beer, P. D.; Drew, M. G. B.; Knubley, R. J.; Ogden, M. I., *J. Chem. Soc., Dalton Trans.* **1995,** (19), 3117-3123.
[50] Roelens, S.; Vacca, A.; Francesconi, O.; Venturi, C., *Chem. Eur. J.* **2009,** *15* (33), 8296-8302.
[51] Hunter, C. A.; Anderson, H. L., *Angew. Chem., Int. Ed.* **2009,** *48* (41), 7488-7499.
[52] Rudkevich, D. M.; Mercerchalmers, J. D.; Verboom, W.; Ungaro, R.; Dejong, F.; Reinhoudt, D. N., *J. Am. Chem. Soc.* **1995,** *117* (22), 6124-6125.
[53] Pelizzi, N.; Casnati, A.; Friggeri, A.; Ungaro, R., *J. Chem. Soc., Perkin trans. 2* **1998,** (6), 1307-1311.
[54] White, D. J.; Laing, N.; Miller, H.; Parsons, S.; Coles, S.; Tasker, P. A., *Chem. Commun.* **1999,** (20), 2077-2078.
[55] Shukla, R.; Kida, T.; Smith, B. D., *Org. Lett.* **2000,** *2* (20), 3099-3102.
[56] Valderrey, V.; Escudero-Adan, E. C.; Ballester, P., *Angew. Chem., Int. Ed.* **2013,** *52* (27), 6898-6902.
[57] Bissell, R. A.; Cordova, E.; Kaifer, A. E.; Stoddart, J. F., *Nature* **1994,** *369* (6476), 133-137.
[58] Livoreil, A.; Dietrichbuchecker, C. O.; Sauvage, J. P., *J. Am. Chem. Soc.* **1994,** *116* (20), 9399-9400.
[59] Balzani, V.; Credi, A.; Raymo, F. M.; Stoddart, J. F., *Angew. Chem., Int. Ed.* **2000,** *39* (19), 3349-3391.
[60] Barrell, M. J.; Leigh, D. A.; Lusby, P. J.; Slawin, A. M. Z., *Angew. Chem., Int. Ed.* **2008,** *47* (42), 8036-8039.
[61] Serpell, C. J.; Chall, R.; Thompson, A. L.; Beer, P. D., *Dalton Trans.* **2011,** *40* (45), 12052-12055.
[62] Barendt, T. A.; Robinson, S. W.; Beer, P. D., *Chem. Sci.* **2016,** *7* (8), 5171-5180.
[63] Barendt, T. A.; Docker, A.; Marques, I.; Felix, V.; Beer, P. D., *Angew. Chem., Int. Ed.* **2016,** *55* (37), 11069-11076.

[64] Jimenez, M. C.; Dietrich-Buchecker, C.; Sauvage, J. P., *Angew. Chem., Int. Ed.* **2000,** *39* (18), 3284-2387.
[65] Goujon, A.; Du, G. Y.; Moulin, E.; Fuks, G.; Maaloum, M.; Buhler, E.; Giuseppone, N., *Angew. Chem., Int. Ed.* **2016,** *55* (2), 703-707.
[66] Badjic, J. D.; Balzani, V.; Credi, A.; Silvi, S.; Stoddart, J. F., *Science* **2004,** *303* (5665), 1845-1849.
[67] Nguyen, T. D.; Tseng, H. R.; Celestre, P. C.; Flood, A. H.; Liu, Y.; Stoddart, J. F.; Zink, J. I., *Proc. Natl. Acad. Sci. U. S. A.* **2005,** *102* (29), 10029-10034.
[68] Green, J. E.; Choi, J. W.; Boukai, A.; Bunimovich, Y.; Johnston-Halperin, E.; DeIonno, E.; Luo, Y.; Sheriff, B. A.; Xu, K.; Shin, Y. S.; Tseng, H. R.; Stoddart, J. F.; Heath, J. R., *Nature* **2007,** *445* (7126), 414-417.

UNIVERSITAT ROVIRA I VIRGILI
INTERLOCKED ARCHITECTURES BASED ON A BIS-CALIX[4]PYRROLE MACROCYCLE FOR ION-PAIR RECOGNITION
Jose Ramon Romero Lopez

Chapter 2

Synthesis of a neutral [2]rotaxane based on a bis-calix[4]pyrrole macrocycle

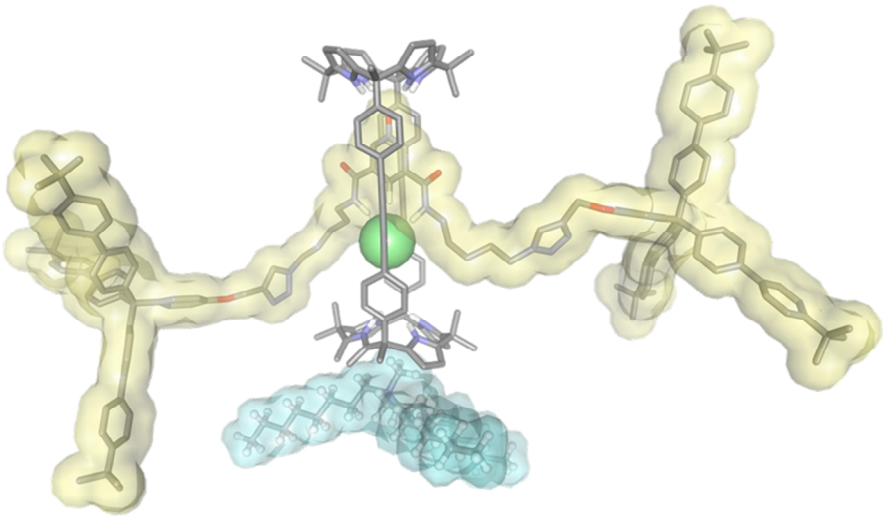

Part of this chapter has been published in:

Romero, J. R.; Aragay, G.; Ballester, P., *Chem. Sci.* **2017,** *8* (1), 491-498.

UNIVERSITAT ROVIRA I VIRGILI
INTERLOCKED ARCHITECTURES BASED ON A BIS-CALIX[4]PYRROLE MACROCYCLE FOR ION-PAIR RECOGNITION
Jose Ramon Romero Lopez

2.1 Introduction

Anion recognition is an important and established field in supramolecular chemistry owing to the fundamental role that negatively charged species play in chemical, biological and environmental processes.[1,2,3]. Mechanically interlocked molecules such as rotaxanes or catenanes present unique three-dimensional cavities for anion recognition that resemble the preorganized pocket of anion binding proteins in nature.[4,5,6] The use of anions as templates in the preparation of interlocked structures has been widely described[7] and is known to generate topologically unique cavities for anion recognition.[8,9,10] However, the majority of anion-template strategies for the assembly of interlocked structures combined strong ion-pairing of the linear axle with hydrogen bonding recognition of the anion by the macrocyclic component.[11,12,13] In 2012, we reported the use of polyatomic anions for the quantitative assembly of [2]pseudorotaxane-like architectures without involving ion-pairing in the linear component.[14] Our approach exploited the exceptional recognition properties exhibited by a neutral interwoven self-assembled receptor **1•2a** towards ion-pairs **3** (Figure 2. 1). In chloroform, at millimolar concentration, an equimolar mixture of bis-calix[4]pyrrole macrocycle **1** and linear bis-amidepyridyl-*N*-oxide **2a** produced the **1•2a** receptor in a partial extent (Figure 2. 1).[15]

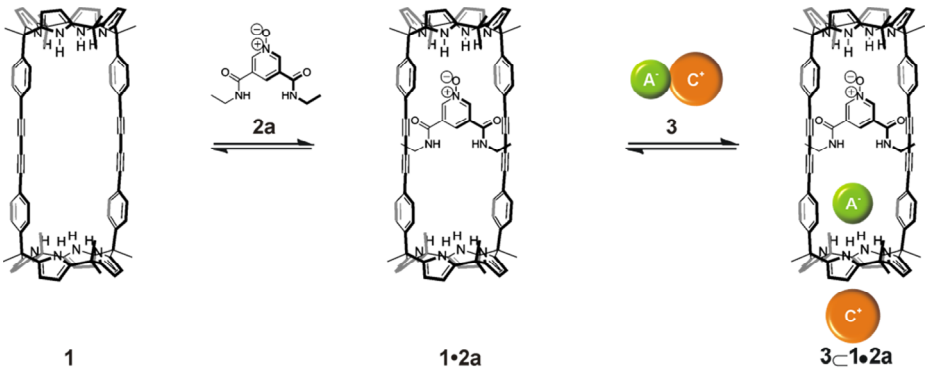

Figure 2. 1. Quantitative self-assembly of complexes **3⊂1•2a** with [2]pseudorotaxane topology. Macrocycle **1**, bis-amidepyridyl-*N*-oxide **2**, ion-pairs **3**; A^-: Anion (^-OCN, Cl^-, NO_3^-); C^+: Cation (TBA^+, $MTOA^+$).

The linear axle threaded the cyclic component by establishing four convergent hydrogen bonds between the oxygen atom of **2a** and the pyrrole NHs of one calix[4]pyrrole unit in **1** (Figure 2. 1). Remarkably, the addition of 1 equiv. of certain polyatomic anions (A^-) as tetrabutylammonium salts ($^+NBu_4$) to the two-components' mixture induced the quantitative assembly of four-particle aggregates $ANBu_4\subset$**1•2a** with [2]pseudorotaxane-like topology. The resulting complexes displayed a cyclic-component separated binding mode of the ion-pair. The anion was included in the polar cavity of the interwoven receptor in which six NHs converged (two from bound bis-amide and four from the opposing calix[4]pyrrole cap of the cyclic component). While the cation was located in the shallow, electron-rich cavity defined by the cone conformation of the calix[4]pyrrole, opposed to the bound anion.

Almost coinciding with our report, Beer and co-workers[16] described the synthesis of neutral [2]rotaxanes that recognized halide anions in aqueous mixtures containing a bis-amidepyridyl-*N*-oxide axle derivative closely related to **2a**. The employed strategy for the assembly and thermodynamic stabilization of the synthetic intermediate displaying pseudorotaxane topology was very similar to ours. They used a subsequent stoppering approach relying on the copper(I)- catalyzed azide-alkyne cycloaddition (CuAAC) reaction to produce the [2]rotaxane. The CuAAC has been extensively and successfully applied in the synthesis of mechanically interlocked molecules i.e. [2]rotaxanes.[17,18,19,20,21]

Inspired by these findings, in this chapter we describe the synthesis of the neutral [2]rotaxane **5** (Scheme 2. 1). The employed stoppering strategy was based on the CuAAC reaction mentioned above. Surprisingly to us, the use of anion templation was detrimental for the synthesis of **5**. The absence of templating anions (i.e. Cl^-, OCN^-) resulted in higher yields of the [2]rotaxane **5**.

2.2 Results and discussion

2.2.1 Design and synthesis of [2]rotaxane **5**

The syntheses of the [2]rotaxane's molecular components (i.e. macrocycle **1**,[14] linear component **2b** and stopper **4a-b**,[22] Figure 2. 2) were performed by following or adapting synthetic procedures described in literature. The selection of the tris(biphenyl) stopper **4a** was not trivial and derived from multiple unsuccessful attempts to isolate the [2]rotaxane when using smaller terphenyl stoppers **4b** (Figure 2. 2). The results obtained using small stopper **4b** in rotaxane synthesis will be discussed in Chapter 4.

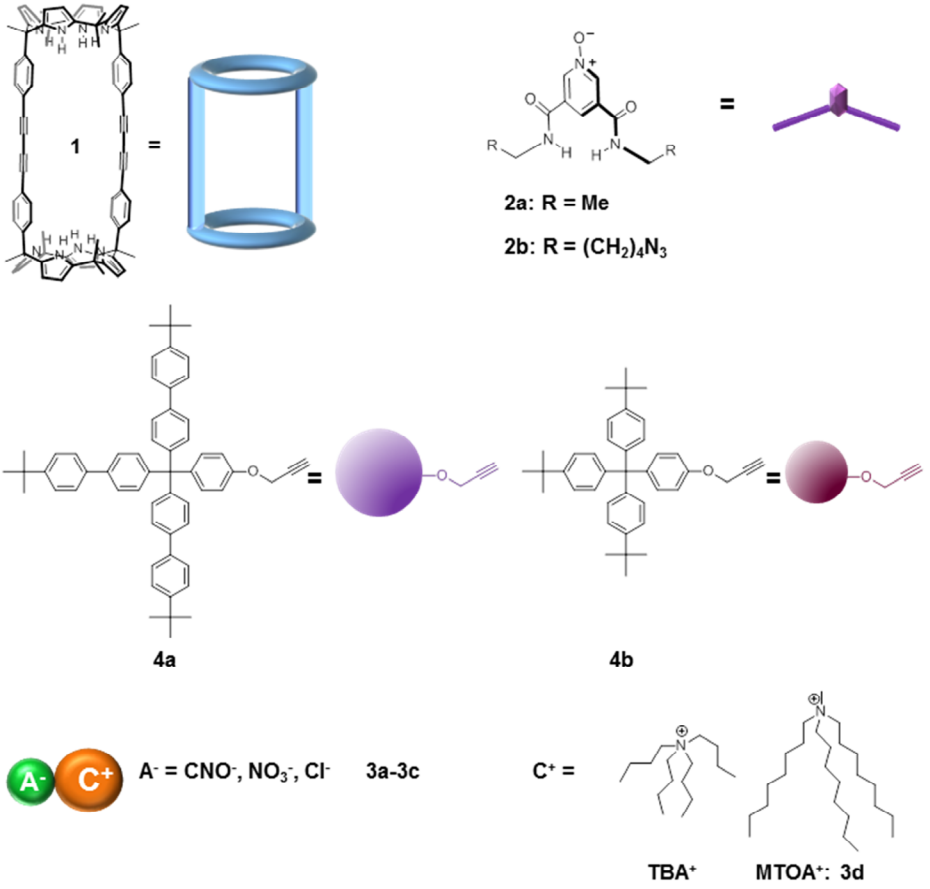

Figure 2. 2 Schematic representation of the molecules used in Chapter 2. Macrocycle **1**, the *bis*-amidepyridyl-*N*-oxides **2**, stoppers **4a** (large stopper) and **4b** (small stopper).

[2]Rotaxane **5** was initially prepared by adding to the 1 mM equimolar mixture of **1** and **2b** in dichloromethane solution, 2 equiv. of the alkyne-functionalized tris(biphenyl) stopper **4a**, 4 equiv. of diisopropyl ethyl amine (DIPEA), and a catalytic amount (5%) of $[Cu(CH_3CN)_4]PF_6$ and tris(benzyltriazoylmethyl)amine (TBTA) (Scheme 2. 1, entry *a* from Table 2. 1). The mixture was stirred at room temperature for 5 hours. [2]Rotaxane **5** was isolated as a white solid in 10% yield after silica column chromatography purification of the crude reaction mixture using $AcOEt/CH_2Cl_2$ 30:70 as eluent.

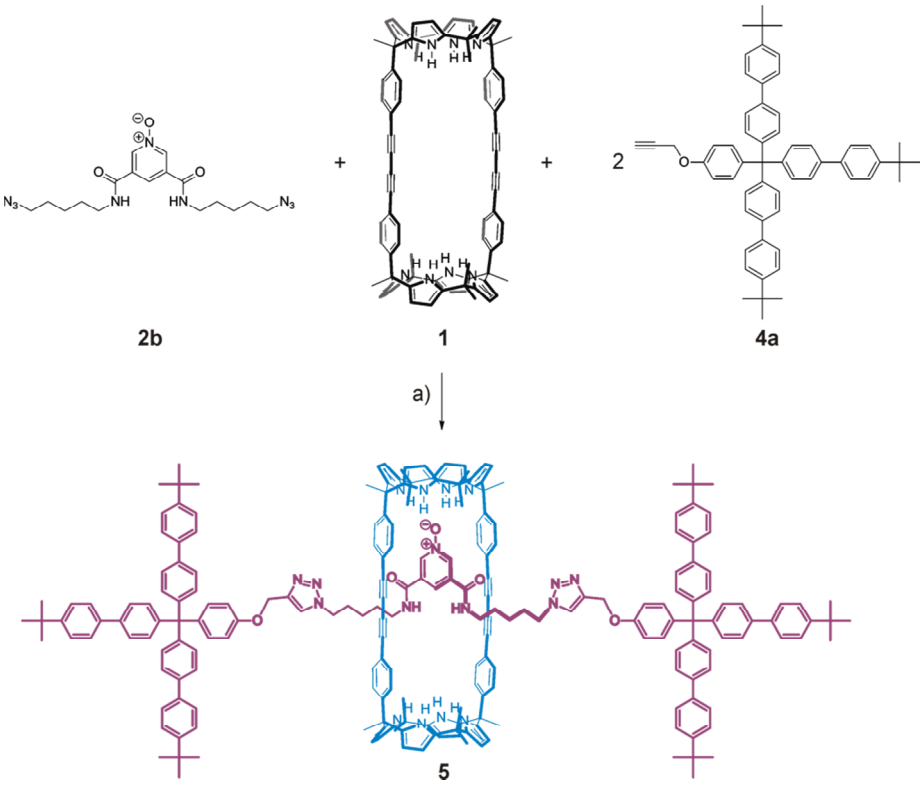

Scheme 2. 1. Synthetic scheme for the preparation of [2]rotaxane **5**. Macrocycle **1**[14] and stopper **4a**[22] were synthetized following a reported procedure. Synthesis of linear component **2b** is in the experimental section of this chapter. a) Reaction conditions: 5% $[Cu[(CH_3CN)_4PF_6]$, 5% TBTA, 4 equiv. DIPEA, DCM.

Table 2. 1. Summary of the different reaction conditions tested for the synthesis of rotaxane **5**. *n.d. not determined. We were not able to isolate pure [2]rotaxane **5**. Solvent CH_2Cl_2

	[**1**]	[**2b**]	[**4**]	[OCNTBA] **3a**	[Cu(I), TBTA]	Yield of **5**
a	1 mM	1 mM	2 mM	-	5%	10%
b	1 mM	1 mM	2 mM	1 mM	5%	n.d.*
c	14 mM	14 mM	28 mM	-	5%	27%
d	8 mM	16 mM	32 mM	-	5%	50%

Rotaxane **5** was characterized by a complete set of high-resolution spectra (1D and 2D NMR spectroscopy and ESI-HRMS+ spectrometry). The ^{1}H NMR spectrum of **5** (Figure 2. 3) in $CDCl_3$ solution displayed both broad and sharp, well-defined signals that were assigned to the protons of its two components, macrocycle and axle, using 2D

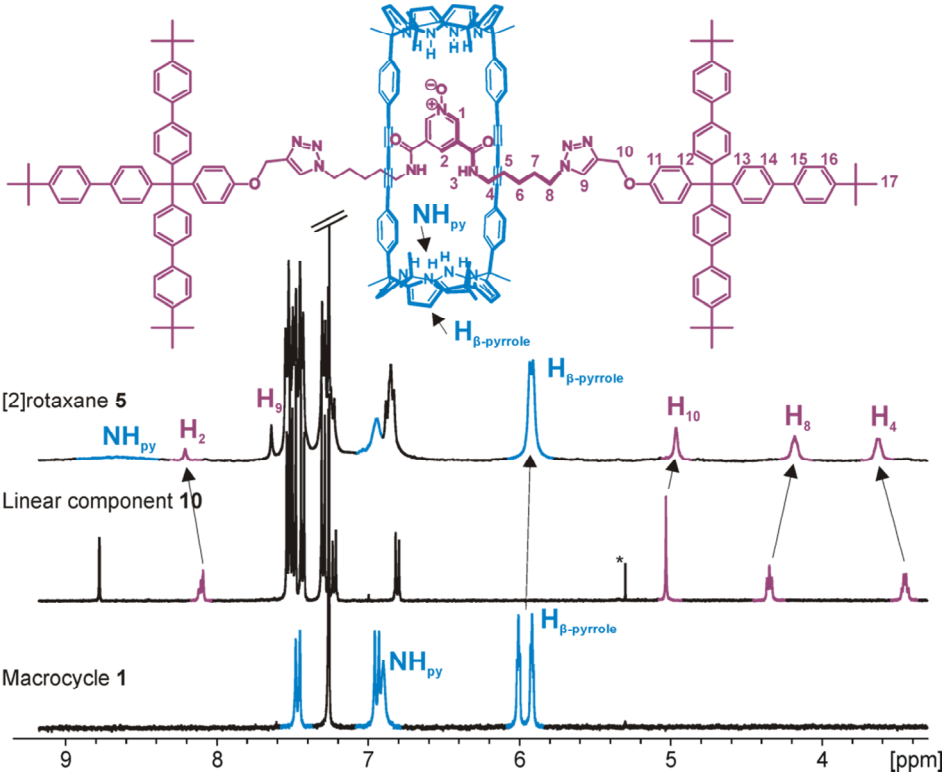

Figure 2. 3. (Top) Molecular structure of [2]rotaxane **5** and proton assignment (Bottom) selected downfield regions of the ^{1}H NMR spectra (500 MHz, $CDCl_3$, 298 K) of the free cyclic (**1**) and linear (**10**) components and [2]rotaxane **5**. (*solvent peak) Notice that macrocycle signals are shown in blue and some signals (but not all) corresponding to the lineal component are shown in purple.

NMR experiments. In particular, the sharp signals observed in the region of 7.5 to 7.2 ppm were attributed to protons of the bulky tris(biphenyl) stopper groups of the axle. The pyrrole NHs resonated at δ = 8.7 ppm as a unique broad signal, which is downfield shifted in comparison to the NHs in the free macrocycle (Figure 2. 3). On the one hand, these observations suggested the existence of hydrogen-bonding interactions between the pyrrole NHs and the oxygen atom of the pyridyl-*N*-oxide group in the threaded linear component. On the other hand, because the cyclic component **1** possesses two identical calix[4]pyrrole binding sites, it must be involved in a dynamic process that most likely encompasses the pirouetting of the pyridyl-*N*-oxide axle within the macrocycle cavity. At room temperature, this dynamic process is fast on the chemical shift timescale providing a single set of signals for the protons of **1** although some of them appear as broad signals i.e NHs pyrrole. The aromatic proton of triazole rings (H_9) resonated as a sharp singlet at δ = 7.6 ppm confirming the covalent connection between the stoppers and the linear axle. Variable temperature ^{1}H NMR experiments performed using a $CDCl_3$ solution of rotaxane **5** showed that at low temperatures many of its broad proton signals split in two or more sharper signals. (Figure 2. 4). Most likely, this is

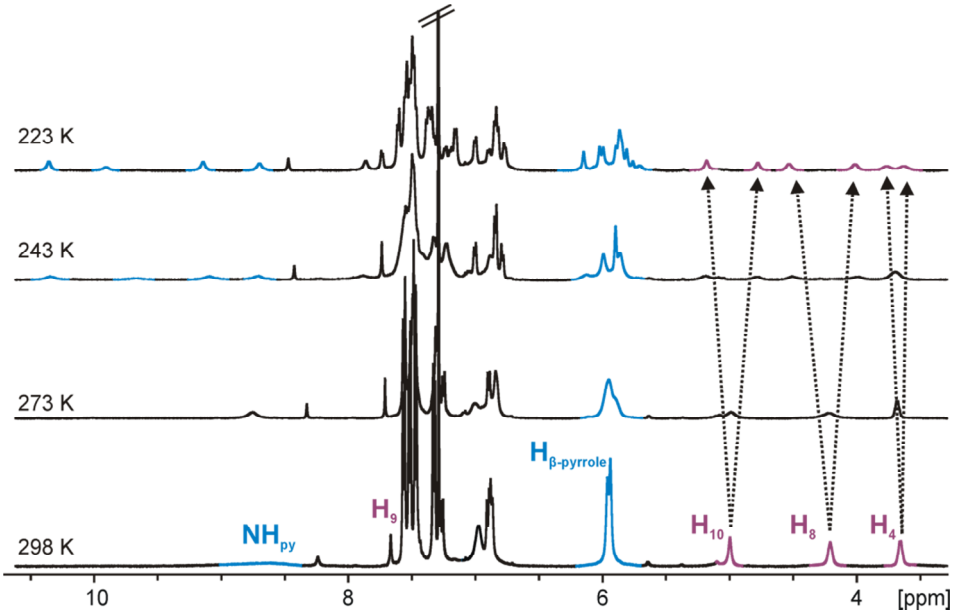

Figure 2. 4. Selected downfield region of the ^{1}H NMR variable temperature (from 298 K to 223 K) experiment of a 1 mM solution of [2]rotaxane **5** in $CDCl_3$.

due to the change in the rate of the pirouetting process experienced by the interlocked linear component of **5**. The process is fast on the chemical shift time scale at 298 K but becomes slow at temperatures close to 233 K.

We also performed Diffusion Ordered SpectroscopY (DOSY) NMR experiments using a millimolar solution of **5** in $CDCl_3$. Despite the size difference between the two molecular components of **5**, the diffusion constant values calculated for the decay of the proton signals' intensities in any of them were identical. This result indicated that the two components were involved in the formation of the interlocked supramolecular species **5**. The diffusion constant determined for **5** was 4.7×10^{-10} m^2/s (Figure 2. 22 from experimental section).

Previously, we reported that in chloroform solution macrotricycle **1** and *N*-oxide **2a** formed a 1:1 complex with [2]pseudorotaxane topology (Figure 2. 1).[14] At room temperature, the ^1H NMR spectrum of the equimolar mixture (1 mM) of **1** and **2a** showed broadening beyond detection for some of the signals of the protons of the two binding partners. Based on ^1H NMR titrations we determined that the stability constant of the **1•2a** complex was 800 M^{-1} at 298 K.[14] Taken together, these results indicate that at this concentration only around 30% of the binding partners are involved in the interwoven **1•2a** or **1•2b** complexes and that the equilibrium process is intermediate/fast on the proton chemical shift timescale. These results are in agreement with the low yield (~10%) of rotaxane **5** isolated under these reaction conditions.

2.2.2 Optimization of the reaction conditions

Study of the anion template effect

Aiming at improving the yield of [2]rotaxane **5**, we considered to undertake its synthesis in the presence of 1 equiv. of tetrabutylammonium cyanate **3a** (OCNTBA) (Scheme 2. 2 **B**, entry *b* Table 2. 1).

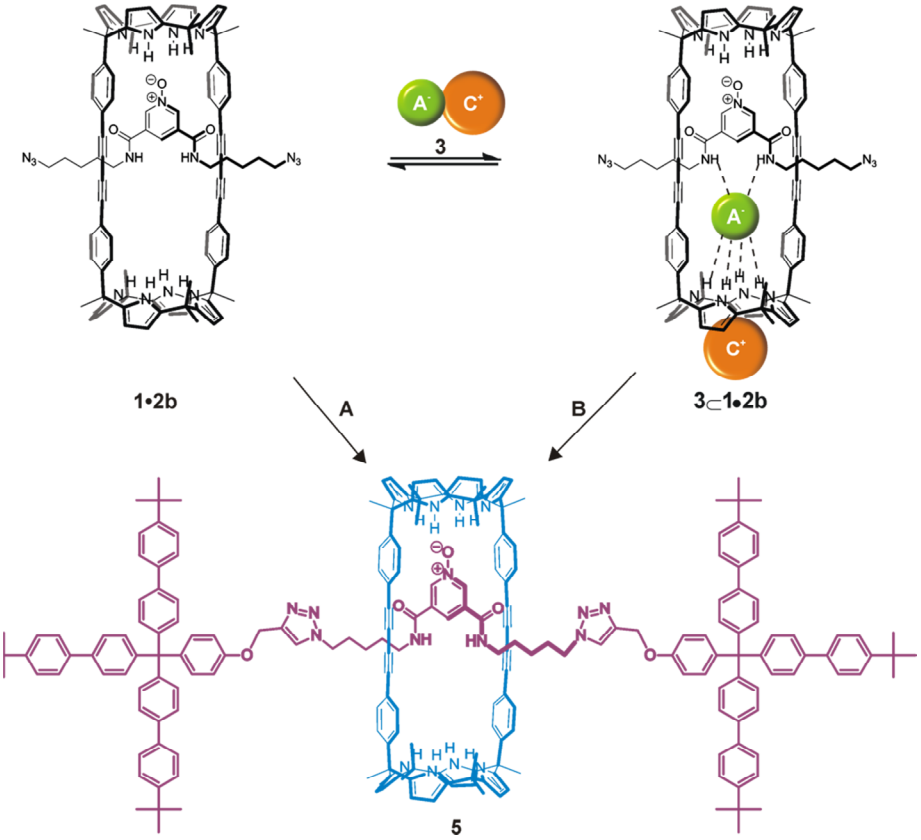

Scheme 2. 2. Synthetic schemes for the preparation of [2]rotaxane **5**. A and B reaction conditions: 2 equiv. **4a**; DIPEA, $[Cu(CH_3CN)_4]PF_6$ and TBTA in CH_2Cl_2, 5h at R.T. A^-: Anion (^-OCN, Cl^-, NO_3^-); C^+: Cation (TBA^+, $MTOA^+$).

We have showed that the addition of 1 equiv. of OCNTBA **3a** to a 1 mM equimolar mixture of **1** and **2a** in $CDCl_3$ solution yielded the quantitative assembly of the **3a⊂1•2a** complex ($K_a \sim 10^{11}$ M^{-2}) featuring [2]pseudorotaxane topology (Figure 2. 1).[14] This result highlighted the important role played by the ion-pair in templating and stabilizing the interwoven structure of the complex formed between **1** and **2a** in solution.

We expected that the concentration increase experienced by the synthetic interwoven intermediate with [2]pseudorotaxane topology from 30% of **1•2b** complex to almost 100% of **3a⊂1•2b** complex in the presence of an equimolar amount of **3a** could be translated in a significant improvement of the isolated yield of [2]rotaxane **5**, (Figure 2. 5).

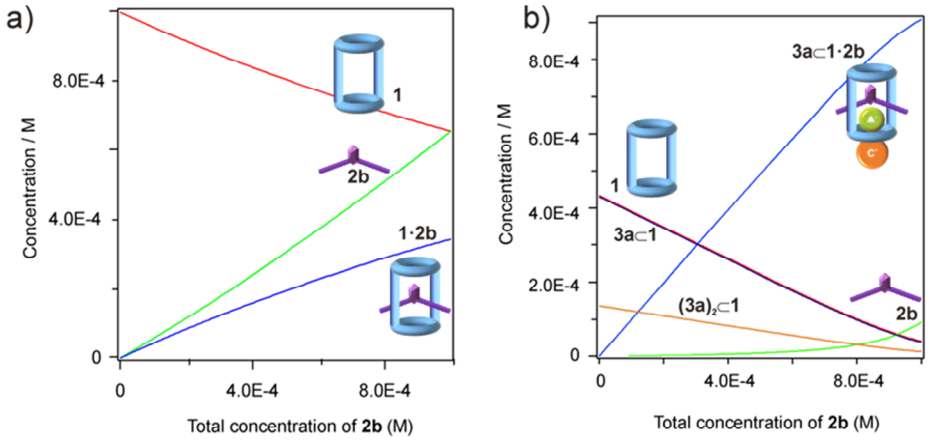

Figure 2. 5. Speciation profiles of the addition of increasing amounts of **2b** (up to 1 equiv.) over a 1 mM solution of macrocycle **1** (a), and over a 1 mM equimolar mixture of **1** and **3a** (b). We considered the association constants determined in previous works: K(**1•2b**) = 800 M^{-1}, K(**3a⊂1**) = 1×10^{5} M^{-1}, K(**$3a_2$⊂1**) =·1×10^{11} M^{-2}, K(**3a⊂1•2b**) = 9.1×10^{10} M^{-2}.[14]

Although we were aware of literature precedents alerting on the inhibitory effects of halides in CuAAC reaction rates in DMSO,[23] aqueous[24] and buffered systems,[25] we repeated the threading and CuAAC stoppering reactions in the presence of 1 equiv. of OCNTBA **3a**. We sought to perform this reaction in a NMR tube with the goal of analyzing the initial assembly of the synthetic [2]pseudorotaxane precursor **3a⊂1•2b** in the presence of the catalytic system (5% TBTA and Cu(I) salt), as well as the evolution of the CuAAC reaction by ^{1}H NMR spectroscopy (Figure 2. 6). We observed that the addition of the catalytic system to a 1 mM equimolar mixture of **1**, **2b** and OCNTBA **3a** and 2 equiv. of the tris(biphenyl) stopper **4a** had a negligible effect on the assembled **3a⊂1•2b** complex in chloroform solution.

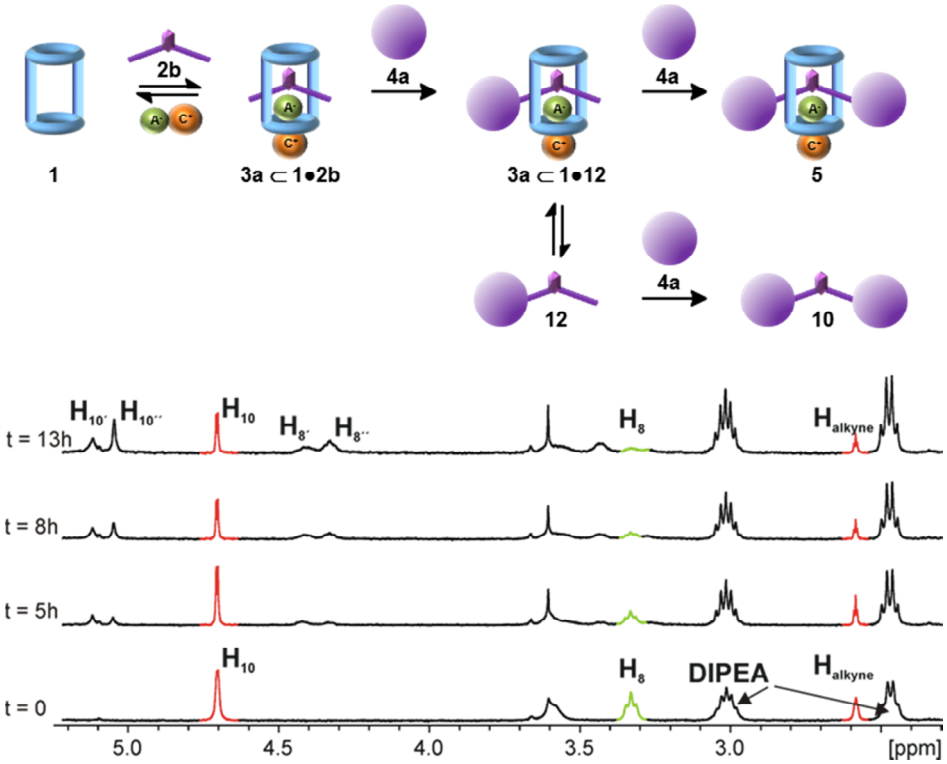

Figure 2. 6. Upper part: schematic representation of the involved species in equilibria during the reaction. Lower part: selected upfield ^{1}H NMR spectra of the reaction crude for the rotaxane synthesis showing the signals for protons H_{10}, H_8, H_{alkyne}. Monitoring of starting material disappearance and product formation. Depicted in red, alkyne proton and proton H_{10} from free stopper **4a**. In green is depicted H_8 from starting N-oxide **2b**. See Figure 2. 3 for proton assignment. (´) Intermediate mono-click product, (´´) [2]rotaxane **5** + free linear component **10**.

Five hours after the addition of the Hünig's base (4 equiv.), the ^{1}H NMR spectrum of the reaction mixture revealed that the signal corresponding to terminal alkyne protons of **4a** and the methylene protons alpha to unreacted azide groups in **2b** (H_8) were still visible. In the NMR spectra at 13h we can detect different sets of signals that we attribute to the multiple species present in solution during the reaction time (Figure 2. 6) namely **2b**, monoclick product **12** (derived from the reaction of only one side of **2b** with stopper **4a**) linear product **10** and rotaxane **5**. Specifically, we identified multiple signals in the region where proton H_8 resonates. We attribute the observed signals to the proton in fee **2b** (H_8), monoclick intermediate **12** ($H_{8'}$) and the linear product **10** ($H_{8''}$), protons H_{10} (corresponding to CH_2 alpha to the oxygen in the stopper) in the monoclick

intermediate **12** ($H_{10'}$) and the linear component **10** ($H_{10''}$) were also observed as separate signals. Moreover, the signal of the H_{10} proton in the free linear component **10** overlapped with that of its counterpart involved in the rotaxane assembly **5**. It is worthy to note that some proton signals appear as broad bands in the ^{1}H NMR spectrum of the reaction mixture. Most likely, this observation is due to the existence of exchange rates that are intermediate on the chemical shift timescale corresponding to different binding equilibria that take place in solution (i.e. free and bound monoclick product **12** and free and bound **2b**), (Figure 2. 6).

We obtained similar results when we replaced the tetrabutylammonium cyanate salt **3a** by methyltrioctylammonium chloride **3d**. These results suggested that the salts, used as templates for the quantitate assembly of the [2]pseudorotaxanes, had a significant effect in the formation rate of the mechanical bond, that is the stoppering reactions on the linear component in the [2]rotaxanes.

In order to gain some insight on the effect played by the tetralkylammonium salts in the CuAAC reaction's rate we performed additional control experiments. First, we determined that the CuAAC reaction of diazide **2b** with 2 equiv. of stopper **4a** in CH_2Cl_2 solution in the absence of macrocycle **1** was completed after 3 hours, (Figure 2. 7 a). Conversely, the same reaction in the presence of 1 equiv. of either ion-pair OCNTBA **3a** or ClMTOA **3d** did not take place even after a period of 24 hours, (Figure 2. 7 b). All together, these results indicated that the presence of 1 equiv of tetralkylammonium salts of coordinating anions, like cyanate or chloride caused the inhibition and deactivation of the copper(I) catalytic system, possibly by competing with the activation of the azide through coordination with the metal center.

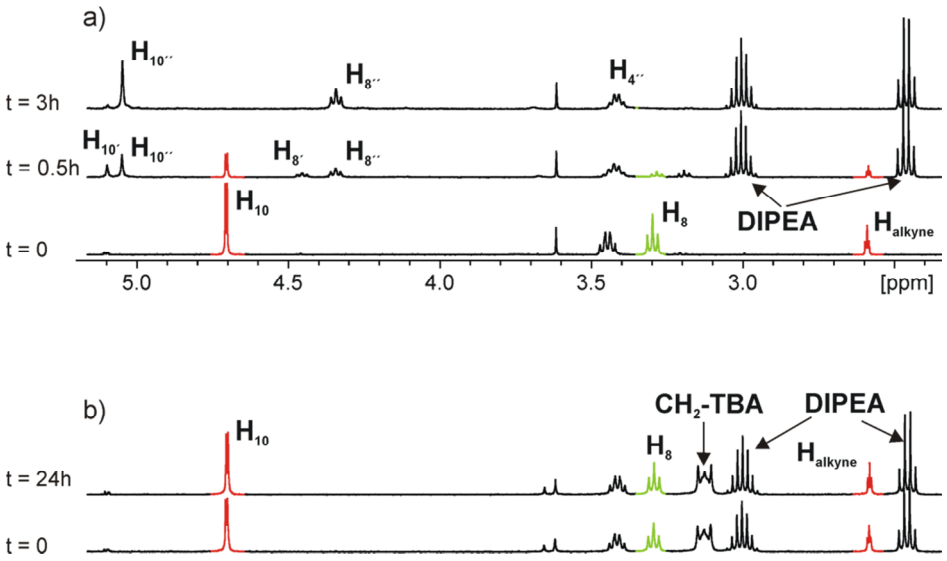

Figure 2. 7. Selected upfield region of the ^{1}H NMR spectra for the synthesis of linear component **10** in the absence (a) and in the presence (b) of OCNTBA. Alkyne protons and proton H_{10} from free stopper **4a** are depicted in red. Protons H_8 from initial *N*-oxide **2b** are depicted in green. See Figure 2. 3 for proton assignment. (′) Intermediate mono-click product, (′′) linear component product **10**.

As mentioned above, the presence of the cyclic component **1** in the stoichiometrically controlled mixture of reactants **2b, 3a** and **4a** allowed the CuAAC reaction to evolve but to a partial extent (Figure 2. 6). Most likely, in this latter case, the complexation of the ion-pair exerted by the self-assembled [2]pseudorotaxanes and the emerging [2]rotaxane significantly reduced the amount of free anions (salt) in solution below 1 equiv. Moreover, the isolation of [2]rotaxane **5** from the crude reaction mixtures obtained using the ion-pair template strategy was not exempt of complications. Surprisingly, the fractions isolated from the column chromatography purification of **5** consisted mainly of mixtures of the free receptor, free linear component and the ion-paired complex, **3**⊂**5**.[26,27]

Concentration effect

Considering the synthetic limitations encountered in the use of ion-pairs as templates for the synthesis of the mechanically interlocked receptor **5** (i.e. purification problems and catalyst deactivation), we explored alternative methodologies that could improve its

isolated yield (entries *c* and *d* from Table 2. 1). We expected that at higher concentrations the formation of the synthetic intermediate with [2]pseudorotaxane topology will be favored. In fact, from the corresponding speciation profiles (Figure 2. 8 a), it is possible to derive that the **1•2b** complex is formed, working under stoichiometric control, in a much higher extent at a concentration of 14mM than at 1 mM, 83% and 30%, respectively (see Figures 2.5 and 2.8a)

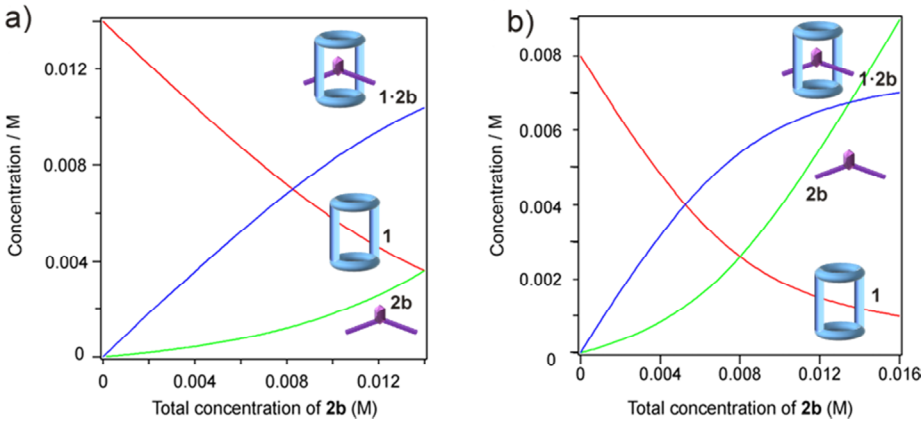

Figure 2. 8. Speciation profiles of: (a) the addition of increasing quantities of **2b** (up to 1 equiv.) over a 14 mM solution of macrocycle **1**. (b) the addition of increasing quantities of **2b** (up to 2 equiv.) over a 8 mM solution of macrocycle **1**. We considered the association constants determined in previous works: K(**1•2b**) = 800 M^{-1}.[14]

Moreover, working at 8 mM concentration for the cyclic component, in order to assure the complete solubility, and doubling the amount of linear component (16mM), induced the assembly of interwoven product concentration **1•2b** complex to a level of 87%, (Figure 2. 8 b). We expected that the use of the latter concentration conditions in the stoppering reaction will translate in a significant improvement of the isolated yield for the [2]rotaxane **5**.

Indeed, a fourteen fold increase in the concentration of reactants ([**2b**] = 14 mM and [**4a**] = 28 mM) and the cyclic component ([**1**] = 14 mM) maintaining a 1:2:1 stoichiometric ratio almost tripled the yield of the isolated [2]rotaxane **5** (27 %). Doubling the stoichiometric ratio of reactants (**2b** and **4a**) with respect to the cyclic component (**1**) and using the latter at a concentration of 8 mM in order to assure the solubility of all compounds, allowed us to isolate the [2]rotaxane **5** in a significant 50%

yield. We used the catalytic system in a 5% load with respect to the concentration of the linear component and all reactions were completed in less than 5 hours. Most likely, the higher concentration attained for the [2]pseudorotaxane precursor in the more concentrated solutions was responsible for the observed increase in isolated yields of **5**.

2.3 Conclusions

In summary, we describe a synthetic methodology for the preparation of [2]rotaxane **5** in a remarkable 50% isolated yield. We conclude that the use of anion templation in the preparation of interlocked structures may limit the application of the CuACC reaction in the stoppering step. In our specific case, we found that the use of ion-pairs as template for the quantitative self-assembly of the synthetic precursor displaying [2]pseudorotaxane topology was associated with two synthetic limitations: (a) difficulties in the isolation of the final [2]rotaxane **5** free from the ion-pair used as template and (b) deactivation of the Cu(I) catalytic process employed to promote the CuAAC reaction in the stoppering step.

2.4 Experimental section

2.4.1 General information and instrumentation

All reagents were obtained from commercial suppliers and used without further purification. Anhydrous solvents were obtained from a solvent purification system SPS-400-6 from Innovative Technologies, Inc. All solvents were of HPLC grade quality, commercially obtained and used without further purification. Routine ^{1}H NMR spectra and kinetic studies were recorded on a Bruker Avance II 400 Ultrashield NMR spectrometer. Variable temperature experiments and 2D NMR spectra were performed on a Bruker Avance 500 (500.1 MHz for ^{1}H NMR) Ultrashield spectrometer. $CDCl_3$ from Sigma Aldrich was used for NMR studies. Chemical shifts are given in ppm, relative to TMS. Analytical HPLC experiments were performed using a HPLC1100 Agilent instrument. UV-Vis measurements were carried out on a Shimadzu UV-2401PC spectrophotometer equipped with a photomultiplier detector, double beam optics and D2 and W light sources. Simulated speciation profiles of pseudorotaxane formation

were obtained for different reaction conditions using the Hyss software. The stability constants used in the simulation were determined in previous works[14] by ^{1}H NMR and ITC experiments.

2.4.2 Synthetic procedures

3-(4-(Tris(4'-tert-butylbiphen-4-yl)methyl)phenoxy)propyne **4a** was synthesized according to reported procedures.[22]

*Synthesis of 3,5-bis((5-azidopentyl)carbamoyl)pyridine **9***

Compound **9** was prepared from commercially available 3,5-pyridinedicarboxylic acid by reaction with oxalyl chloride and a catalytic amount of DMF to obtain the corresponding acid chloride **8**. To a solution of **8** in DCM (1.2 mM, 10 mL) a solution of 5-azidopentan-1-amine **6**[28] (1.53g, 11.9 mmol), Et_3N (2.8 mL) and DMAP (0.69 g, 5.7 mmol) in dry CH_2Cl_2 (5 mL) was added dropwise at 0ºC. The reaction mixture was stirred at room temperature for 2h. After 2 hours, the reaction crude was washed with 0.01 N HCl (2×10 mL) followed by washes of saturated $NaHCO_3$ (2x10 mL). The organic layer was dried over anhydrous Na_2SO_4 and concentrated *in vacuo*. Purification of the residue by column chromatography (AcOEt as eluent) afforded **9** as yellow solid (1.13 g, 51 %). ^{1}H NMR (400 MHz, Chloroform-*d*) δ 9.08 (s, 2H), 8.44 (s, 1H), 6.65 (br, 2H), 3.51 (m, 4H), 3.30 (m, 4H,), 1.67 (m, 8H), 1.48 (m, 4H).

*Synthesis of 3,5-bis((5-azidopentyl)carbamoyl)pyridine 1-oxide **2b***

In a round bottom flask (250 mL) 3,5-bis((5-azidopentyl)carbamoyl)pyridine ***9*** (1.1 g, 2.9 mmol) and sodium hydrogen carbonate (7.4 g, 87.5 mmol) were dissolved in 30 mL mixture of H_2O/2-butanone 1:1. The solution was stirred vigorously for 5 min. Oxone was added dropwise to the solution (7 g in 10 mL of water). After 4 hours, the reaction mixture was treated with brine (20 mL) and the desired product was extracted with $CHCl_3$ (2x10 mL). The combined organic layers were dried over anhydrous Na_2SO_4 and concentrated *in vacuo* to obtain a yellow solid (993 mg, 84%). ^{1}H NMR (400 MHz, Chloroform-*d*) δ 8.87 (s, 2H), 8.10 (s, 1H), 7.14 (br, 2H), 3.51 (m, 4H), 3.33 (m, 4H), 1.70 (m, 8H), 1.52 (m, 4H). ^{13}C{^{1}H} NMR (125 MHz, Chloroform-*d*) δ 162.4, 140.3,

134.2, 124.8, 51.4, 40.5, 29.0, 28.7, 24.3. IR νmax/cm^{-1}: 2935 (C-H, st), 2090 (N=N, st), 1645 (C=O, st), 1543 (N-O, st). HR-MS (ESI-TOF ES+) m/z calculated for $C_{17}H_{25}N_9O_3$ $([M+H])^+$ 404.2153 found $([M+H])^+$ 404.2145

*Synthesis of linear component **10***

A mixture of **2b** (32 mg, 0.08 mmol), **4a** (127 mg, 0.16 mmol), $Cu(CH_3CN)_4PF_6$ (30 mg, 0.08 mmol) and TBTA (43 mg, 0.08 mmol) were dissolved in dry DCM (4 mL) in a two necked round bottom flask (50 mL). Finally, *N*-ethyl-*N*-isopropylpropan-2-amine (0.056 ml, 0.32 mmol) was added to the reaction mixture. The reaction was stirred at room temperature under argon for 3 hours. After 3 hours, the crude was washed with water (2x40 mL). The organic layer was dried over anhydrous Na_2SO_4 and concentrated *in vacuo*. The product was purified by silica column chromatography using DCM as eluent in order to collect the excess of stopper **4a.** The eluent was changed to 5% MeOH/DCM to collect the desired product as a white solid (85 mg, 54%). ^{1}H NMR (400 MHz, Chloroform-*d*) δ 8.78 (s, 2H), 8.1 (br, 1H), 8.09 (s, 2H), 7.53 (d, *J* = 8.4 Hz, 12H), 7.52 (s, 2H), 7.49 (d, *J* = 8.4 Hz, 12H), 7.43 (d, *J* = 8.4 Hz, 12H), 7.29 (d, *J* = 8.4 Hz, 12H), 7.22 (d, *J* = 8.8 Hz, 4H), 6.8 (d, *J* = 8.8 Hz, 4H), 5.08 (s, 4H), 4.35 (m, 4H), 3.4 (m, 4H), 1.84 (m, 4H), 1.64 (m, 4H), 1.34 (s, 54H, CH_3-*t*But), 1.28 (m, 4H). ^{13}C{^{1}H} NMR (125 MHz, Chloroform-*d*) δ 162.8, 156.3, 150.4, 145.7, 144.4, 141.2, 140.9, 140.1, 138,6, 137.8, 132.5, 131.7, 126.7, 126.2, 125.8, 123.3, 121.5, 113.6, 64.0, 61.8, 49.8, 39.6, 34.8, 31.5, 29.5, 27.7, 22.8. IR νmax/cm^{-1}: 2959 (C-H, st), 2867 (C-H, st), 1494(C=N, C=C, st), 815 (C=C, st). HR-MS (ESI-TOF ES+) m/z calculated for $C_{133}H_{141}N_9O_3Na$ $([M+Na])^+$ 1967.0948 found $([M+Na])^+$ 1967.0938

*Synthesis of [2]rotaxane **5***

Conditions a: Macrocycle **1**[14] (21.1 mg, 0.018 mmol), pyridine *N*-oxide **2b** (7.1 mg, 0.018 mmol), **4a** (27.2 mg, 0.035 mmol), TBTA (0.50 mg, $0{,}9\times10^{-3}$ mmol) and the catalyst $Cu[(CH_3CN)_4PF_6]$ (0.34 mg, 0.9×10^{-3} mmol) were placed in a two necked round bottom flask (25 mL) and dissolved in dry DCM (7 mL). Finally, the Hünig's base (0.012 ml, 0.070 mmol) was added to the reaction mixture and was stirred at room temperature under Ar for 5 hours. The reaction could be monitored by TLC (2%

MeOH/DCM, Rf rotaxane=0.36; Rf macrocycle=1; Rf linear component=0). The reaction mixture was washed with water (2×40 mL). The organic phase was dried over anhydrous Na_2SO_4 and the solvent was removed *in vacuo*. The residue was purified by column chromatography (30% AcOEt/DCM) to give the desired product as a white solid (6 mg, 11%). Upon changing the eluent to 5% MeOH/DCM we could isolate the free linear component.

Conditions b (using MTOACl as template): In a two necked round bottom flask (25 mL) macrocycle **1** (21.1 mg, 0.018 mmol), pyridine *N*-oxide **2b** (7.1 mg, 0.018 mmol), MTOACl **3d** (7.3 mg, 0.018 mmol) were dissolved in dry DCM (7 mL). The formation of the 1:1:1 [**1**]:[**2b**]:[**3d**] pseudorotaxane complex was monitored by ^{1}H NMR. After confirming the exclusive formation of the 1:1:1 complex in solution, **4a** (27.2 mg, 0.035 mmol), TBTA (0.50 mg, 0.9×10^{-3} mmol) and the catalyst $Cu[(CH_3CN)_4PF_6]$ (0.34 mg, 0.9×10^{-3} mmol) were added to the reaction mixture. Finally, Hünig's base (0.012 ml, 0.070 mmol) was added and the reaction mixture was stirred at room temperature under Ar for 5 hours. After 5 hours the reaction crude was washed with water (2×40 mL). The organic phase was collected and dried over anhydrous Na_2SO_4 and the solvent was removed *in vacuo*. The crude was purified by silica column chromatography, using 30% AcOEt/DCM as eluent. Different fractions were collected but none of them contained the pure free rotaxane but mixtures of the free macrocycle **1**, free linear component **10** and the ion-paired complex **3**⊂**5**. Other separation mixtures (e.g. MeOH:DCM 5:95) were also tried without separation success.

Conditions c (higher concentration of the reactants, 14 mM): In a two necked round bottom flask (25 mL) macrocycle **1** (100 mg, 0.084 mmol), pyridine *N*-oxide **2b** (33.7 mg, 0.084 mmol), **4a** (129 mg, 0.167 mmol), TBTA (2.2 mg, 4.2×10^{-3} mmol) and the catalyst $Cu[(CH_3CN)_4PF_6]$ (1.5 mg, 4.2×10^{-3} mmol) were dissolved in dry DCM (6 mL). Finally, Hünig's base (0.06 ml, 0.33 mmol) was added to the reaction mixture. The reaction was stirred at room temperature under Ar for 5 hour. After 5 hours, the reaction crude was washed with water (2×40 mL). The organic phase was collected and dried over anhydrous Na_2SO_4 and the solvent was removed *in vacuo*. The residue was purified by column chromatography (30% AcOEt/DCM) to give pure [2]rotaxane **5** as a white solid (72 mg, 27%).).

Conditions d (1:2:4 [**1**]:[**2b**]:[**4a**] molar ratios, and 8 mM): In a two necked round bottom flask (25 mL) macrocycle **1** (100 mg, 0.084 mmol), pyridine *N*-oxide **2b** (67.4 mg, 0.167 mmol), **4a** (258 mg, 0.334 mmol), TBTA (22 mg, 0.04 mmol) and the catalyst $Cu[(CH_3CN)_4PF_6]$ (16 mg, 0.04 mmol) were dissolved in dry DCM (10 mL). Finally, Hünig's base (0.1 ml, 0.7 mmol) was added to the reaction mixture. The reaction was stirred at room temperature under Ar for 5 hours. After 5 hours the reaction crude was washed with water (2×40 mL). The organic phase was collected and dried over anhydrous Na_2SO_4 and the solvent was removed *in vacuo*. The residue was purified by column chromatography (30% AcOEt/DCM) to give pure [2]rotaxane **5** as a white solid (130 mg, 50%).

^{1}H NMR (500 MHz, Chloroform-*d*) δ 8.73 (br, 8H, NHe,f), 8.20 (s, 1H, H2), 7.64 (s, 2H, H9), 7.54 (d, *J* = 8.5 Hz, 12H, H15), 7.49 (d, *J* = 8.5 Hz, 12H, H16), 7.44 (d, *J* = 8.5 Hz, 12H, H14), 7.29 (d, *J* = 8.5 Hz, 12H, H13), 7.24 (m, 4H, H12), 6.96 (br, 8H, Hb, Hd), 6.88 (m, 12H, H11, Ha, Hc), 5.93 (m, 16H, Hg-j), 4.97 (br, 4H, H10), 4.18 (m, 4H, H8), 3.6 (br, 4H, H4), 1.92 (m, 4H, H7), 1.75 (br, 16H, H5, Hk-l), 1.55 (br, 24H, Hm,n), 1.35 (s, 54H, H17). $^{13}C\{^1H\}$ NMR (125 MHz, Chloroform-*d*) δ 162.3, 156.2, 150.2, 149.6, 145.7, 143.9, 139.7, 139.3, 138.8, 138.4, 137.7, 135.9, 133.5, 132.3, 131.6, 131.4, 127.1, 126.6, 126.1, 125.9, 125.7, 123.9, 118.9, 113.4, 105.5, 102.9, 81.6, 74.2, 63.7, 61.3, 49.9, 45.4, 39.3, 34.8, 34.5, 31.5, 31.4, 29.8, 29.7, 28.8, 27.9, 22.9. IR νmax/cm^{-1}: 3344 (N-H, st), 2960 (C-H, st), 2867 (C-H, st), 1494(C=N, C=C, st), 814 (C=C, st), 767 (C-H, δ oop). HR-MS (ESI-TOF ES+) m/z calculated for $C_{217}H_{217}N_{17}O_5Na_2$ $([M+2Na])^{2+}$ 1593.3517, found $([M+2Na])^{2+}$ 1593.3474.

2.4.3 Experimental section: Figures

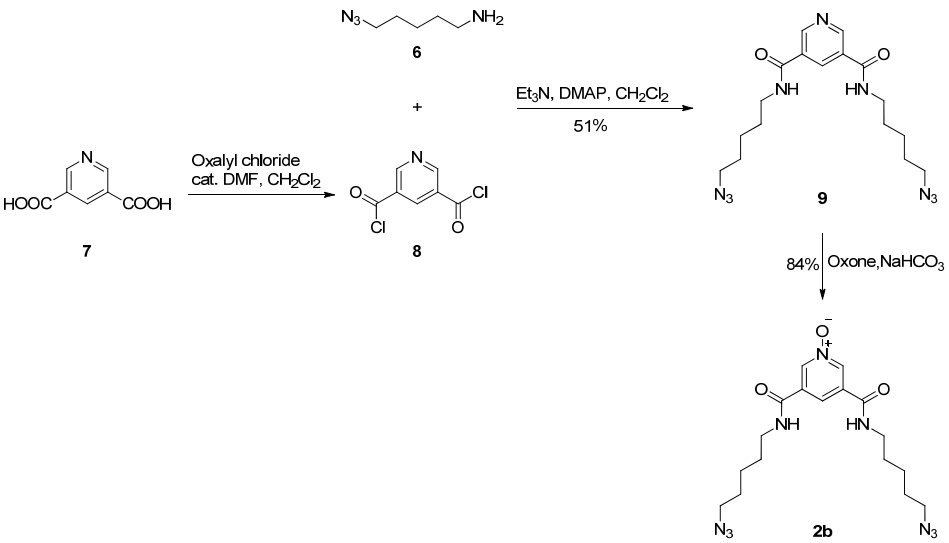

Scheme 2. 3. Synthetic scheme for the preparation of *N*-oxide (**2b**). 5-azidopentan-1-amine (**6**) was synthesized following a reported procedure.[29,30]

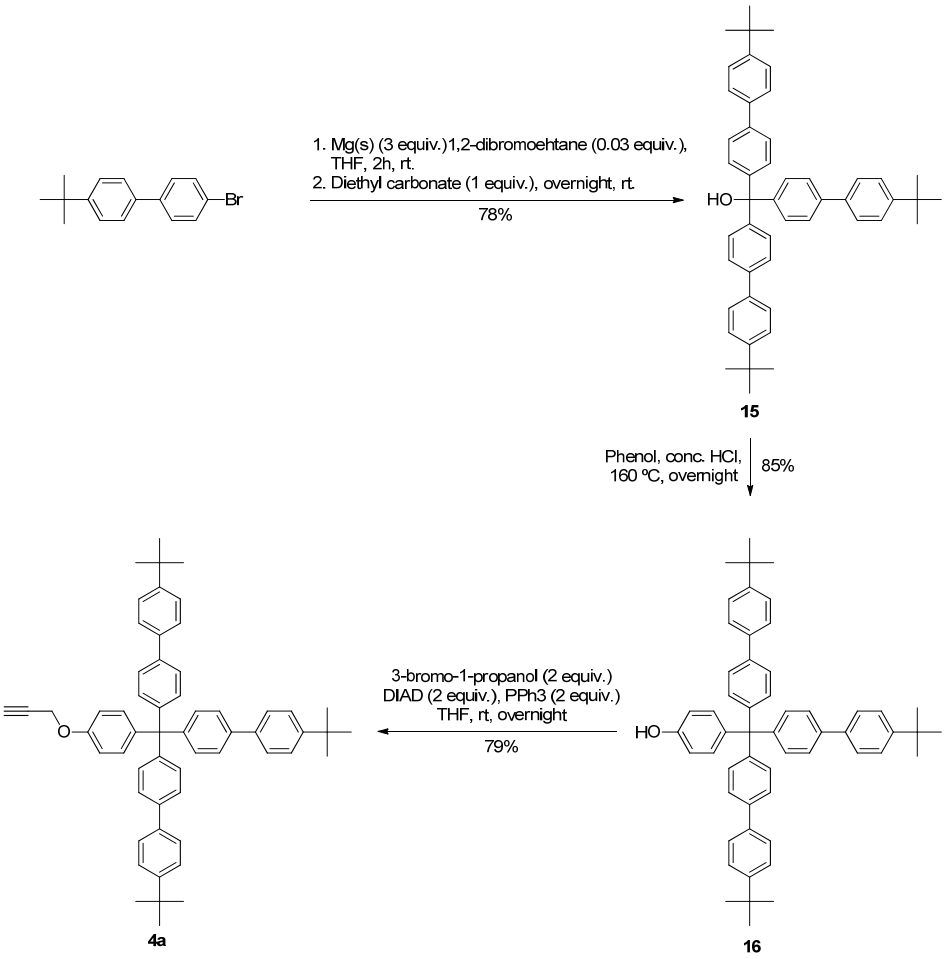

Scheme 2. 4. Schematic synthesis of large stopper **4a**.[22]

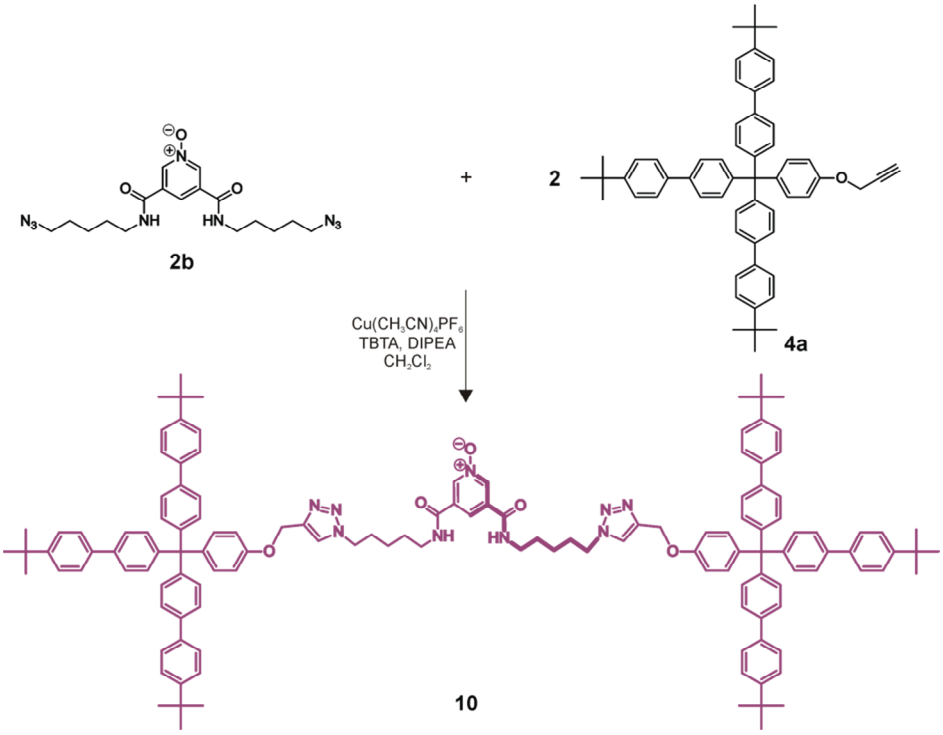

Scheme 2. 5. Synthetic scheme for the preparation of the linear component (**10**).

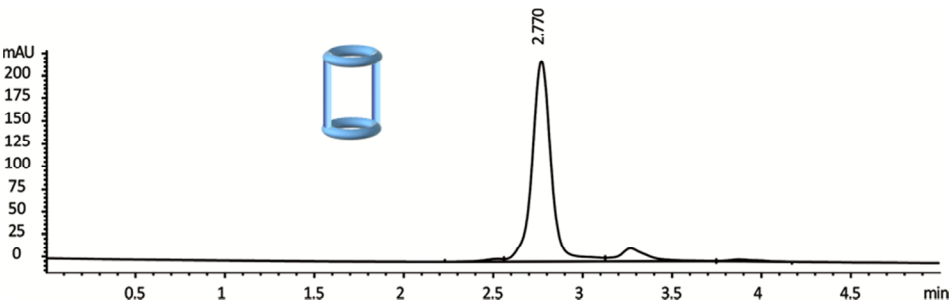

Figure 2. 9. HPLC trace of a 1 mM solution of pure macrocycle **1**.

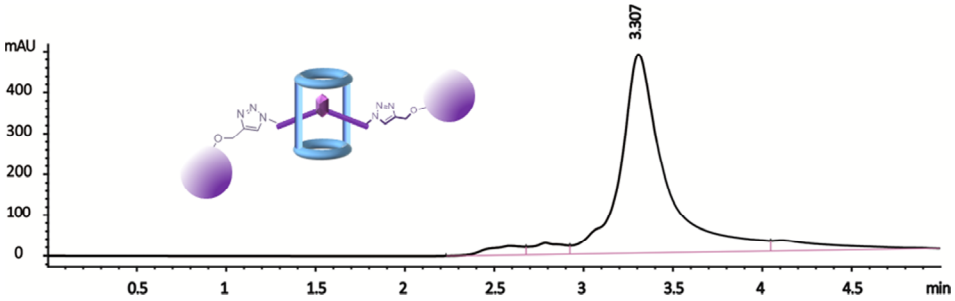

Figure 2. 10. HPLC trace of a 1 mM solution of pure [2]rotaxane **5**.

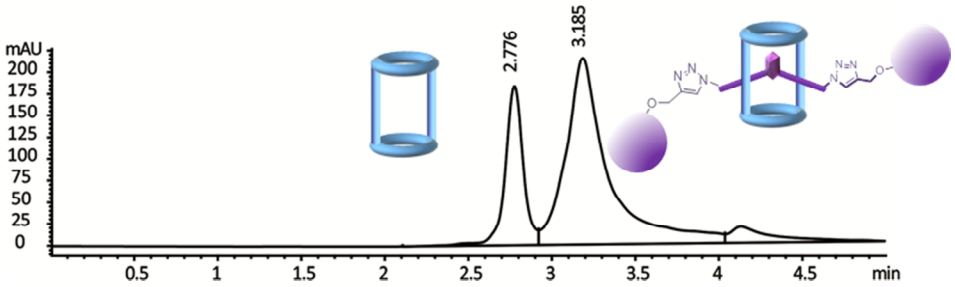

Figure 2. 11. HPLC trace of a 1 mM solution of an equimolar mixture [2]rotaxane **5** and macrocycle **1**.

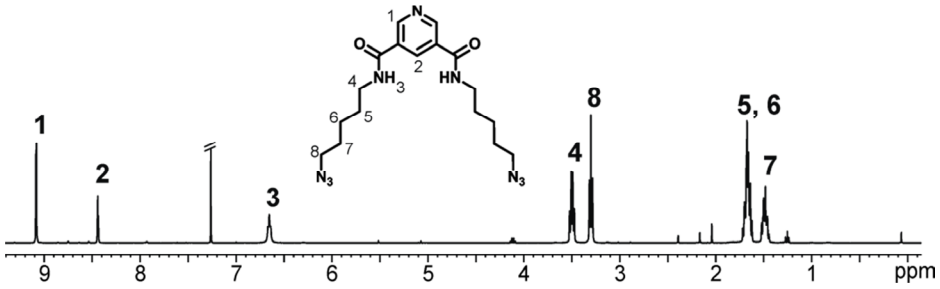

Figure 2. 12. ^{1}H NMR spectrum of **9** ($CDCl_3$, 400 MHz, 298 K) with the corresponding proton assignment.

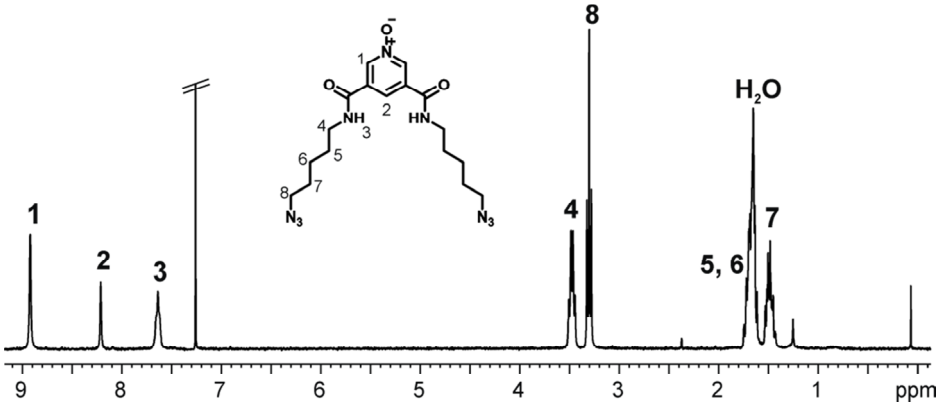

Figure 2. 13. ^{1}H NMR spectrum of N-oxide **2b** ($CDCl_3$, 400 MHz, 298 K) with the corresponding proton assignment.

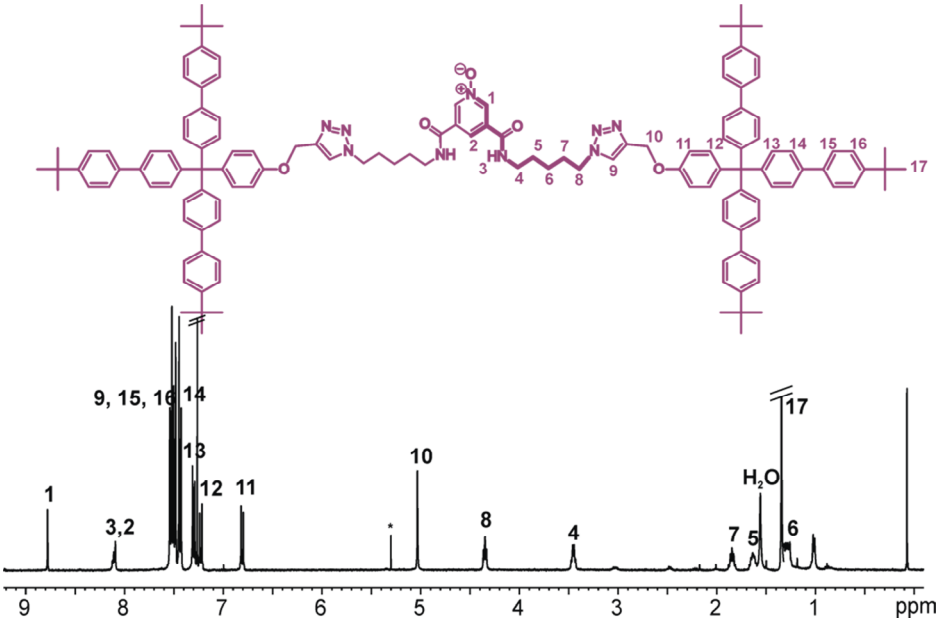

Figure 2. 14. ^{1}H NMR spectrum of linear component **10** ($CDCl_3$, 400 MHz, 298K) with the corresponding proton assignment.* solvent signal.

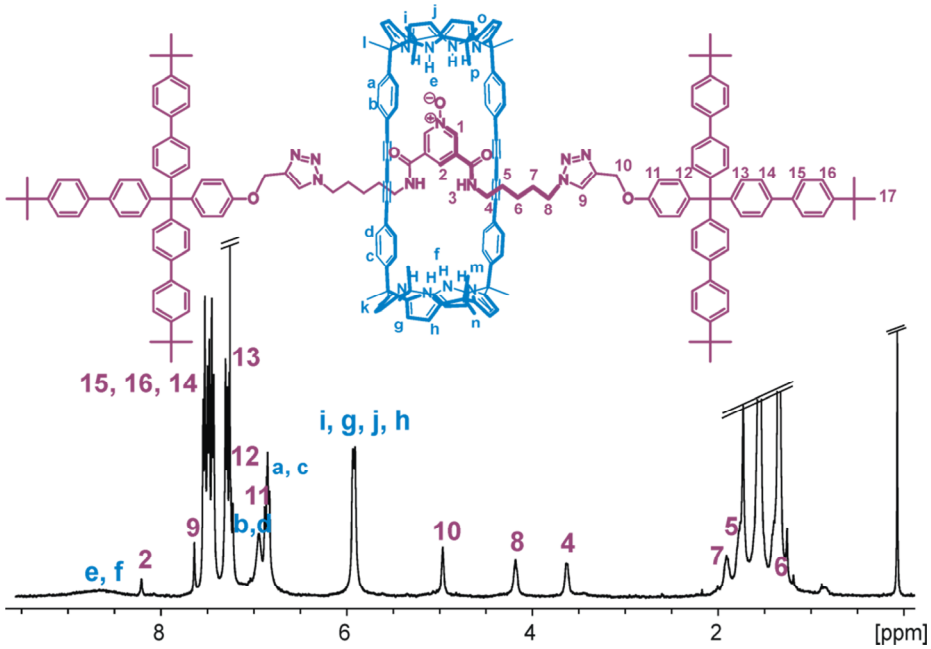

Figure 2. 15. ^{1}H NMR spectrum of a 1 mM solution of [2]rotaxane **5** ($CDCl_3$, 500 MHz, 298 K) with the corresponding proton assignment.

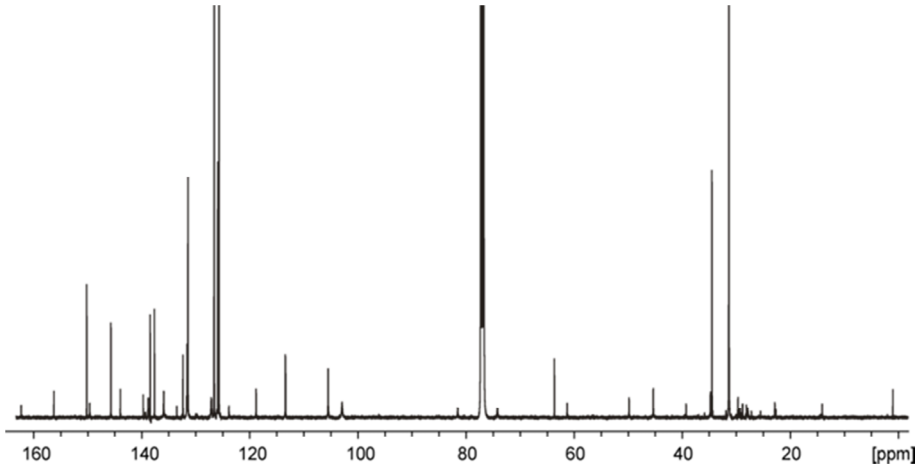

Figure 2. 16. $^{13}C\{^{1}H\}$ NMR spectrum (125 MHz with cryoprobe, $CDCl_3$, 298 K) of a 1 mM solution of [2]rotaxane 5.

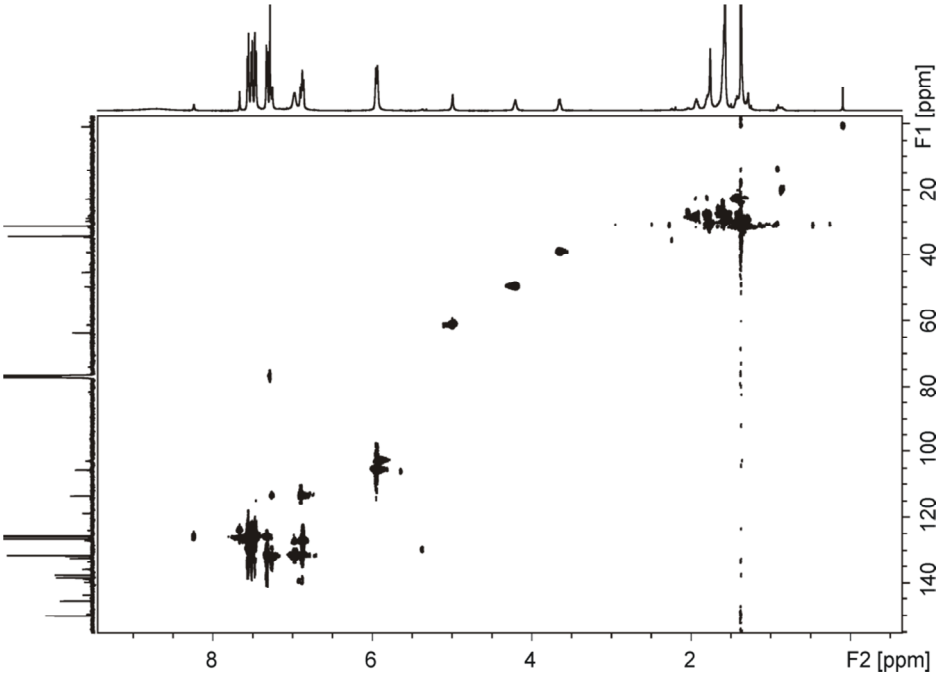

Figure 2. 17. ^{1}H-^{13}C HSQC spectrum (125 MHz with cryoprobe, $CDCl_3$, 298 K) of a 1 mM solution of [2]rotaxane **5**.

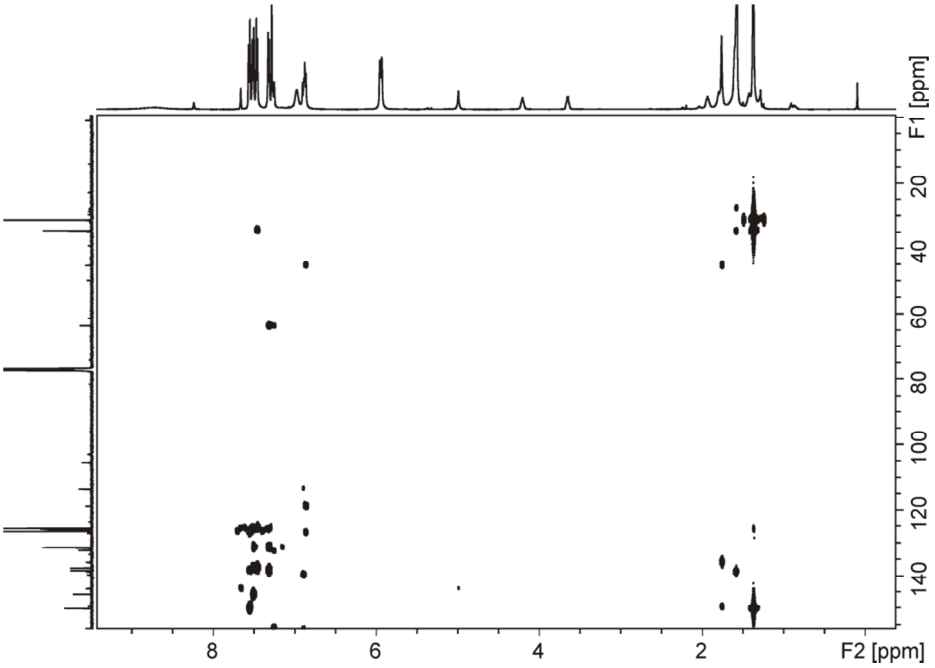

Figure 2. 18. ^{1}H-^{13}C HMBC spectrum (125 MHz with cryoprobe, $CDCl_3$, 298 K) of a 1 mM solution of [2]rotaxane **5**.

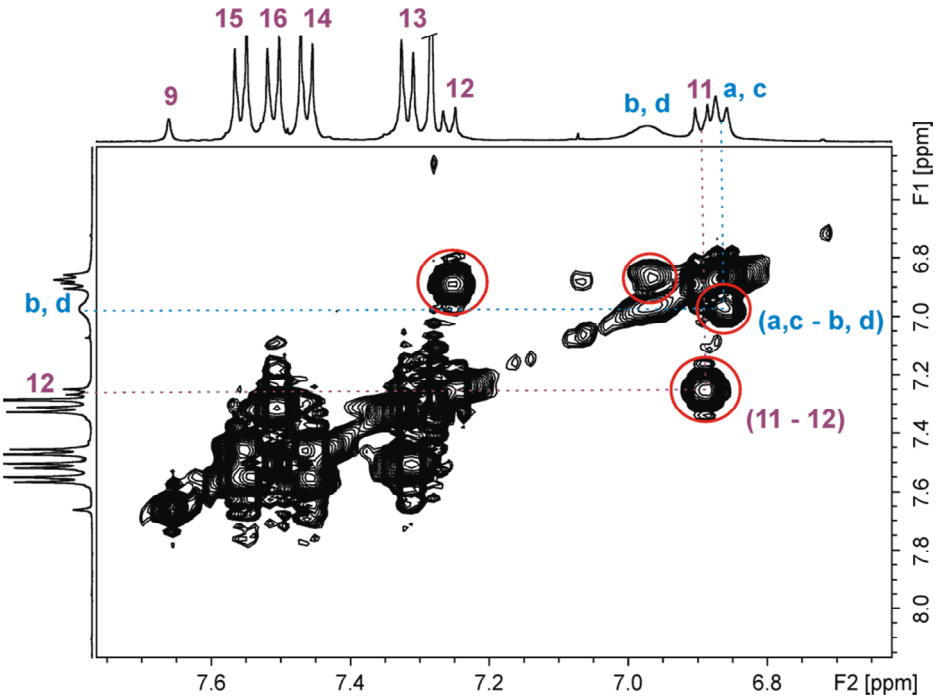

Figure 2. 19. Selected downfield region of the COSY experiment ($CDCl_3$, 500 MHz, 298 K) of a 1 mM solution of [2]rotaxane **5** showing the assignment of some relevant cross-peaks.

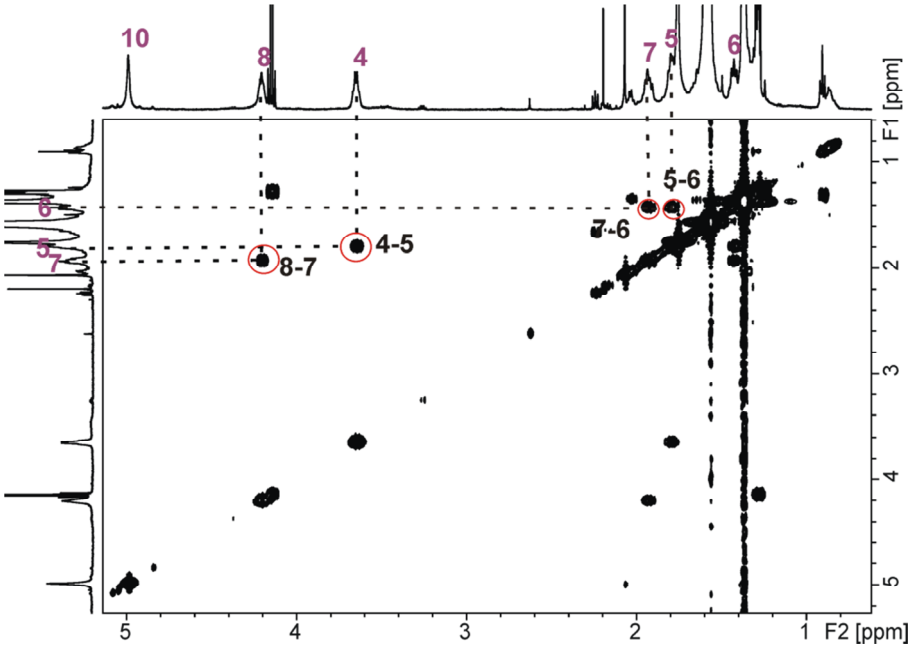

Figure 2. 20. Selected upfield region of the COSY experiment ($CDCl_3$, 500 MHz, 298 K) of a 1 mM solution of [2]rotaxane **5** showing the assignment of some relevant cross-peaks from the aliphatic chain of the linear component.

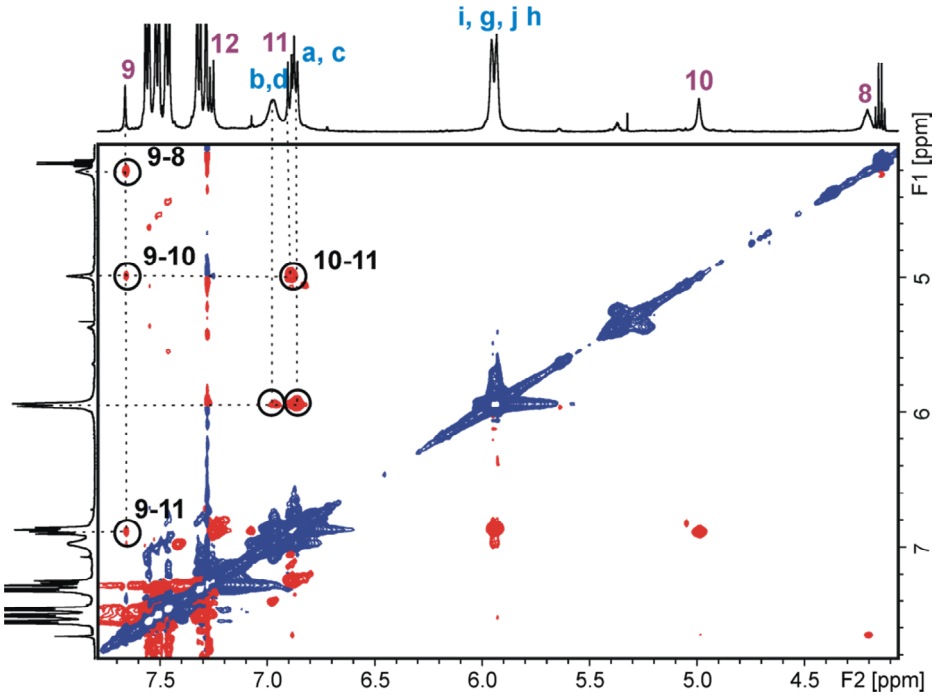

Figure 2. 21. Selected region of the ROESY experiment ($CDCl_3$, 500 MHz, 298 K) of a 1 mM solution of [2]rotaxane **5** showing the assignment of some relevant cross-peaks.

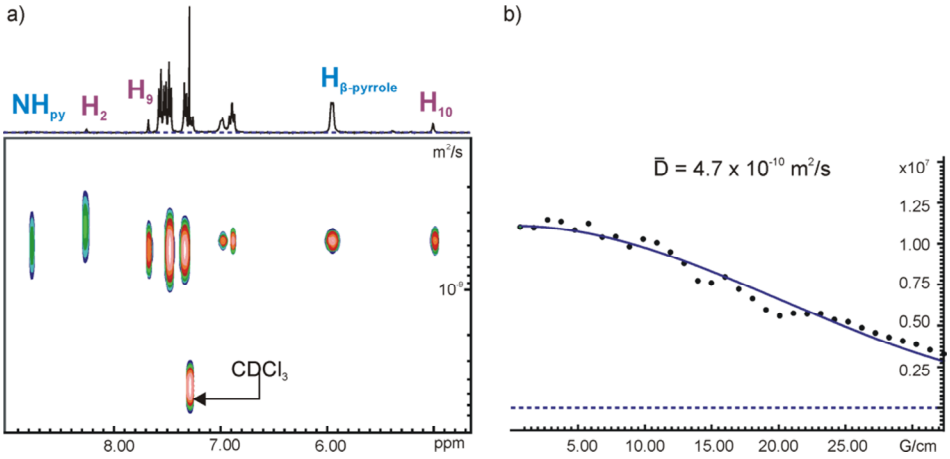

Figure 2. 22. ^1H pseudo-2D DOSY ($CDCl_3$, 500 MHz, 298 K) of a millimolar solution of [2]rotaxane **5** (a) and fit of the decay in the peak height at 4.99 ppm to a monoexponential function (b).

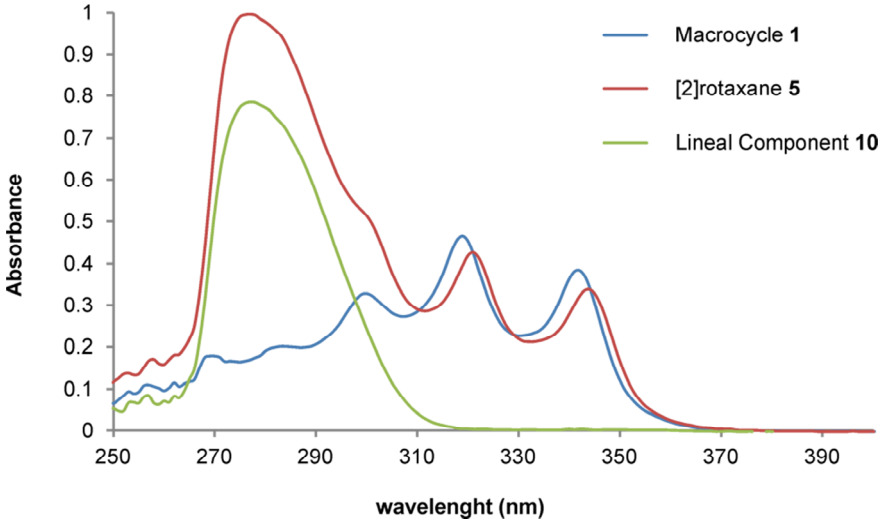

Figure 2. 23. UV-visible spectrum of a micromolar DCM solution of free macrocycle **1** (blue line), linear component **10** (green line) and [2]rotaxane **5** (red line).

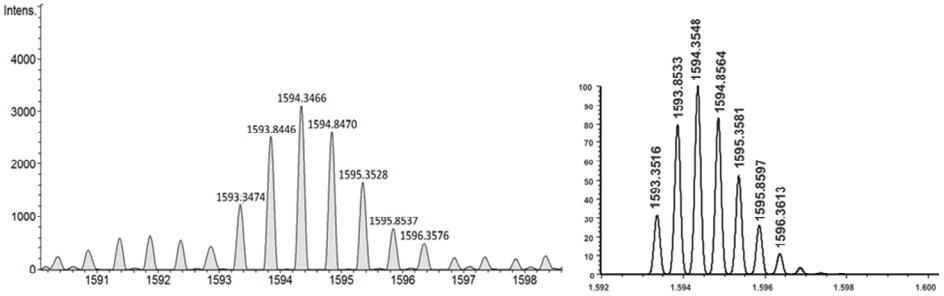

Figure 2. 24. Experimental (left) and theoretical (right) isotopic pattern of HR-MS spectrum of [2]rotaxane **5**.

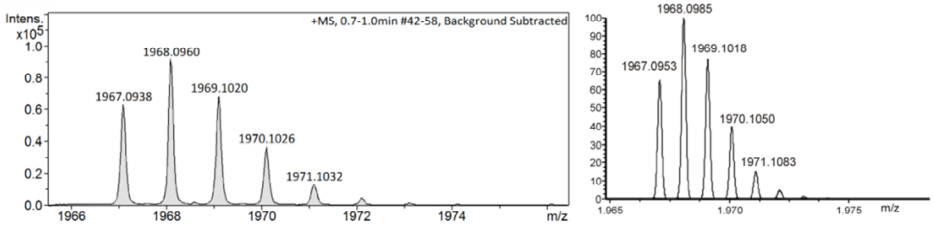

Figure 2. 25. Experimental (left) and theoretical (right) isotopic pattern of HR-MS spectrum of: linear component **10**.

2.5 References and notes

[1] Busschaert, N.; Caltagirone, C.; Van Rossom, W.; Gale, P. A., *Chem. Rev. (Washington, DC, U. S.)* **2015,** *115* (15), 8038-8155.
[2] Bregovic, V. B.; Basaric, N.; Mlinaric-Majerski, K., *Coord. Chem. Rev.* **2015,** *295*, 80-124.
[3] Gale, P. A.; Busschaert, N.; Haynes, C. J. E.; Karagiannidis, L. E.; Kirby, I. L., *Chem. Soc. Rev.* **2014,** *43* (1), 205-241.
[4] Caballero, A.; Zapata, F.; Beer, P. D., *Coord. Chem. Rev.* **2013,** *257* (17–18), 2434-2455.
[5] Xue, M.; Yang, Y.; Chi, X.; Yan, X.; Huang, F., *Chem. Rev. (Washington, DC, U. S.)* **2015,** *115* (15), 7398-7501.
[6] Langton, M. J.; Serpell, C. J.; Beer, P. D., *Angew. Chem., Int. Ed.* **2016,** *55* (6), 1974-1987.
[7] Hubner, G. M.; Glaser, J.; Seel, C.; Vogtle, F., *Angew. Chem., Int. Ed.* **1999,** *38* (3), 383-386.
[8] Vickers, M. S.; Beer, P. D., *Chem. Soc. Rev.* **2007,** *36* (2), 211-225.
[9] Beer, P. D.; Sambrook, M. R.; Curiel, D., *Chem. Commun.* **2006,** (20), 2105-2117.
[10] Chae, M. K.; Suk, J.-m.; Jeong, K.-S., *Tetrahedron Lett.* **2010,** *51* (32), 4240-4242.
[11] Brown, A.; Beer, P. D., *Dalton Trans.* **2012,** *41* (1), 118-129.
[12] Rezanka, M.; Langton, M. J.; Beer, P. D., *Chem. Commun.* **2015,** *51* (21), 4499-4502.
[13] Lankshear, M. D.; Evans, N. H.; Bayly, S. R.; Beer, P. D., *Chem. Eur. J.* **2007,** *13* (14), 3861-3870.
[14] Valderrey, V.; Escudero-Adán, E. C.; Ballester, P., *J. Am. Chem. Soc.* **2012,** *134* (26), 10733-10736.
[15] For other examples of [2]rotaxanes and pseudorotaxanes that use pyridine-N-oxide motifs in the axle component see: a) Knighton, R. C.; Beer, P. D., *Chem. Commun.* **2014,** *50* (13), 1540-1542. b) Hancock, L. M.; Beer, P. D., *Chem. Commun.* **2011,** *47* (21), 6012-6014. c) Chen, M. J.; Han, S. J.; Jiang, L. S.; Zhou, S. G.; Jiang, F.; Xu, Z. K.; Liang, J. D.; Zhang, S. H., *Chem. Commun.* **2010,** *46* (22), 3932-3934. d) Zapata, F.; Blackburn, O. A.; Langton, M. J.; Faulkner, S.; Beer, P. D., *Chem. Commun.* **2013,** *49* (74), 8157-8159.
[16] Mercurio, J. M.; Tyrrell, F.; Cookson, J.; Beer, P. D., *Chem. Commun.* **2013,** *49* (92), 10793-10795.
[17] Hanni, K. D.; Leigh, D. A., *Chem. Soc. Rev.* **2010,** *39* (4), 1240-1251.
[18] Lim, J. Y. C.; Cunningham, M. J.; Davis, J. J.; Beer, P. D., *Dalton Trans.* **2014,** *43* (46), 17274-17282.
[19] Ke, C.; Smaldone, R. A.; Kikuchi, T.; Li, H.; Davis, A. P.; Stoddart, J. F., *Angew. Chem., Int. Ed.* **2013,** *52* (1), 381-387.
[20] Miljanić, O. Š.; Dichtel, W. R.; Aprahamian, I.; Rohde, R. D.; Agnew, H. D.; Heath, J. R.; Fraser Stoddart, J., *QSAR Comb. Sci.* **2007,** *26* (11-12), 1165-1174.
[21] Aucagne, V.; Berná, J.; Crowley, J. D.; Goldup, S. M.; Hänni, K. D.; Leigh, D. A.; Lusby, P. J.; Ronaldson, V. E.; Slawin, A. M. Z.; Viterisi, A.; Walker, D. B., *J. Am. Chem. Soc.* **2007,** *129* (39), 11950-11963.
[22] Clever, G. H.; Shionoya, M., *Chem. Eur. J.* **2010,** *16* (39), 11792-11796.
[23] Lal, S.; Diez-Gonzalez, S., *J. Org. Chem.* **2011,** *76* (7), 2367-2373.
[24] Moorman, R. M.; Collier, M. B.; Frohock, B. H.; Womble, M. D.; Chalker, J. M., *Org. Biomol. Chem.* **2015,** *13* (7), 1974-1978.
[25] Rodionov, V. O.; Presolski, S. I.; Diaz, D. D.; Fokin, V. V.; Finn, M. G., *J. Am. Chem. Soc.* **2007,** *129* (42), 12705-12712.
[26] Successive water washes did not allow the extraction of the salt from the host cavity.
[27] Column chromatography performed on an equimolar mixture of rotaxane **5** and ion-pair OCNTBA **3a** using a 3:7 mixture of AcOEt:CH_2Cl_2 as eluent, did not allow the isolation of the pure free rotaxane but mixtures of rotaxane with different amounts of the ion-pair.
[28] Careful attention should be taken in the handling and storage of diazide **6** owing to its rather low molecular weight.

[29] Wang, H.; Zhu, Y. J.; Ren, X. N.; Zhang, H.; Tan, Y. B., *Colloid Polym. Sci.* **2012,** *290* (11), 1065-1075.
[30] Thomas, J. R.; Liu, X. J.; Hergenrother, P. J., *J. Am. Chem. Soc.* **2005,** *127* (36), 12434-12435.

Chapter 3

Binding Studies of [2]rotaxane 5 with ion-pairs

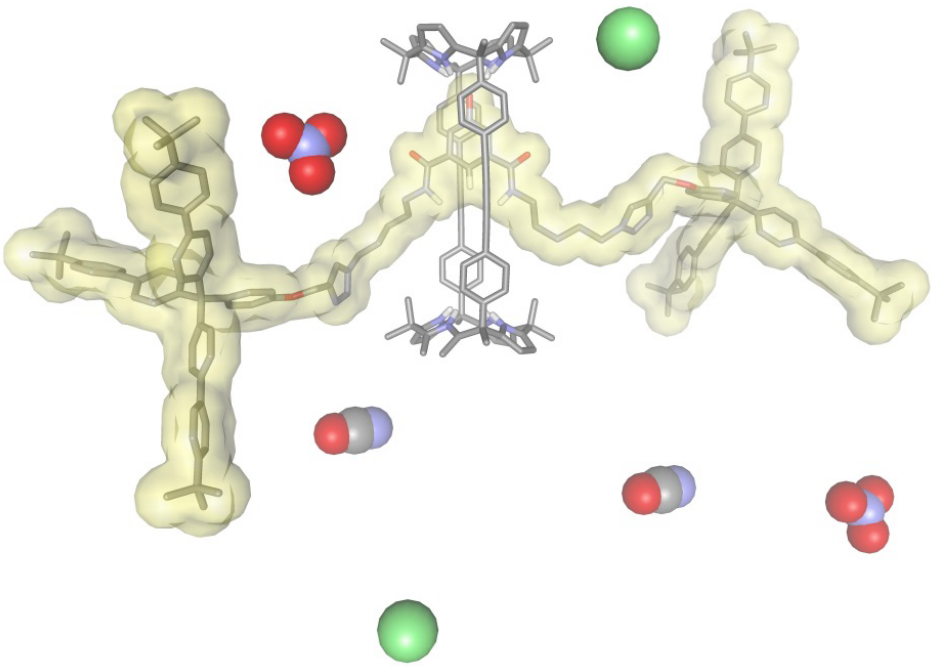

Part of this chapter has been published in:

Romero, J. R.; Aragay, G.; Ballester, P., *Chem. Sci.* **2017,** *8* (1), 491-498.

UNIVERSITAT ROVIRA I VIRGILI
INTERLOCKED ARCHITECTURES BASED ON A BIS-CALIX[4]PYRROLE MACROCYCLE FOR ION-PAIR RECOGNITION
Jose Ramon Romero Lopez

3.1 Introduction

The design and synthesis of receptors capable of recognizing ion-pairs (heteroditopic receptors)[1] instead of hosts able to bind either an anion or a cation has attracted increasing interest in the last years since they exhibit improved properties in terms of selectivity and sensitivity.[2] The nature of these enhanced binding properties is not easy to address. Cooperative interactions exerted between the co-bound ions and cooperative allosteric effects are known to contribute to this improvement. Moreover, the binding of the counter-ion of the targeted ion is also known to reduce interferences arising from ion-pairing and solvation effects.[3]

In this area, the use of interlocked molecules as ion-pair receptors is still a poorly explored field. This is surprising given the unique three-dimensional topological interlocked cavity design that they possess featuring superior binding properties in comparison to their non-interlocked counterparts.[4] Thus, rotaxanes and catenanes are ideal candidates for the development of ion-pair receptors able to operate in competitive media such as aqueous media.[5]

In this chapter we describe the binding properties of rotaxane **5** with a series of tetraalkylammonium salts containing hydrogen-bonding anions such as chloride, nitrate and cyanate, by means of ^{1}H NMR spectroscopy and Isothermal Titrations Calorimetry (ITC) experiments. We probed the interaction in two different solvents chloroform, a non-polar non-protic solvent, and acetone, a polar non-protic solvent. The influence of the anion's size and shape (monoatomic anion such as chloride or polyatomic anions such as cyanate or nitrate), as well as the nature of the ammonium cation (tetraalkyl or methyltrialkyl) on the binding affinity for receptor **5** were also investigated.

3.2 Results and discussion

3.2.1 Binding studies in chloroform

The interaction of [2]rotaxane **5** with several ion-pairs in $CDCl_3$ solution was probed by means of ^1H NMR titration experiments. The titration experiments were performed in a 5 mm NMR tube by adding incremental amounts of guests (**3a-d**) to a millimolar solution of the host in $CDCl_3$. The concentration of the host was maintained constant throughout the titration.

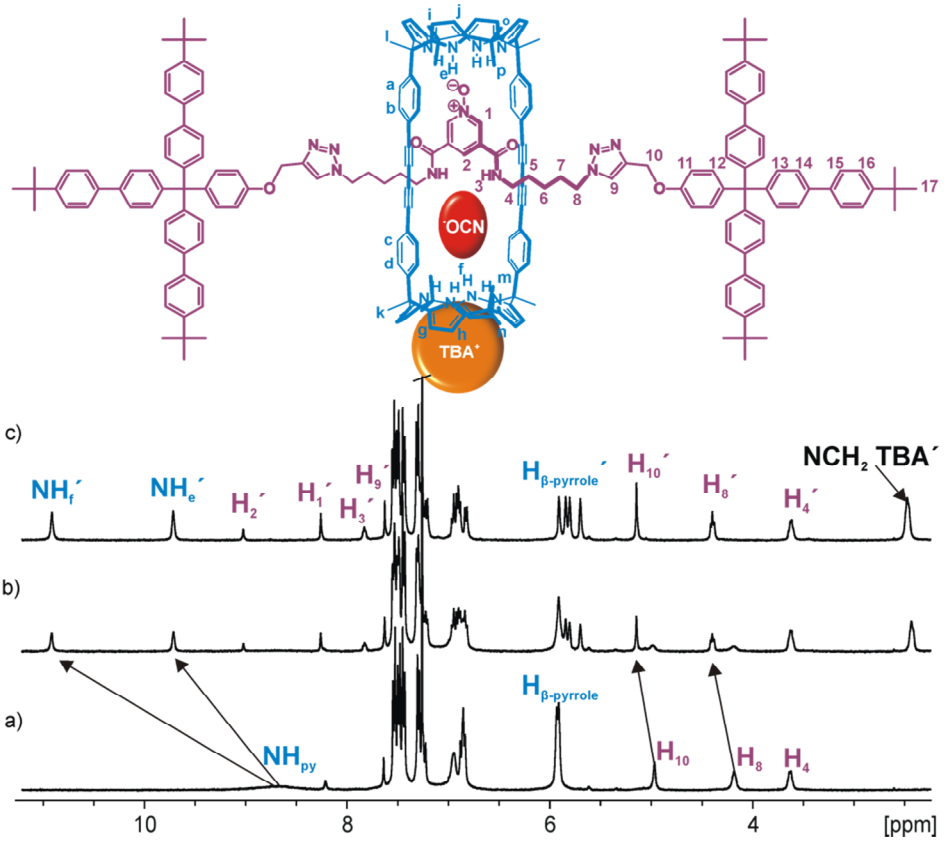

Figure 3. 1. (Top) Molecular structure of the **3a⊂5** complex. The [2]rotaxane **5** includes a hydrogen-bonded cyanate anion in the polar and cylindrical cavity defined by its threaded structure and binds the TBA cation in the shallow aromatic cavity opposite to the anion and defined by the calix[4]pyrrole in cone conformation. (Bottom) Selected regions of the ^1H NMR spectra acquired during the titration of free [2]rotaxane **5** (a) in $CDCl_3$ with incremental amounts of **3a**: 0.5 equiv. (b) and 1 equiv. (c). Primed numbers and letters indicate the proton signals in the complex, blue color for macrocycle component, purple color for linear component.

Addition of 0.5 equiv. of OCNTBA **3a** to a millimolar $CDCl_3$ solution of **5** (Figure 3. 1b) produced the observation of separate signals for the hydrogen atoms in the bound and free rotaxane indicating that the binding equilibrium was slow on the ^1H NMR timescale. When 1 equiv. of OCNTBA **3a** was added (Figure 3. 1c), only the signals corresponding to the protons in the bound rotaxane were detected. This observation supported the formation of a complex with 1:1 stoichiometry and an association constant larger than 10^4 M^{-1}. In the 1:1 complex, all the proton signals related to **5** were sharp and well-defined suggesting that the putative pirouetting process of the axle component within the macrocycle was slow on the chemical shift timescale. The slow dynamics of this process was also evidenced by the observation of two separate and highly downfield shifted proton signals corresponding to the pyrrole NHs of **1**. This observation was in agreement with their involvement in hydrogen bonding interactions with two different acceptor moieties (i.e. one hemisphere binds the *N*-oxide unit of the axle and the other binds the cyanate anion). The β-pyrrole protons resonated as two sets of two signals in the range of 5.9 to 5.7 ppm. This finding also supported the existence of two chemically non-equivalent hemispheres in the resulting 1:1 complex. The amide NH protons (H_3') of the linear component in the 1:1 complex appeared as a singlet at δ = 7.8 ppm. Finally, in the initial stage of the titration, the signal for the methylene protons alpha to the nitrogen atom of the TBA cation experienced an upfield shift with respect to the cation in the free OCNTBA salt, **3a**. However, the incremental addition of **3a** produced a gradual downfield shift of this signal, which became more evident when more than 1 equiv. of the salt was added. These observations supported the binding of the TBA cation in the electron-rich and shallow aromatic cavity opposed to the bound cyanate and defined by the calix[4]pyrrole core in cone conformation. In short, [2]rotaxane **5** acted as a heteroditopic receptor for the recognition of OCNTBA in $CDCl_3$ solution and the resulting 1:1 complex displayed a host-separated ion-pair binding geometry. Remarkably, the inspection of different exchange dynamics on the chemical shift timescale between free and bound **5** (slow) and between free and bound TBA cation (fast) was indicative of two dissimilar exchange mechanisms. Because the anion is included and hydrogen bonded in the polar cavity defined by the interlocked structure, the exchange between free and bound host requires the cleavage of multiple

hydrogen bonds and a conformational reorganization. Both processes are typically associated with energetically demanding transition states. Conversely, the exchange between the free and bound TBA cation can occur without such strict energetic requirements owing to the exposed nature of its binding mode.

A ^{1}H-^{1}H ROESY experiment performed on a millimolar $CDCl_3$ solution containing the quantitatively formed **3a⊂5** complex revealed the presence of cross-peaks due to through-space proximity between the H_1 *ortho*-protons of the pyridyl-*N*-oxide unit in the linear axle and the calix[4]pyrrole NHs, H_e, of the cyclic component hemisphere that are hydrogen bonded (Figure 3. 2 a).

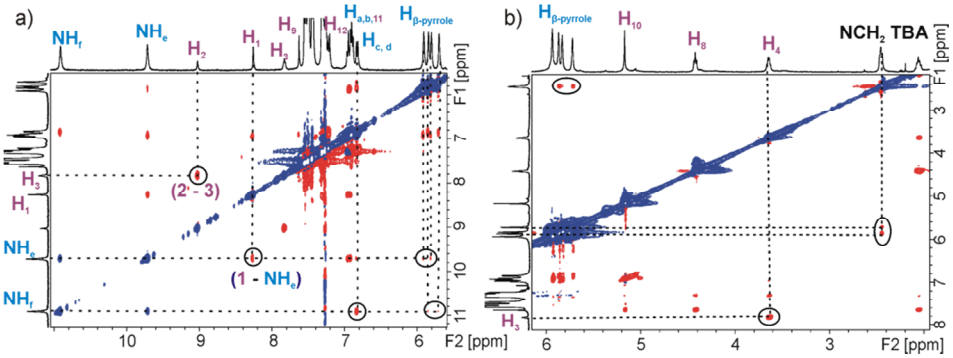

Figure 3. 2. Selected regions of the ROESY experiment ($CDCl_3$, 500 MHz, 298 K, mixing time=0.3 s, power level=120 dB) of a millimolar solution of an equimolar mixture of [2]rotaxane **5** and tetrabutylammonium cyanate (**3a**). Some relevant cross-peaks have been highlighted.

Other cross peaks due to through-space proximity were observed between the calix[4]pyrrole β-protons of the cyclic component's hemisphere, to which the cyanate is hydrogen bonded, and the methylene protons alpha to the N atom of the TBA cation (NCH_2 TBA', Figure 3. 2 b). This observation is in complete agreement with the macrocycle-separated binding mode assigned to OCNTBA **3a** in the **3a⊂5** ion-paired complex. Altogether, the above ROESY spectroscopic observations provided additional support to the interlocked nature and binding mode assigned to the **3a⊂5** complex.

The results of a DOSY experiment allowed us to assign very similar diffusion constants for the signals of the bound receptor **5** and the ones corresponding to the bound TBA cation (Figure 3. 3). This result also supported the formation of the ion-paired **3a⊂5** complex in $CDCl_3$ solution. We determined the diffusion constant for **3a⊂5** complex as 4.0×10^{-10} m^2/s. This value is slightly smaller than the one reported in Chapter 2 for the

free [2]rotaxane **5** (4.7×10^{-10} m^2/s) and it's in agreement with the gain in hydrodynamic radii for the **3a⊂5** complex produced by the peripheral complexation of the TBA cation.

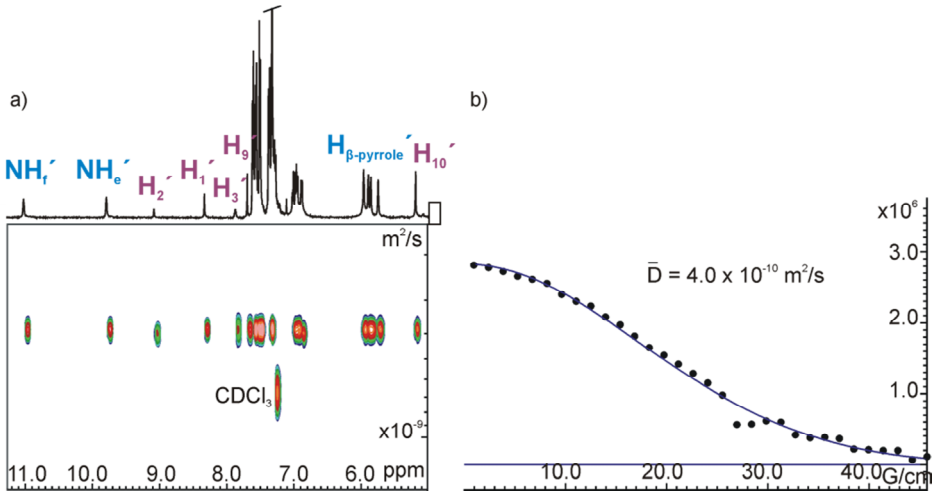

Figure 3. 3. ^{1}H pseudo-2D DOSY ($CDCl_3$, 500 MHz, 298 K) of a millimolar solution of an equimolar mixture of **3a** and [2]rotaxane **5** (a) and fit of the decay in the peak height at 5.17 ppm to a monoexponential function (b).

We also performed ^{1}H NMR titration experiments with **3b** (NO_3TBA) (Figure 3. 4). The spectroscopic changes observed in the ^{1}H NMR titration were similar to those already described for **3a**. In the case of the nitrate anion, at 298 K the chemical exchange between the free and bound [2]rotaxane **5** was intermediate on the chemical shift timescale producing broad bands for some of its proton signals. At low temperature (263 K) an equimolar mixture of **5** and NO_3TBA **3b** produced a single set of sharp proton signals that were indicative for the quantitative formation of the **3b⊂5** complex (Figure 3. 5).

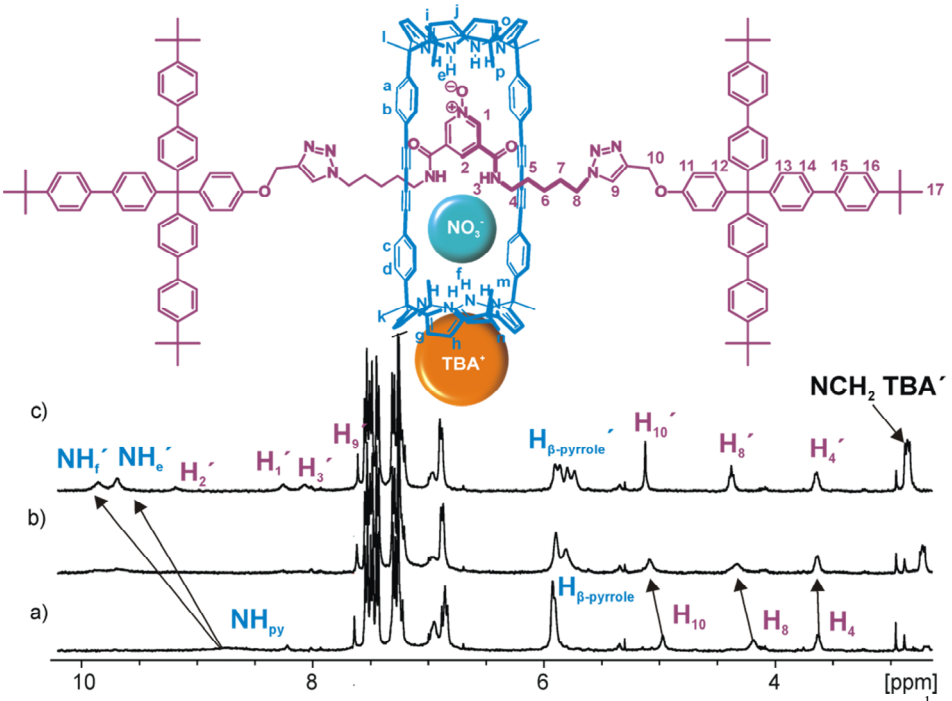

Figure 3. 4. (Top) Molecular structure of the **3b⊂5** complex. (Bottom) Selected region of the ^{1}H NMR spectra acquired during the titration ($CDCl_3$, 400 MHz, 298 K) of a millimolar solution of [2]rotaxane **5** with successive additions of tetrabutylammonium nitrate (**3b**). Free rotaxane a) 0.5 equiv. b) 1 equiv. c)

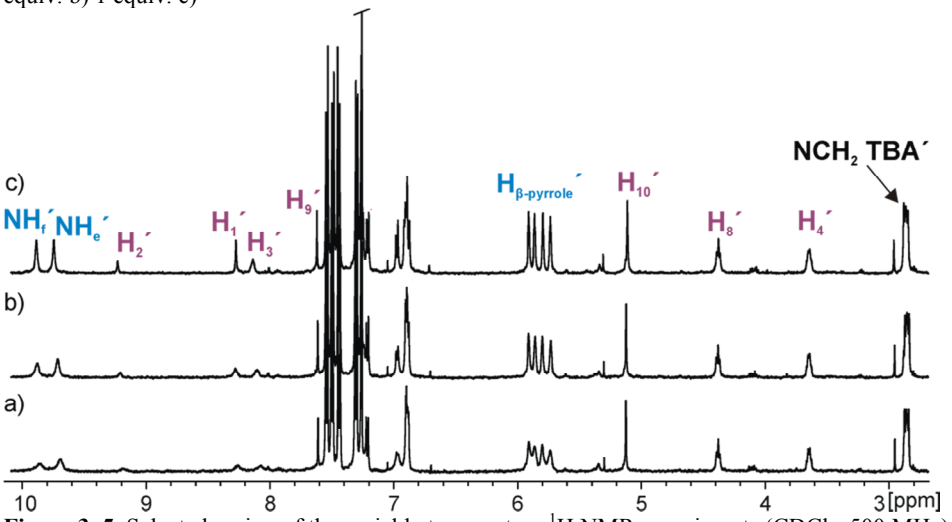

Figure 3. 5. Selected region of the variable temperature ^{1}H NMR experiments ($CDCl_3$, 500 MHz) performed on an equimolar mixture of [2]rotaxane and tetrabutylammonium nitrate (**3b**) at 298 K a) 288 K b) 263 K c).

A ^{1}H-^{1}H ROESY experiment performed on a millimolar $CDCl_3$ solution containing the quantitatively formed **3b⊂5** complex at 263 K revealed the presence of cross-peaks due to through-space proximity between the H_1 *ortho*-protons of the pyridyl-*N*-oxide unit in the linear axle and the calix[4]pyrrole NHs, H_e, of the cyclic component hemisphere that are hydrogen bonded (Figure 3. 6). Other cross peaks due to through-space proximity were observed for aromatics phenyl protons from the macrocycle and H_1 proton as reported previously in the case of the cyanate anion.

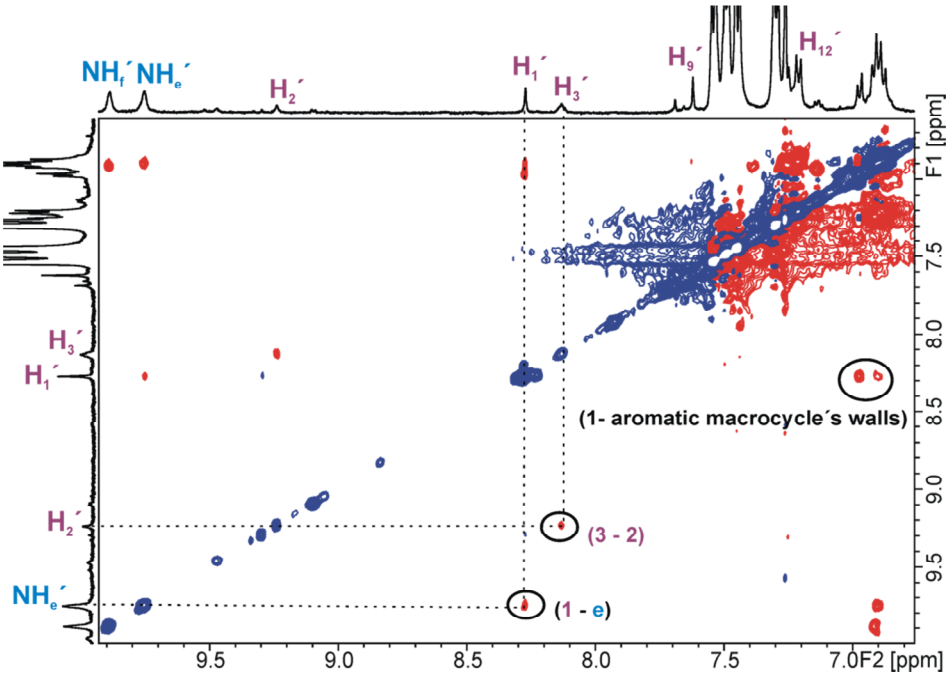

Figure 3. 6. Selected region of the ROESY experiment ($CDCl_3$, 500 MHz, 263 K, mixing time=0.4 s, power level=24.74 dB) performed on an equimolar mixture of [2]rotaxane and tetrabutylammonium nitrate (**3b**) at 263 K showing the most relevant close contact peaks.

The addition of **3c** (ClTBA) to a chloroform solution of [2]rotaxane **5** gave similar results to the ones obtained for the ion-pairs of polyatomic anions (Figure 3. 7). It is worth noting that the addition of incremental amounts of **3c** provoked a greater broadening of the rotaxane proton signals in comparison to the ones observed in the ^{1}H NMR titrations with previous anions **3a-3b**. This observation indicates that in the case of the chloride anion the equilibrium between bound and free host is intermediate in the NMR timescale. On the other hand, the observed gradual downfield shift of the proton

signal corresponding to the CH_2 alpha to the nitrogen of the tetrabutylammonium cation indicated that the cation is in fast exchange between the free and bound species in the chemical shift timescale.

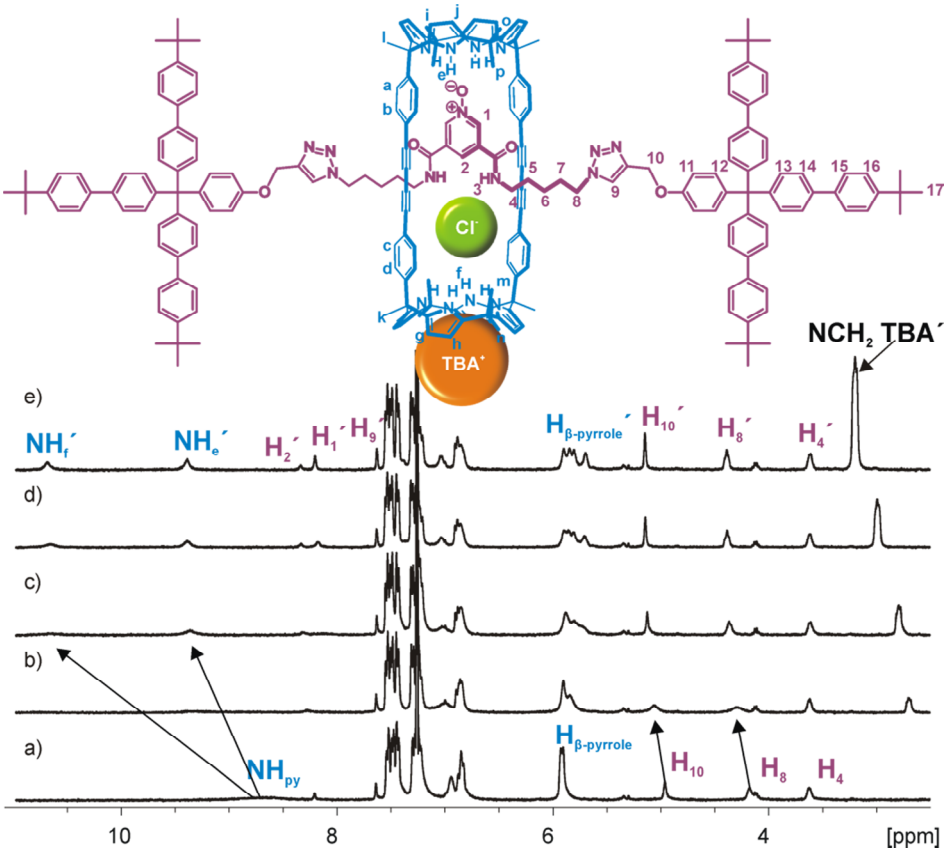

Figure 3. 7. (Top) Molecular structure of the **3c⊂5** complex. (Bottom) Selected region of the ^{1}H NMR spectra acquired during the titration ($CDCl_3$, 400 MHz, 298 K) of a millimolar solution of [2]rotaxane **5** with successive additions of tetrabutylammonium chloride (**3c**). Free rotaxane a) 0.5 equiv. b) 1 equiv. c) 1.7 equiv. d) 3.7 equiv. e).

The accurate determination of the binding constant values for the ion-paired interlocked complexes **3⊂5** was undertaken using isothermal titration calorimetry (ITC) experiments. We performed the titration experiments at 298 K by the incremental addition of a chloroform solution containing the ion-pair (**3a-c**) to a solution of the rotaxane **5** in the same solvent. We observed a regular heat release upon salt addition that was caused by the exothermicity of the binding process. All ITC experiments

showed good fits to the theoretical binding isotherm for the formation of a 1:1 complex (Figure 3. 8).[6]

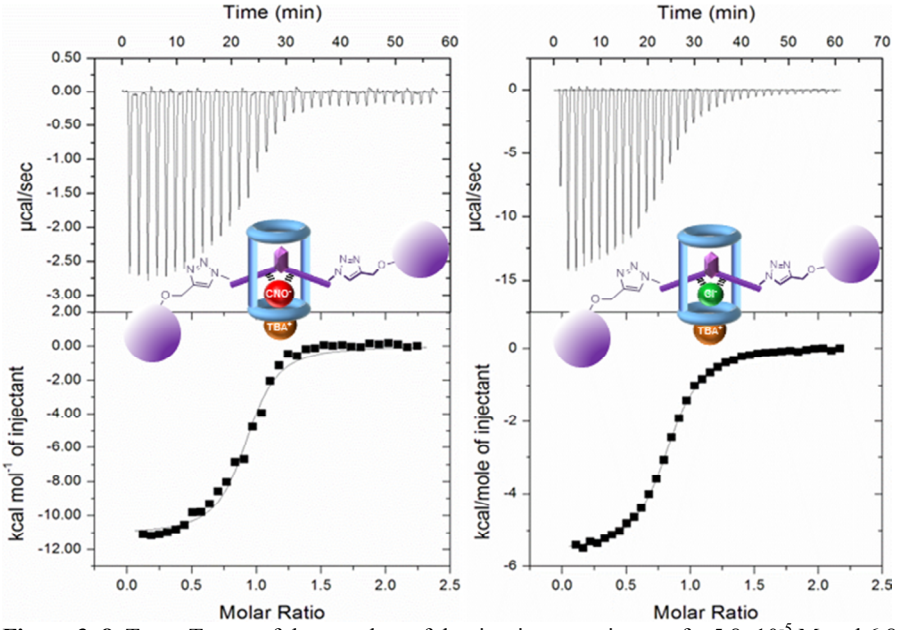

Figure 3. 8. Top – Traces of the raw data of the titration experiment of a 5.8×10^{-5} M and 6.8×10^{-4} M solution respectively, of rotaxane **5** with the tetrabutylammonium salts (OCNTBA **3a**, 0.68×10^{-3} M (left) and ClTBA **3c**, 6.4×10^{-3} M (right)) in $CHCl_3$. Bottom – Binding isotherms of the calorimetric titration shown on top. To determine the values of the thermodynamic variables the ITC data was fitted to a 1:1 binding model (black line).

The obtained results demonstrated the high selectivity exhibited by [2]rotaxane **5** in the complexation of the cyanate tetrabutylammonium salt **3a** in front of the nitrate **3b** or chloride **3c** tetrabutylammonium counterparts (i.e. $K_{\mathbf{3a}\subset\mathbf{5}}$ is almost 20-fold larger than $K_{\mathbf{3b}\subset\mathbf{5}}$ and $K_{\mathbf{3c}\subset\mathbf{5}}$), see Table 3. 1. Most likely, the observed differences derived from the better shape and size complementarity that existed between the cyanate anion and the polar three-dimensional cylindrical cavity contained in the [2]rotaxane topology of the heteroditopic receptor **5**. Indeed, simple molecular modelling studies showed that the binding pocket of **5**, featuring six convergent hydrogen-bond donors, is highly complementary in shape and size to the cyanate anion (Figure 3. 9). The smaller and

Table 3. 1. Association constant values (M^{-1}), free energies of complexation (ΔG, kcal mol^{-1}) and values for the enthalpic (ΔH, kcal mol^{-1}) and entropic components ($T\Delta S$, kcal mol^{-1}, 298 K) for the complexes formed between [2]rotaxane **5** and the different ammonium salts **3a-d** determined in chloroform solution using ITC experiments.

	$K_a \times 10^{-5}$	ΔG	ΔH	$T\Delta S$
3a	7.9±0.2	-8.0±0.02	-11.7±1.7	-3.7±1.7
3b	0.4±0.1	-6.3±0.1	-10.7±2.1	-4.4±2.1
3c	0.5±0.2	-6.4±0.2	-6.3±0.4	0.1±0.4
3d	158±16	-9.8±0.06	-9.6±0.3	0.2±0.3

spherical chloride anion and the trigonal and planar nitrate are considerably worst fits to the cylindrical internal cavity of **5** equipped with six hydrogen bond donor sites.

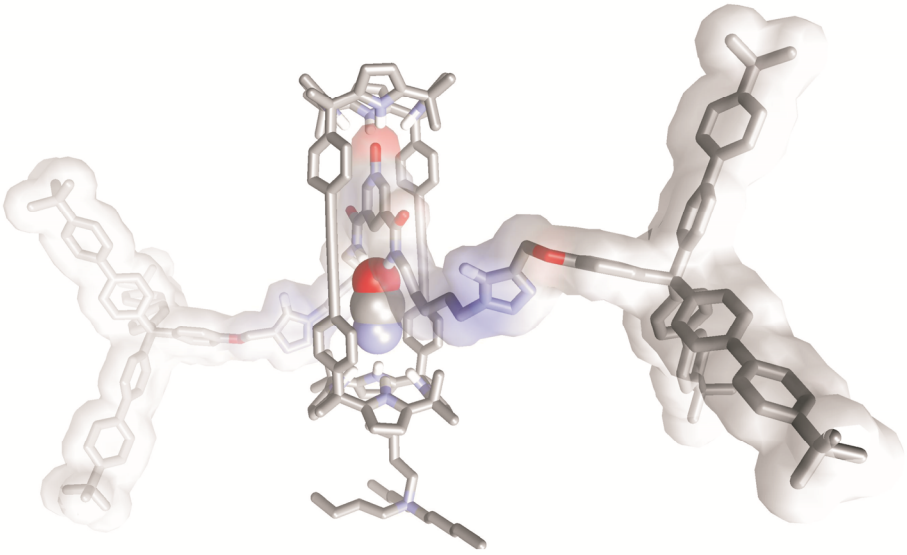

Figure 3. 9. Energy minimized structure (MM3) of the **3a⊂5** complex. Included anion shown as CPK model. The rest of the molecule is depicted in stick representation. The lineal component is depicted with a van der waals surface. Non-polar hydrogens were removed for clarity.[7]

We were interested in providing further evidence on the functioning of [2]rotaxane **5** as a heteroditopic receptor for ion-pairs in chloroform solution. The methyl trioctylammonium cation (i.e. $MTOA^+$) is known to be a better fit than the TBA^+ cation for the electron rich and shallow cup defined by the calix[4]pyrroles in cone conformation.[8,9] The stability constant measured for the **3d⊂5** complex was three orders

of magnitude larger than for the **3c⊂5** counterpart with the only difference between the two complexes being the nature of the cation of the ion-pair: $MTOA^+$ in **3d** and TBA^+ in **3c**. This result proved the functioning of [2]rotaxane **5** as a heteroditopic receptor of organic ion-pairs in chloroform solution. The noticeable affinity and selectivity exhibited by **5** in the recognition of ClMTOA **3d** directly derived from the better cation-receptor complementarity.

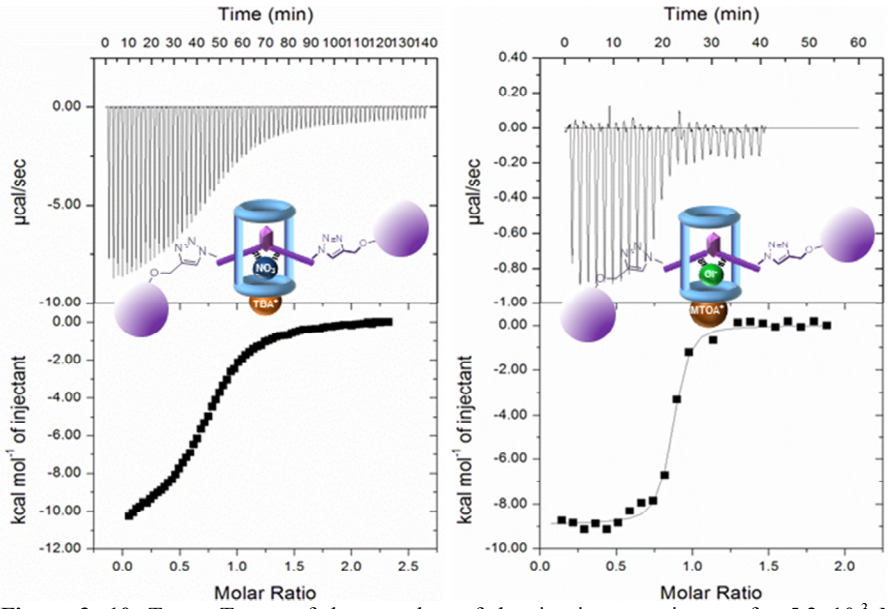

Figure 3. 10. Top – Traces of the raw data of the titration experiment of a 5.2×10^{-3} M and 1.7×10^{-4} M solution of rotaxane 5, respectively with the tetraalkylammonium salts ($TBANO_3$ **3b**, 5.2×10^{-3} M (left) and MTOACl **3c**, 0.17×10^{-3} M (right)) in $CHCl_3$. Bottom – Binding isotherms of the calorimetric titration shown on top. To determine the values of the thermodynamic variables the ITC data was fitted to a 1:1 binding model (black line).

In non-polar solvents, anion binding by synthetic receptors is mainly dominated by the use of hydrogen-bonding interactions. The formation of hydrogen bonds with anions in non-polar solvents is associated with a high enthalpy gain. In this line, Table 3. 1 shows that for all the studied anions, the binding processes in chloroform solution are enthalpy driven and highly exothermic. Remarkably, the binding processes leading to complexes **3a⊂5** and **3b⊂5**, with OCNTBA and NO_3TBA, respectively, did not obey the enthalpy-entropy compensation principle.[10] Unexpectedly, we also determined that the formation of complexes with the chloride anion, **3c⊂5** and **3d⊂5**, were not significantly opposed by entropy. Taken in concert, these thermodynamic observations are quite significant

because the binding processes occur in a nonpolar solvent (chloroform) that minimizes solvation effects and better approximates to a gas phase host-guest complexation process. We are convinced that the use of ion-pairs as guest complicated the analysis of the enthalpic and entropic terms using a simplistic 1:1 binding process in the gas phase, where enthalpically more favorable interactions should led to thermodynamically more stable complexes. We concluded that the solvation/desolvation effects occurring during the binding processes are important and difficult to predict. This is related to the deep inclusion geometry of the anion and the separated binding mode of the ion-pair being present in the formed complexes.

The assessment of the relative thermodynamic stabilities of ion-paired complexes formed with receptors featuring [2]pseudorotaxane and [2]rotaxane topology is complicated owing to their different stoichiometries (number of involved components). In our case, we considered that a sensible solution to address this problem would consist in determining the required amounts of salt that have to be added to 1 mM solutions of the supramolecular 1:1 ion-paired complexes, either with [2]rotaxane or [2]pseudorotaxane topologies, in order to induce the observation of higher stoichiometry complexes with respect to the salt, as well as the complete disassembly of the parent 1:1 complex (Figure 3. 11).

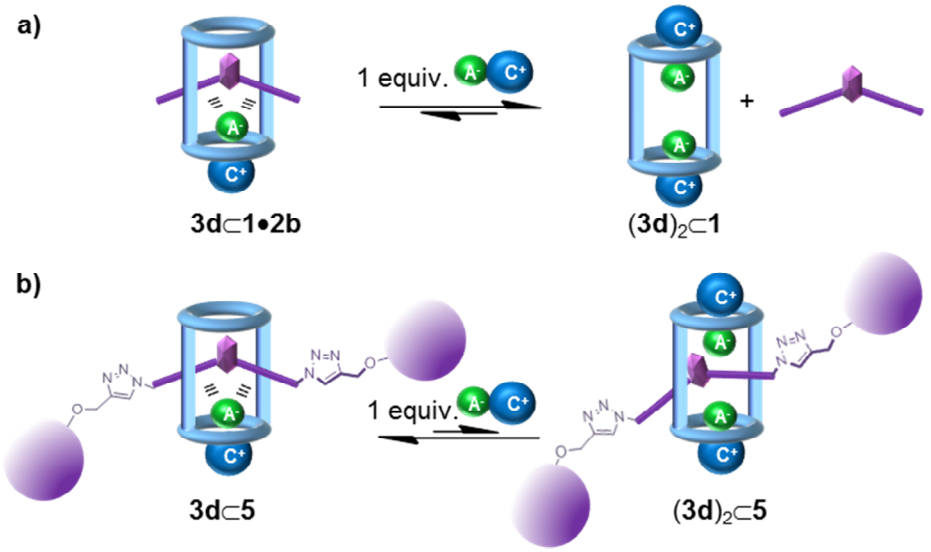

Figure 3. 11. Schematic representation of the plausible equilibria involved in the disassembly of 1:1 ion-paired complexes of pseudorotaxane (a) and rotaxane (b) structures.

In other words, we were interested in forcing the replacement of the pyridine-*N*-oxide unit of the axle, which is ditopically bound to the macrocycle, and the anion in the 1:1 complex, by a second ion-pair that will coordinate the cyclic component in a receptor separated binding mode (Figure 3. 11). In this vein, we previously reported that macrocycle **1** coordinated ClMTOA through a non-cooperative process yielding a dimeric ion-paired aggregate (**3d**)$_2$⊂**1**. Both ion-pairs were bound to the tetratopic macrocycle **1** and displayed receptor-separated binding geometry.**Error! Bookmark not defined.**

In the case of the [2]pseudorotaxane complex **3d**⊂**1**•**2b** (1 mM), the addition of slightly more than 1 equiv. of the ClMTOA ion-pair induced the initial disassembly of the interlocked structure and the concomitant formation of higher order aggregates (i.e. (**3d**)$_2$⊂**1** complex). The disassembly process was monitored using ^{1}H NMR spectroscopy by following the intensity changes of diagnostic proton signals of the two species that were involved in a slow chemical exchange on the proton chemical shift timescale (Figure 3. 12).

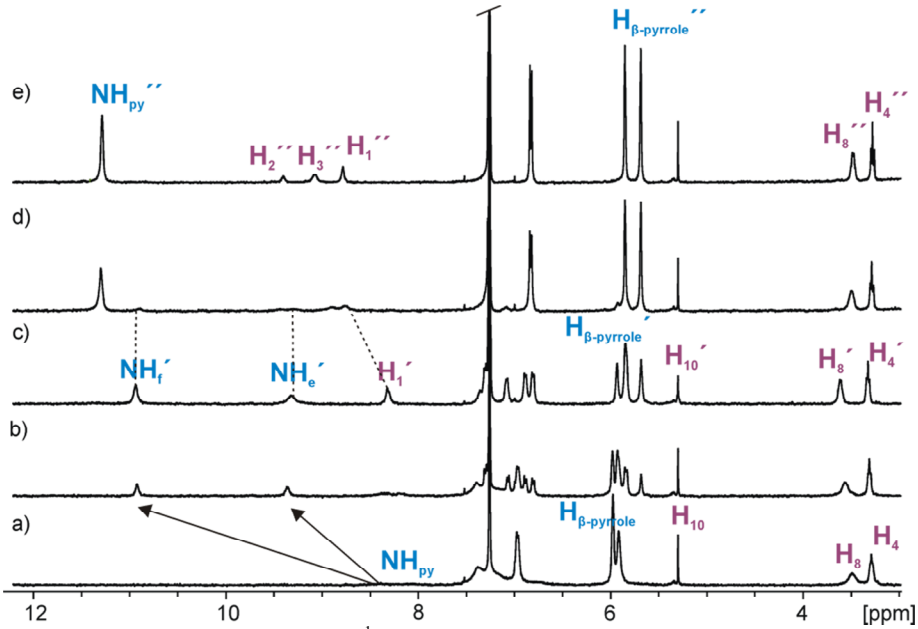

Figure 3. 12. Selected region of the ^{1}H NMR spectra registered during the titration ($CDCl_3$, 400 MHz, 298 K) of an equimolar solution of **1** and **2b** (1 mM) a) with successive additions of MTOACl **3d**, 0.5 equiv. b) 1 equiv. c) 1.5 equiv. d) 2.2 equiv. e).(´) signals refer to [2]pseudorotaxane **3d**⊂**1**•**2b** (´´) signals refer to 2:1 complex. H_1´´- H_3´´ refers to **2b**•**3d** complex.

The proton signals corresponding to **3d⊂1•2b**, 1:1 complex with [2]pseudorotaxane topology, disappeared completely after the addition of 2 equiv. of ClMTOA **3d**. In contrast, in the mechanically locked **3d⊂5** complex, even after the addition of 8 equiv. of ClMTOA ion-pair **3d** we could observe the characteristic proton signals of the 1:1 complex with [2]rotaxane topology (Figure 3. 13).

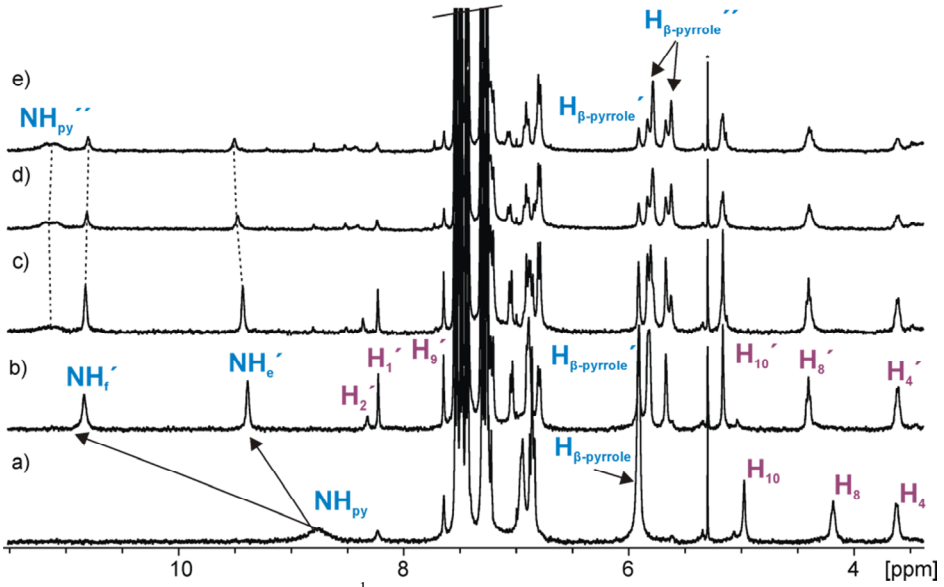

Figure 3. 13. Selected region of the ^{1}H NMR titration ($CDCl_3$, 400 MHz, 298 K) of a solution of rotaxane **5** (1 mM) a) with successive additions of methyltrioctylammonium chloride **3d**, 1 equiv. b) 1.7 equiv. c) 3.3 equiv. d) 8 equiv. e).

These results suggested that the increase in local concentration of the pyridyl-*N*-oxide unit exerted by the mechanical bond of **5** provided a measurable thermodynamic stabilization to its ditopic interaction with one calix[4]pyrrole hemisphere of the cyclic component and the bound chloride. Nonetheless, the emergence of a new set of proton signals in the ^{1}H NMR spectrum of a 1 mM $CDCl_3$ of the **3d⊂5** complex became evident after addition of more than an extra equiv. of ClMTOA **3d**. Upon incremental addition of **3d**, the new set of signals grew in intensity at the expenses of those assigned to the **3d⊂5** complex. We assigned this new set of proton signals to a higher stoichiometry complex between **3d** and **5** (i.e. 2:1) for which we have not fully determined its structure.

3.2.1 Binding studies in acetone

The thermodynamic signatures of the complexation processes determined in chloroform augur well for the application of the interlocked structure for anion recognition in more polar solvents. Thus, we decided to move our solution studies to acetone which can compete for hydrogen bond interactions. The polar nature of the solvent could also have an effect on the structure of the final complex. While in chloroform solution, binding of tetraalkylammonium salts occurs through the formation of 1:1 ion-paired complexes with host-separated geometry, in acetone the salt and the final complex are expected to have a more ion-pair dissociated nature.

We performed ^{1}H NMR titration experiments of rotaxane **5** in acetone with both chloride salts, **3c** and **3d**. The ^{1}H NMR spectrum of rotaxane **5** in acetone showed sharp and well-defined signals for most of the protons (Figure 3. 14 a). However, the pyrrole NHs signal appeared broadened in the downfield region of the ^{1}H NMR spectrum. Addition of 1 equiv of **3c** produced the appearance of a new set of sharp and well defined signals that we attributed to the bound rotaxane.

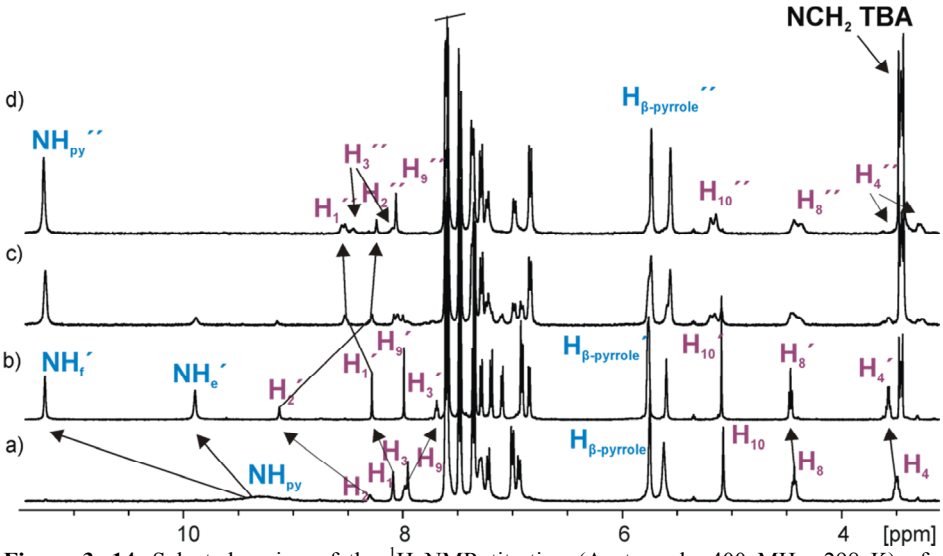

Figure 3. 14. Selected region of the ^{1}H NMR titration (Acetone-d_6, 400 MHz, 298 K) of a solution of rotaxane **5** (1 mM) a) with successive additions of tetrabutylammonium chloride (**3c**), 1 equiv. b) 2 equiv. c) 3 equiv. d). Primed numbers and letters indicate the proton signals in the 1:1 complex. Double-primed numbers and letters indicate the proton signals in the 2:1 complex. Blue color for macrocycle component, purple color for linear component.

As described for the same binding process in $CDCl_3$, two different pyrrole NHs were detected for bound **5**. These signals were significantly downfield shifted compared to that of the NHs in free **5**. This result indicated the involvement of the pyrrole NHs of bound **5** in hydrogen bonding interactions with different guests: the *N*-oxide knob of the lineal component and the chloride anion. Conversely to the results obtained in $CDCl_3$, in acetone solution the signal of the methylene protons alpha to the nitrogen of the TBA cation did not experience any chemical shift change during the titration, simply its intensity was increased upon incremental addition of **3c**. Most likely, the good solvation experienced by the cation with the acetone molecules opposes to the formation of an ion-paired complex.

Incremental addition of **3c** to the equimolar mixture of **5** and **3c** in acetone produced further changes in the ^{1}H NMR spectrum. The most remarkable changes were related to the disappearance of the signal of the protons assigned to the pyrrole NHs of **5** that we assigned as bound to the *N*-oxide moiety. A slight increase of the intensity of the signal corresponding to the pyrrole NHs bound to the anion was also observed. Moreover, significant broadening was detected for the signals attributed to the pyridine *N*-oxide ring and for the H_{10}-H_8-H_4 protons.

A ROESY experiment performed on a millimolar acetone solution containing the equimolar mixture of rotaxane **5** and salt **3c** (Figure 3. 15) showed cross peaks between the NHs protons resonating at 8.28 ppm and the H_1 protons *ortho* to the pyridine *N*-oxide from the lineal axle. This observation supported the binding of the *N*-oxide moiety within one hemisphere of the calix[4]pyrrole macrocycle.

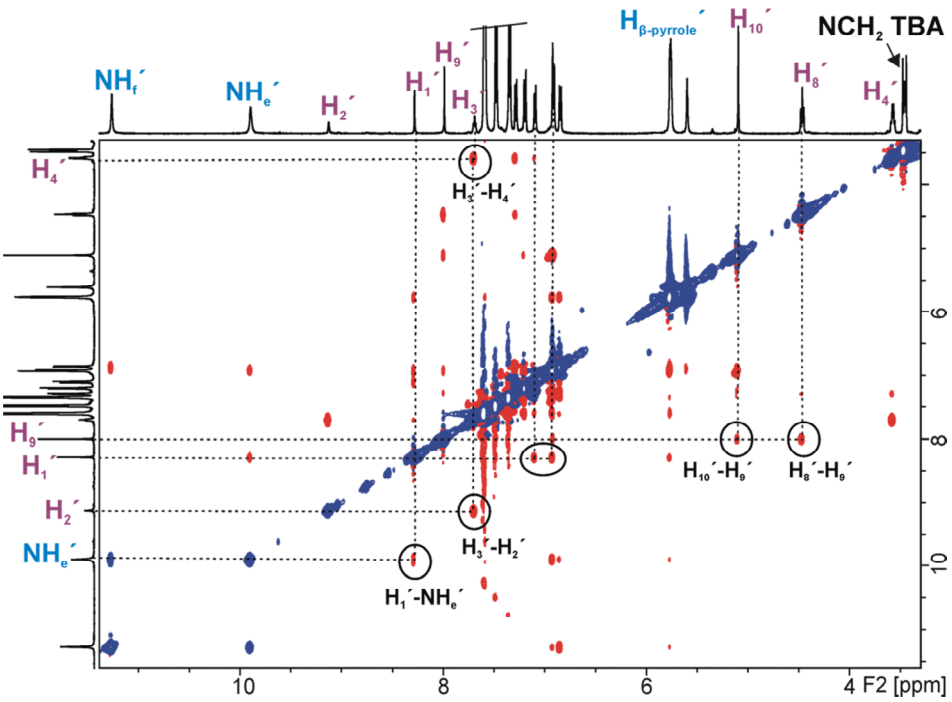

Figure 3. 15. Selected region of the ROESY experiment (Acetone-d_6, 500 MHz, mixing time= 0.3 s, power level=120 dB) performed on an equimolar mixture of [2]rotaxane and tetrabutylammonium chloride (**3c**) at 298 K showing the most relevant close contact peaks.

Remarkably, these intermolecular close contacts were not observed when the ROESY experiment was performed in an acetone solution of **5** containing an excess of **3c** (Figure 3. 16). Taken together, these observations suggested the dissociation of the pyridine *N*-oxide moiety from one of the calix[4]pyrrole binding units of the macrocycle owing to the competitive coordination of a second anion yielding a 2:1 complex. This complex will consist on two chloride anions included in the internal cavity of the macrocycle and bound at the two opposed calix[4]pyrrole units. The pyridine *N*-oxide unit of the threaded linear component might be displaced from the internal cavity of the macrocycle owing to the competitive binding of the second chloride anion.

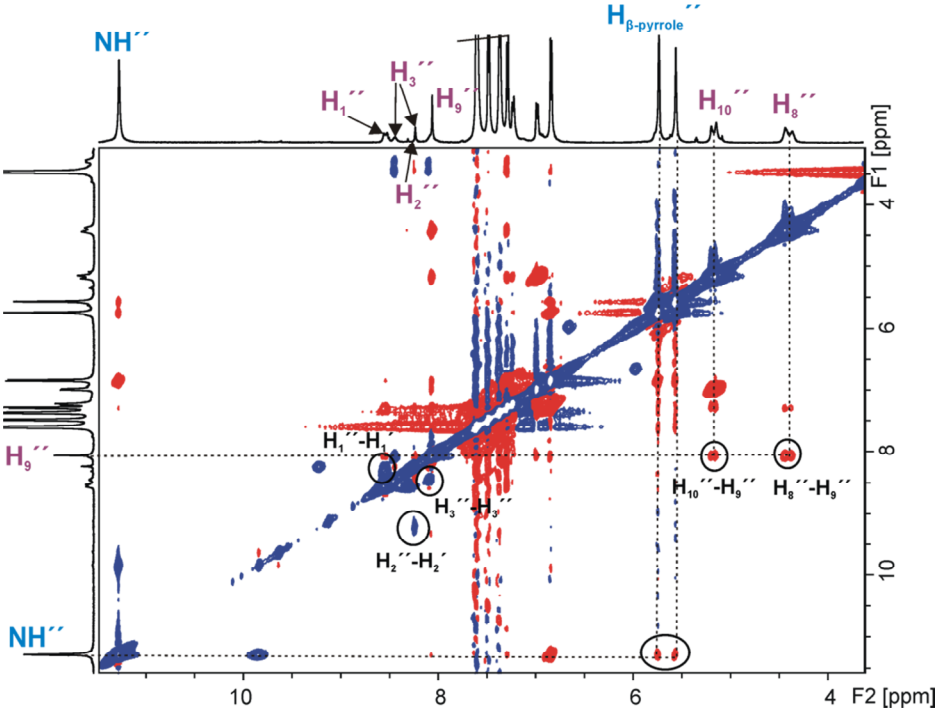

Figure 3. 16. Selected region of the ROESY experiment (Acetone-d_6, 500 MHz, mixing time= 0.3 s, power level=120 dB) performed on an mixture of [2]rotaxane and excess of tetrabutylammonium chloride (**3c**) at 298 K showing the most relevant close contact peaks. Primed numbers and letters indicate the proton signals in the 1:1 complex. Double-primed numbers and letters indicate the proton signals in the 2:1 complex. Blue color for macrocycle component, purple color for linear component.

Figure 3. 17 shows the MM3 energy minimized structure of the putative 2:1 complex.

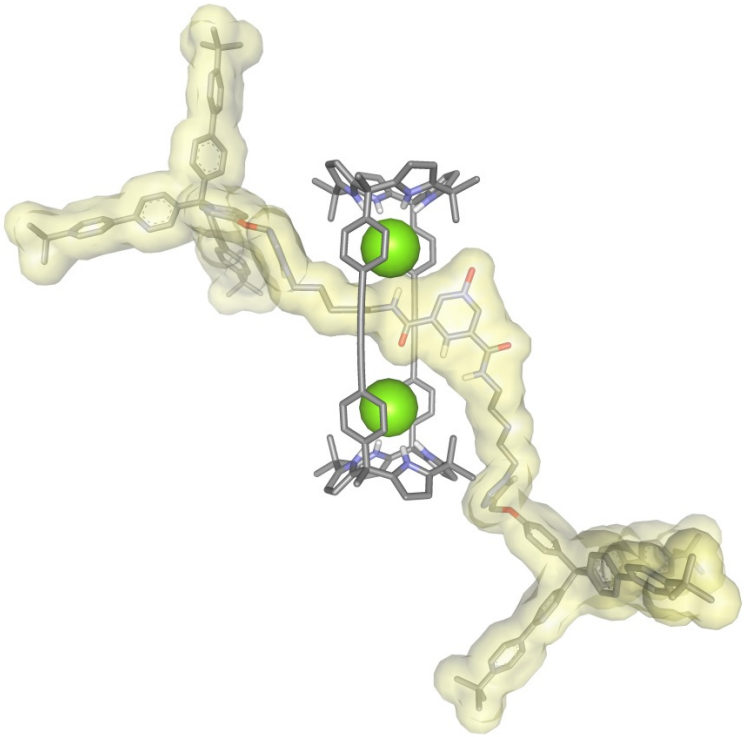

Figure 3. 17. Energy minimized structure (MM3) of the **(3c)$_2$⊂5** complex. Included anion shown as CPK model. The rest of the molecule is depicted in stick representation. The lineal component is depicted with a van der waals surface. Non-polar hydrogens were removed for clarity.

^{1}H NMR titrations of **5** with **3d** in acetone solution showed practically identical changes in the ^{1}H NMR spectra than the ones observed in the titration with **3c**, (Figure 3. 18).

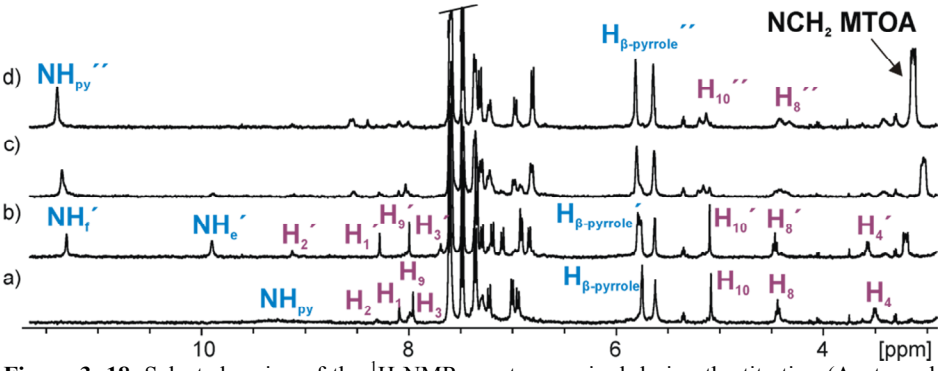

Figure 3. 18. Selected region of the ^{1}H NMR spectra acquired during the titration (Acetone-d_6, 400 MHz, 298 K) of a solution of rotaxane **5** (1 mM) a) with successive additions of methyltrioctylammonium chloride (**3d**), 1 equiv. b) 2 equiv. c) 4 equiv. d).

Complexation-induced changes were observed for the methylene protons alpha to the nitrogen of the MTOA cation (Figure 3. 18). The chemical shift change of the alpha-methylene protons in the alkylammmonium salts was not observed in the ^{1}H NMR titration using ClTBA. Most likely, the good fit of the methyl group in the MTOA cation and the external aromatic cavity of the receptor defined by the pyrrole rings of the calix in cone conformation are responsible of this difference.

Next, we decided to probe the binding of alkylammonium salts of polyatomic anions with **5** in acetone solution using ^{1}H NMR spectroscopy. The addition of 1 equiv. of **3a** to a millimolar acetone solution of **5** showed one single set of sharp and well-defined proton signals. We assigned this set of signals to the 1:1 complex that was quantitatively assembled (Figure 3. 19).

The incremental addition of **3a** to the equimolar mixture (up to 5 equiv.) provoked the gradual appearance of a new set of signals that grew to the expenses of those assigned to the 1:1 complex. We assigned the new set of signals to the 2:1 complex. It is worth noting that this new set of proton signals showed significant broadening compared to the ones of the 2:1 complex involving the chloride anion. Most likely, this observation is related to the superior thermodynamic stability of the complexes of **5** and chloride, which in turn improves their kinetic stability and produces a reduced exchange rate of their equilibrium.

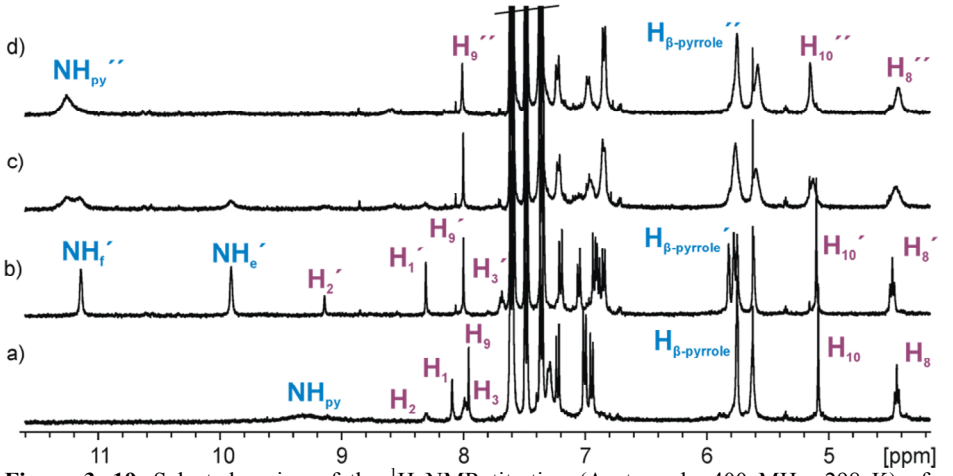

Figure 3. 19. Selected region of the ^{1}H NMR titration (Acetone-d_6, 400 MHz, 298 K) of a solution of rotaxane **5** (1 mM) a) with successive additions of tetrabutylammonium cyanate (**3a**), 1 equiv. b) 3 equiv. c) 5 equiv. d).

Finally, the ^{1}H NMR titration of **5** with NO_3TBA **3b** in acetone solution demonstrated the quantitative complexation of the nitrate anion in the equimolar millimolar mixture (Figure 3. 20). All the proton signals corresponding to the 1:1 complex were easily assigned. The diagnostic features for the existence of two different hydrogen-bonded hemispheres of the macrocyclic were readily observed. In this case, the addition of an excess of salt, up to 6 equiv., did not produce significant changes to the signals in the ^{1}H NMR spectrum. This observation indicated that the binding of a second nitrate anion in the cavity of **5**, as we previously observed for the Cl^- and CNO^- anions, have not taken place for nitrate in the range of studied concentrations. Either the size and the shape of the trigonal nitrate anion disfavors the formation of the 2:1 complex or their hydrogen-bonding competitive properties with respect to the pyridyl-*N*-oxide are reduced.

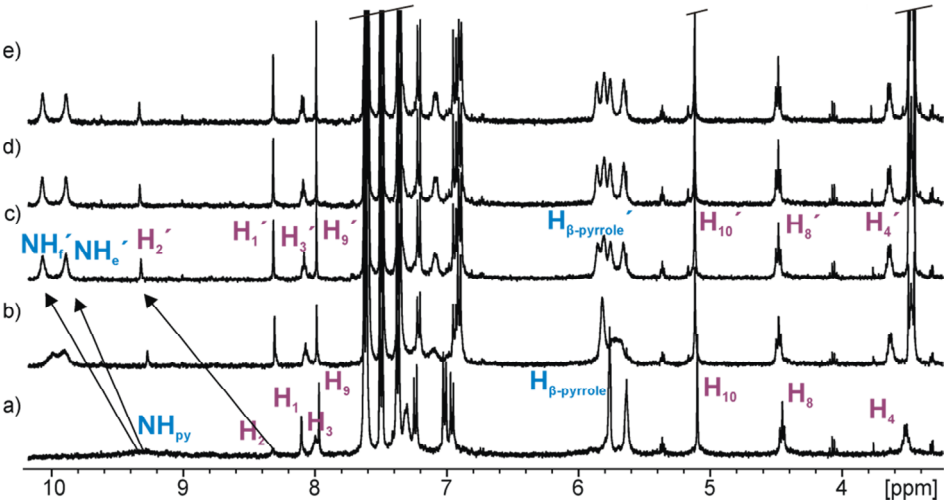

Figure 3. 20. Selected region of the ^{1}H NMR spectra acquired during the titration (Acetone-d_6, 400 MHz, 298 K) of a solution of rotaxane **5** (1 mM) a) with successive additions of tetrabutylammonium nitrate (**3b**), 1 equiv. b) 2 equiv. c) 4 equiv. d) 6 equiv. e).

The association constant values in acetone were also determined using ITC experiments. The ITC data of the binding of **3a** and **3b** to rotaxane **5** in acetone showed good fits to a theoretical binding isotherm that assumes the formation of a simple 1:1 complex (Figure 3. 21). The lower concentration used in the ITC experiments and the reduced excess of added tetralkylammonium salts (up to 2 equiv.) made that the presence of species with stoichiometries higher than 1:1 were negligible.

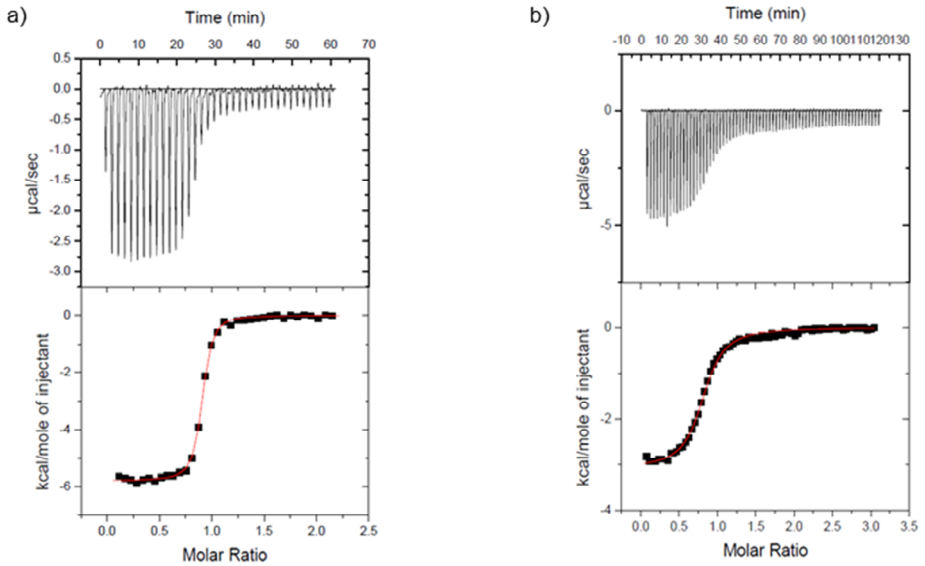

Figure 3. 21. Top – Traces of the raw data of the titration experiment of a 1.2×10^{-4} M and 5.3×10^{-4} M solution of rotaxane **5**, respectively with the tetraalkylammonium salts (OCNTBA 1.2×10^{-3} M (left) and NO_3TBA 7.29×10^{-3} M (right)) in acetone. Bottom – Binding isotherms of the calorimetric titration shown on top. To determine the values of the thermodynamic variables the ITC data was fitted to a 1:1 binding model (red line).

Surprisingly, the derived association constant values for the complexes of both polyatomic anions with **5** were almost one order of magnitude larger than those measured for their counterparts in chloroform solution. In addition, the dissection of the Gibbs energy into the enthalpic and entropic terms also presented significant differences. The binding enthalpy in acetone was lower than the one determined in chloroform. This result is in agreement with the competitive nature of the solvent. On the other hand, the entropy values in acetone became positive. We learnt from previous binding studies that solvation/desolvation effects can be responsible for this observation. Most likely, the desolvation of the receptor's cavity with concomitant release of acetone molecules to the bulk solution could explain this gain in entropy.

Remarkably, the analysis of the ITC binding data for the chloride anion (i.e. **3c** and **3d**) in acetone yielded results that were expected from the previous results observed by ^{1}H NMR titration. The binding isotherm showed two sigmoidal curves with inflection points centered at molar ratio values of **5**/**3c** = 1 and 2. This result indicated that two different binding events were taking place in solution producing two complexes with

different stoichiometry, a 1:1 and a 2:1 complex. Similar results were obtained with **3d** (Figure 3. 22).

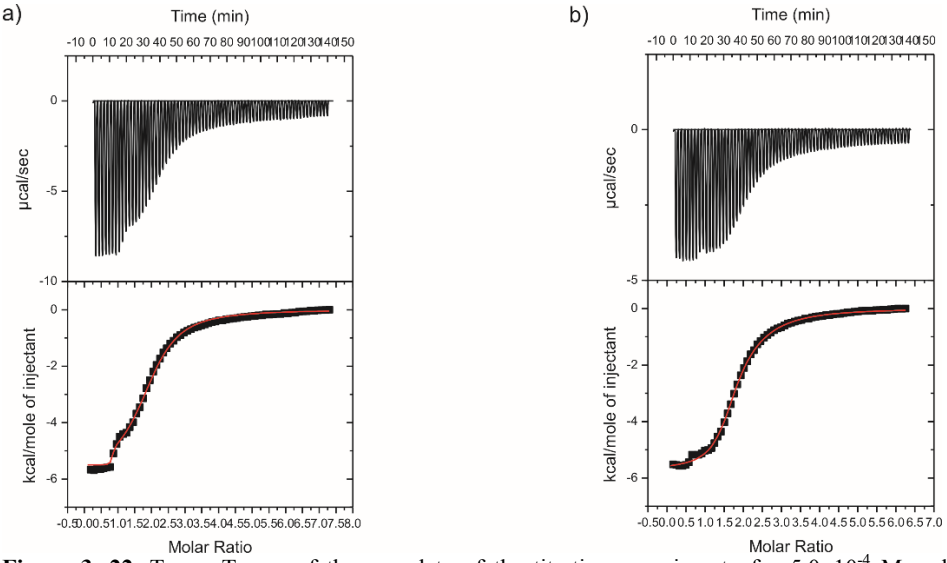

Figure 3. 22. Top – Traces of the raw data of the titration experiment of a 5.0×10^{-4} M and 3.2×10^{-4} M solution of rotaxane **5**, respectively with the **3c-3d** salts (ClTBA 17×10^{-3} M (left) and ClMTOA 8.74×10^{-3} M (right)) in acetone. Bottom – Binding isotherms of the calorimetric titration shown on top. To determine the values of the thermodynamic variables the ITC data was fitted considering a 1:1 and a 2:1 binding model (red line).

We analyzed the experimental binding isotherms obtained in acetone using a binding model that considered the formation of 1:1 and 2:1 complexes, **3c**⊂**5** and (**3c**)$_2$⊂**5**, respectively (Figure 3. 22). The thermodynamic values derived from the fitting procedure are summarized in Table 3. 2. The association constant value for the first binding event, which would yield the anionic complex **Cl**$^-$⊂**5**, is in the order of 10^7 M^{-1}. The thermodynamic parameters derived from the ITC experiment revealed that this binding event was both enthalpically and entropically driven. In contrast, the binding constant value associated to the second binding event, that is the formation of the (**Cl**$^-$)$_2$⊂**5** complex starting from the **Cl**$^-$⊂**5** complex, was determined to be aproximately 3 orders of magnitude smaller (~10^4 M^{-1}). The reduction for chloride affinity in this second binding event was accompanied with a decrease of both the enthalpic and entropic terms when compared to the binding of the first chloride. These observations support the competitive nature of the second chloride binding with respect to that of the *N*-oxide.

Table 3. 2. Association constant values (M^{-1}), free energies of complexation (ΔG, kcal mol^{-1}) and values for the enthalpic (ΔH, kcal mol^{-1}) and entropic components ($T\Delta S$, kcal mol^{-1}, 298 K) for the complexes formed between [2]rotaxane **5** and the different ammonium salts **3a-d** determined in acetone solution using ITC experiments.

	$K_a \times 10^{-5}$	ΔG	ΔH	$T\Delta S$	n
3a	30.6±5.9	-8.8±0.1	-5.9±0.1	2.9±0.1	1
3b	1.06±0.4	-6.9±0.2	-2.9±0.2	4.0±0.4	1
3c	K_1=156±49.4 K_2=0.094±0.001	ΔG_1 = -9.7±0.2 ΔG_2 = -5.4±0.01	ΔH_1 = -5.5±0.2 ΔH_2 = -3.6±0.1	$T\Delta S_1$ = 4.2±0.3 $T\Delta S_2$ = 1.8±0.1	2
3d	K_1=800±35.3 K_2=0.4±0.1	ΔG_1 = -10.8±0.03 ΔG_2 = -6.3±0.1	ΔH_1 = -5.5±0.1 ΔH_2 = -5.6±0.1	$T\Delta S_1$ = 5.3±0.1 $T\Delta S_2$ = 0.7±0.2	2

Not surprisingly, in acetone solution the association constant values derived from the binding of **3d** (i.e. MTOA cation) were only slightly larger than those determined for **3c** (i.e. TBA cation). This result gives support to the idea that, in acetone solution, the free salt **3c** and both 1:1 and 2:1 complexes of chloride with **5** exist to a significant extent as almost fully dissociated ion-pairs.

3.3 Conclusions

In chloroform solution, [2]rotaxane **5** functioned as an efficient heteroditopic receptor for tetraalkylammonium salts, **3a-d**, containing mono- (Cl^-) or polyatomic anions (NO_3^- or ^-OCN). In all cases, we observed the formation of kinetically and thermodynamically stable 1:1 ion-paired complexes featuring cyclic-component separated binding mode. The determined K_a values indicated that [2]rotaxane **5** was selective for the complexation of cyanate *vs* chloride or nitrate when the ion-pair precursors were TBA salts. This selectivity was attributed to the superior complementarity that existed between the cylindrical polar cavity of the interlocked receptor and the polyatomic linear geometry of the cyanate anion. Remarkably, the change of the TBA^+ cation for $MTOA^+$ produced an increase in binding affinity of almost three orders of magnitude in the case of chloride salts. This result highlighted the functioning of **5** as a heteroditopic receptor for ion-pairs in chloroform and supported the better fit of the methyl group in

the $MTOA^+$ cation in the electron-rich and shallow cavity opposed to the bound anion that defined the cone conformation of the calix[4]pyrrole.

Unfortunately, the accurate comparison of the thermodynamic stabilities of 1:1 ion paired complexes of salts with receptors featuring [2]rotaxane and [2]pseudorotaxane topologies is challenging. In any case, we assigned a higher thermodynamic stability to the 1:1 ion-paired complexes resulting from the [2]rotaxane **5** receptor with respect to the ones derived from the assembled [2]pseudorotaxane counterpart. We based this conclusion on the salt's excess that is required to produce aggregates of higher stoichiometry (i.e. 2:1 complexes). We are aware that this reasoning is limited and does not take into account the difference in thermodynamic stability of the higher stoichiometry produced complexes.

In acetone solution, the selectivity displayed by the [2]rotaxane **5** in the formation of 1:1 complexes using TBA salts as anion precursors is reversed. The interlocked receptor features a K_a value with monoatomic spherical Cl^- that is five-fold larger than for cylindrical ^-OCN and more than two orders of magnitude larger than for trigonal and planar NO_3^-. We attribute this selectivity to the superior hydrogen bonding properties of chloride (same charge but small size), which are better expressed in a polar solvent, like acetone, that promotes ion-pair dissociation by nicely solvating the cation. The solvent influence in ion-pair dissociation is also substantiated by the fact that the cation effect is significantly reduced in acetone. The MTOA chloride binds only four-fold stronger than the TBA counterpart. This represents a drop of more than two order of magnitude in ion-pair recognition when compared to the results obtained in chloroform solution. In acetone, the cation effect is less important owing to the more dissociated nature of the resulting 1:1 complex. Significantly, the magnitude of the calculated binding constants for all anionic complexes is quite similar in both solvents. We surmise that this results has to do with the interwoven nature of the binding site that provides a reduced access to hydrogen bonding competing solvent molecules. However, the polar nature of acetone revealed a known but unexpected binding behavior of **5**, the formation of 2:1 anion complexes. On the one hand, acetone competes better for the hydrogen bonding acceptor properties of the calix[4]pyrroles with the *N*-oxides. On the other hand, in acetone anions are loosely solvated but dissociated from their cations, which makes

them very prone to get involved in hydrogen bonding interactions. The combination of both effects, produces in the case of chloride and cyanate anions added in excess a competition with the N-oxide unit for hydrogen bonding with one calix[4]pyrrole core. The net result of this competition is the emergence of 2:1 complexes, in which [2]rotaxane **5** binds two anions in the internal cavity of the macrocycle, when not working under a strict stoichiometric control.

3.4 Experimental section

3.4.1 General information and instrumentation

All solvents were of HPLC grade quality, commercially obtained and used without further purification. Routine ^{1}H NMR spectra were recorded on a Bruker Avance II 400 Ultrashield NMR spectrometer. Variable temperature experiments and 2D NMR spectra were performed on a Bruker Avance 500 (500.1 MHz for ^{1}H NMR) Ultrashield spectrometer. $CDCl_3$ and acetone-d_6 from Sigma Aldrich was used for NMR studies. Chemical shifts are given in ppm, relative to TMS. Isothermal titration calorimetry experiments were performed using a Microcal VP-ITC Microcalorimeter. All the titrations were carried out in chloroform and acetone solution at 298 K. Titrations of rotaxane **5** with tetraalkylammonium salts **3a-3d** were carried out by adding aliquots of a solution of the salt into a solution of rotaxane in the same solvent. The concentration of guests' solution was approximately 10 times more concentrated than for the host. The association constants and the thermodynamic parameters were obtained from the fit of the titration data to a simple 1:1 or 2:1 binding model using the Microcal ITC Data Analysis module. The association constant (K_a), $T\Delta S$ and ΔH values for the binding process were determined by averaging the values from at least two titration experiments.

3.4.2 Experimental section: Figures

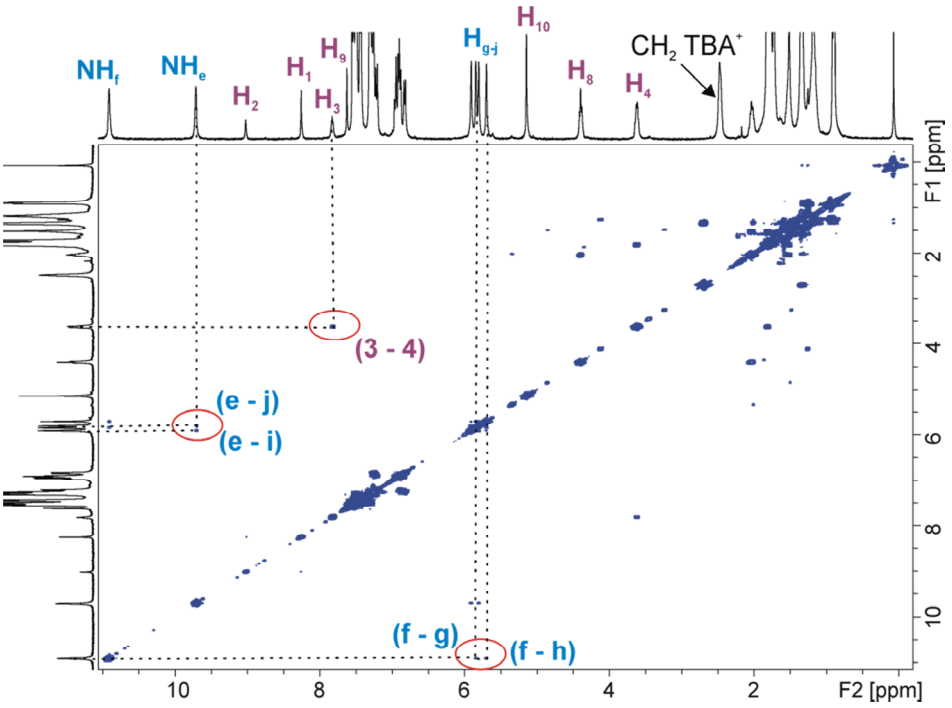

Figure 3. 23. COSY NMR experiment ($CDCl_3$, 500 MHz, 298 K) of a millimolar solution of an equimolar mixture of [2]rotaxane **5** and tetrabutylammonium cyanate (**3a**).

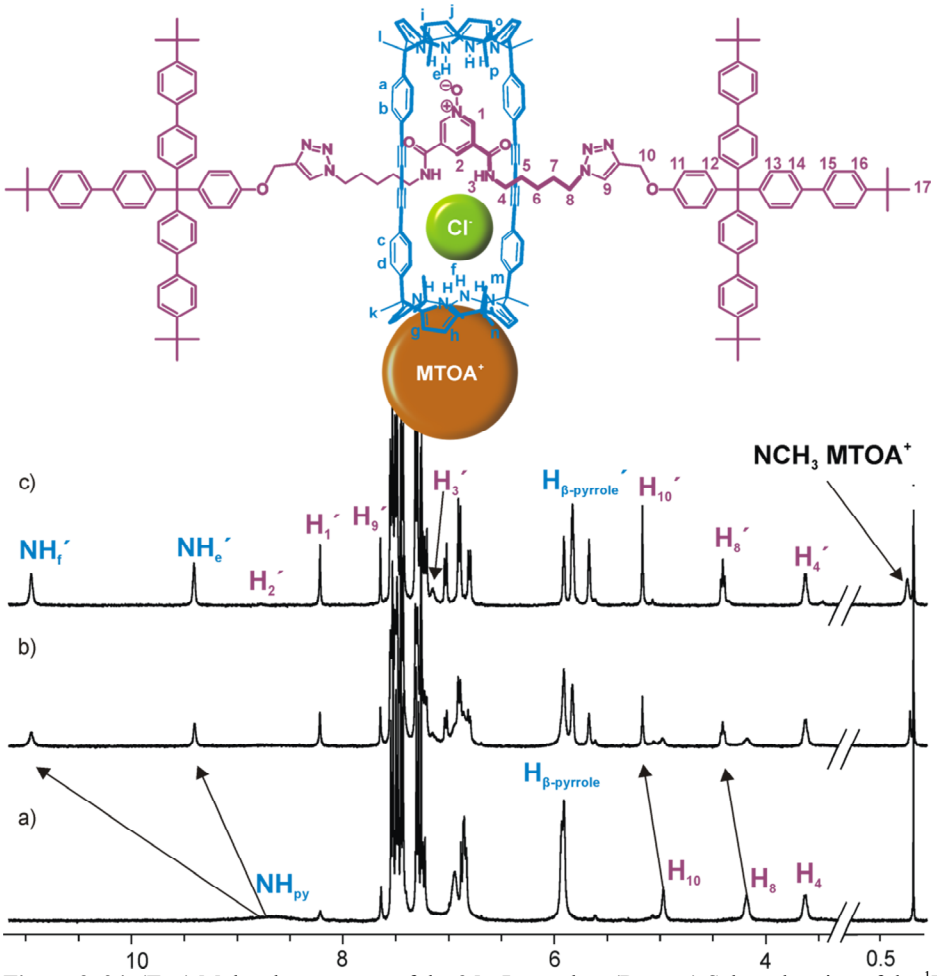

Figure 3. 24. (Top) Molecular structure of the **3d⊂5** complex. (Bottom) Selected region of the ^{1}H NMR titration ($CDCl_3$, 400 MHz, 298 K) of a millimolar solution of [2]rotaxane **5** with successive additions of methyltrioctylammonium chloride (**3d**). Free rotaxane a) 0.5 equiv. b) 1 equiv. c).

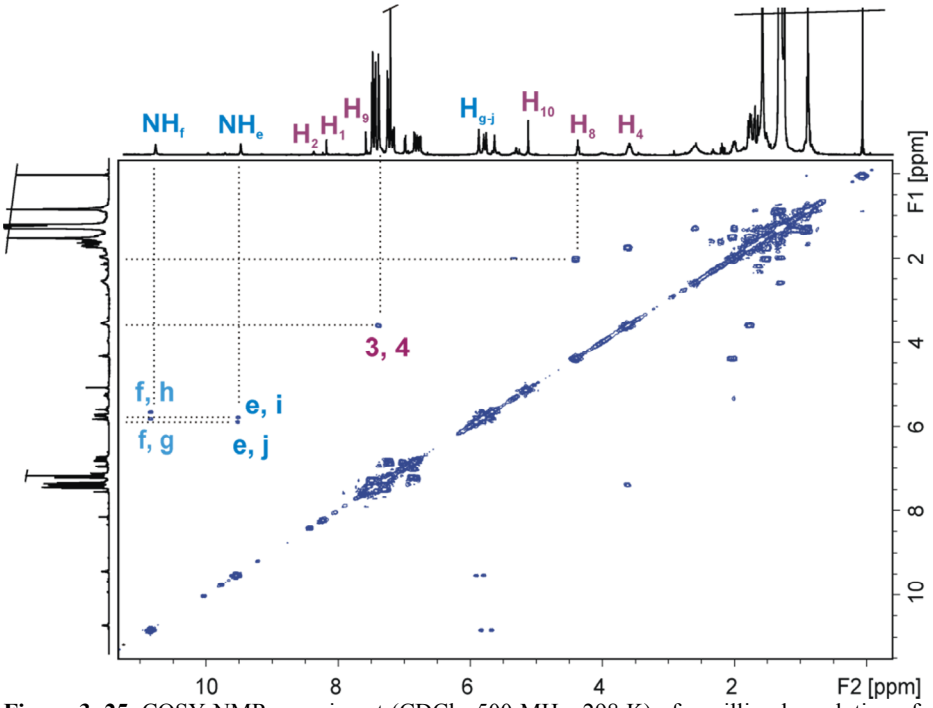

Figure 3. 25. COSY NMR experiment ($CDCl_3$, 500 MHz, 298 K) of a millimolar solution of an equimolar mixture of [2]rotaxane **5** and methyltrioctylammonium chloride (**3d**). Some relevant cross-peaks are highlighted.

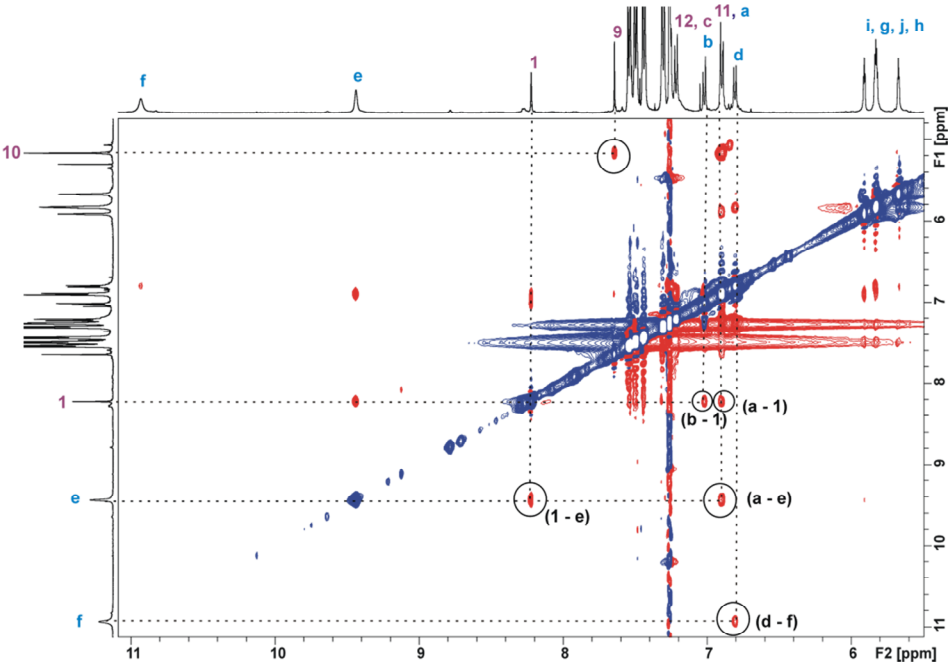

Figure 3. 26. Selected region of the T-ROESY experiment ($CDCl_3$, 500 MHz, 263 K) of an equimolar mixture of [2]rotaxane **5** and methyltrioctylammonium chloride (**3d**) highlighting some relevant close-contact cross-peaks. T-ROESY experiments were preferred to classical ROESY experiments as this sequence provides reliable dipolar cross-peaks with a minimal contribution of scalar transfer.

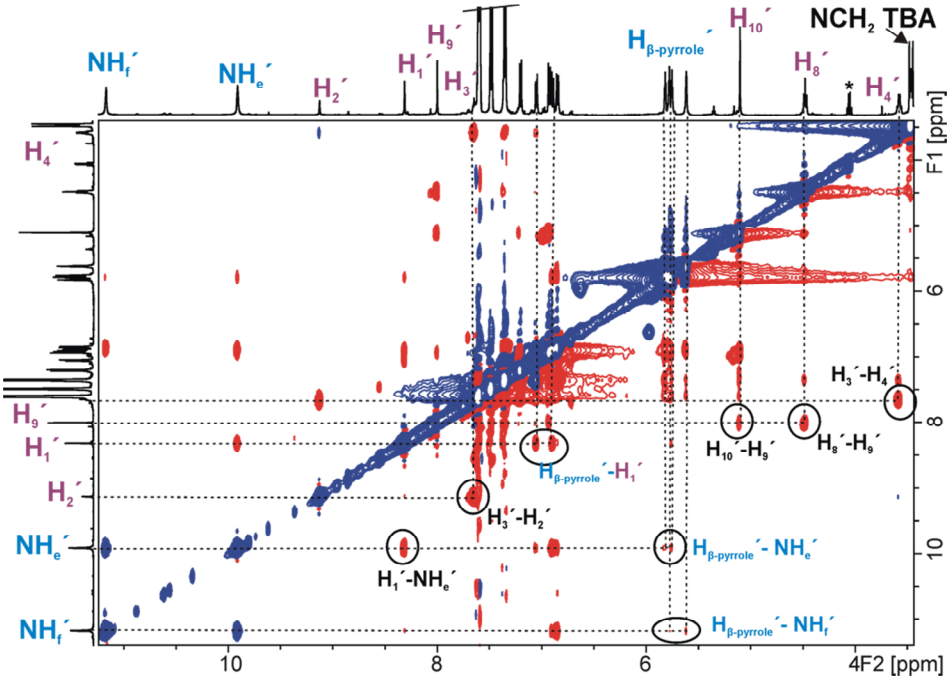

Figure 3. 27. Selected region of the ROESY experiment (Acetone-d_6, 500 MHz) performed on an equimolar mixture of [2]rotaxane and tetrabutylammonium chloride (**3a**) at 298 K showing the most relevant close contact peaks.

3.5 References and notes

[1] McConnell, A. J.; Beer, P. D., *Angew. Chem., Int. Ed.* **2012,** *51* (21), 5052-5061.
[2] Kim, S. K.; Sessler, J. L., *Chem. Soc. Rev.* **2010,** *39* (10), 3784-3809.
[3] Sambrook, M. R.; Beer, P. D.; Wisner, J. A.; Paul, R. L.; Cowley, A. R.; Szemes, F.; Drew, M. G. B., *J. Am. Chem. Soc.* **2005,** *127* (7), 2292-2302.
[4] Knighton, R. C.; Beer, P. D., *Chem. Commun.* **2014,** *50* (13), 1540-1542.
[5] Mercurio, J. M.; Tyrrell, F.; Cookson, J.; Beer, P. D., *Chem. Commun.* **2013,** *49* (92), 10793-10795.
[6] The low concentration used in the ITC experiments and the reduced excess of added tetralkylammonium salts (up to 2 equiv.) made that the presence of species with stoichiometries higher than 1:1 was negligible.
[7] The energy minimized structure was obtained using the software package Fujitsu Scigress Version 2.2.0. The structure was optimized by performing a geometry calculation using the implemented molecular mechanics force field with augmented MM3 parameters.
[8] Gross, D. E.; Schmidtchen, F. P.; Antonius, W.; Gale, P. A.; Lynch, V. M.; Sessler, J. L., *Chem-Eur J* **2008,** *14* (26), 7822-7827.
[9] Valderrey, V.; Escudero-Adan, E. C.; Ballester, P., *Angew. Chem., Int. Ed.* **2013,** *52* (27), 6898-6902.
[10] Dunitz, J. D., *Chem. Biol.* **1995,** *2* (11), 709-712.

Chapter 4

Influence of the stopper's size in the rotaxane synthesis

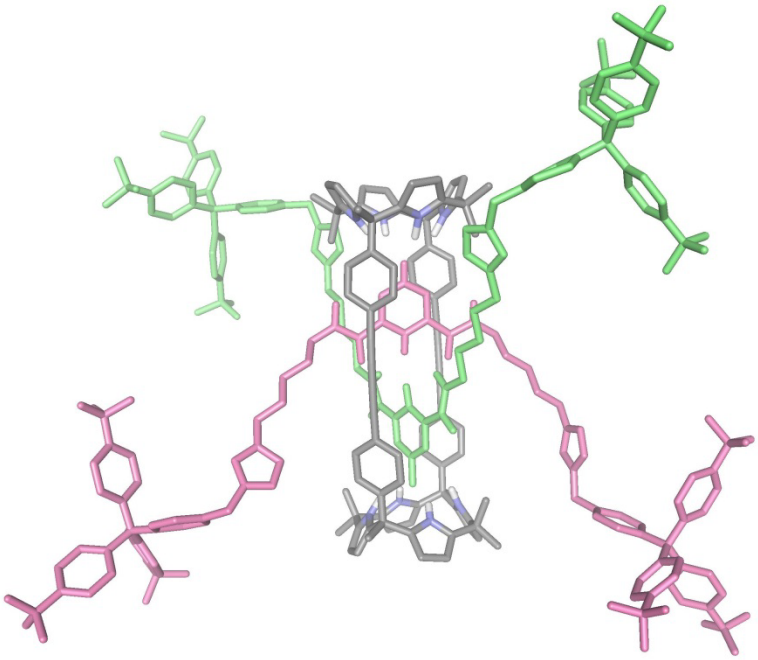

UNIVERSITAT ROVIRA I VIRGILI
INTERLOCKED ARCHITECTURES BASED ON A BIS-CALIX[4]PYRROLE MACROCYCLE FOR ION-PAIR RECOGNITION
Jose Ramon Romero Lopez

4.1 Introduction

The synthesis of interlocked molecules, such as rotaxanes or catenanes requires very specific conditions, for example in terms of concentration, solvent and suitable design of the initial components.

The size complementarity between the macrocyclic and the linear component's stoppers is crucial for the kinetic stability of rotaxane structures.[1,2,3,4,5,6,7,8,9,10,11,12,13,14,15] Axle stoppers must be bulky enough to avoid the dethreading from the macrocycle and the establishment of an equilibrium between the interlocked structure and its free components without the cleavage of any covalent bond.[16] Saito´s group reported detailed studies concerning the relationship that existed between the size of the stoppers (blocking groups) and the kinetic stability of the corresponding rotaxanes.[17,18,19,20] They demonstrate that small structural changes either in the macrocycle or in the blocking groups can cause large effects on the stability of the rotaxane structure. Moreover, the macrocycle size limits the synthesis of this type of interlocked structures as it requires large blocking groups (i.e. dendrimers,[21,22,23] porphyrins[24,25,26,27,28] or cyclodextrins[29,30,31,32]) that involve more challenging and longer synthetic pathways.

The considerations above are basically true for the synthesis of [2]rotaxanes which involves one macrocycle and one lineal component. However, in the synthesis of more complex structures such as [3]- or [4]-rotaxanes other considerations must be taken into account. The vast majority of reported [*n*]rotaxane structures are those involving *n*-1 macrocyclic components threaded on a single axle.[33,34,35,36,37,38] However, examples of [*n*]rotaxane structures that involve *n*-1 linear components threading a single macrocycle are scarce.[39,40,41,42,43,44,45] The synthesis of multithreaded [*n*]rotaxanes is limited to macrocyclic components that are large enough to accommodate two or more axles in its cavity but, at the same time, they must be also small enough to prevent the dethreading process.[46,47,48] In this sense, the size of the stoppers is also determining. The use of relatively small blocking groups in the axle is necessary to allow the multithreading of the cyclic component by more than one axle. The use of large stoppers, generally, disfavors a second threading process and leads to the formation of a [2]rotaxane as the main product.

In this chapter, we disclose our investigations on the effect of the stopper's size employed in the synthesis of interlocked structures using the bis(calix[4]pyrrole) **1** as cyclic component and the 3,5-bis-amidepyridyl-*N*-oxide derivative **2b** as linear component, that were introduced previously in Chapter 2, in combination with a significantly smaller terphenyl unit **4b** as blocking group.

4.2 Results and discussion

4.2.1 Attempts to obtain [2]rotaxane **15**

In Chapter 2, we described the synthesis of the neutral [2]rotaxane **5**. We used as synthetic precursor the [2]-pseudorotaxane assembled by the interaction of the calix[4]pyrrole **1** as cyclic component, and the 3,5-*bis*-amidepyridyl-*N*-oxide derivative **2b** as axle.[49] The selection of the tris(biphenyl) group **4a** as blocking group for the synthesis of **5** was not trivial. All our attempts to isolate an analogous [2]rotaxane using the smaller terphenyl stoppers **4b** were unsuccessful.

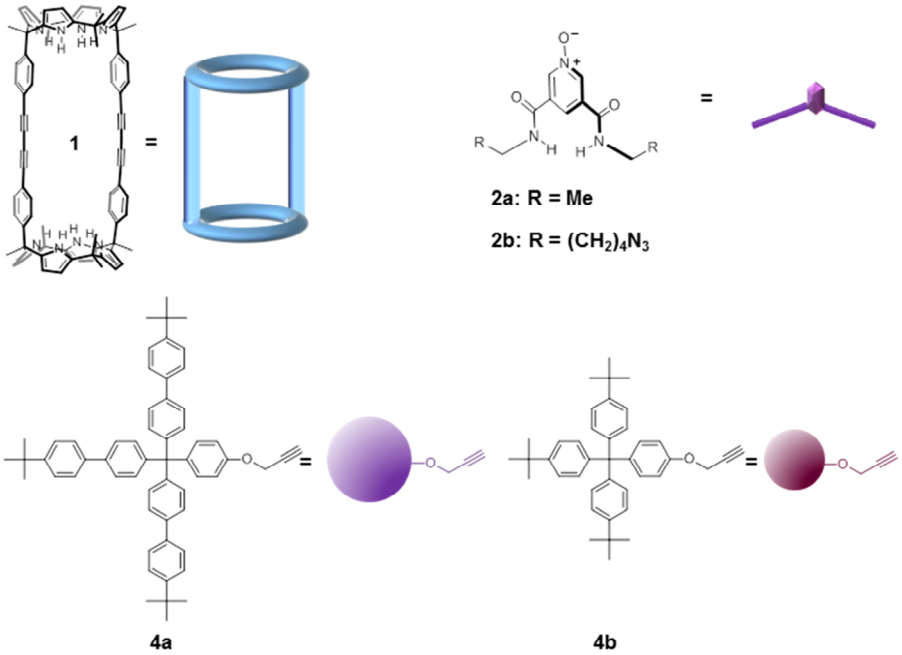

Figure 4. 1. Molecular structures of macrocycle **1**, *bis*-amidepyridyl-*N*-oxide axle **2b**, and stoppers **4a-b** used in this chapter.

We attempted the synthesis of [2]rotaxane **15** (Scheme 4. 1) under the same reaction conditions used for the synthesis of rotaxane **5**. That is, to a 10 mM equimolar mixture of **1** and **2b** in dichloromethane we added 2 equiv. of the alkyne-functionalized terphenyl stopper **4b**, 4 equiv. of diisopropyl ethyl amine (DIPEA), and a catalytic amount (5%) of $[Cu(CH_3CN)_2]PF_6$ and tris(benzyltriazoylmethyl)amine (TBTA) (Scheme 4. 1). The mixture was stirred at room temperature for 5 hours. The reaction was monitored by ^{1}H NMR spectroscopy. The ^{1}H NMR spectrum of the reaction crude at 5 hours showed broad signals that did not help us to identify the presence of the desired [2]rotaxane **15**. We were able to assign some of the signals to protons in the free macrocycle **1** and the linear component functionalized with two blocking groups **11**.

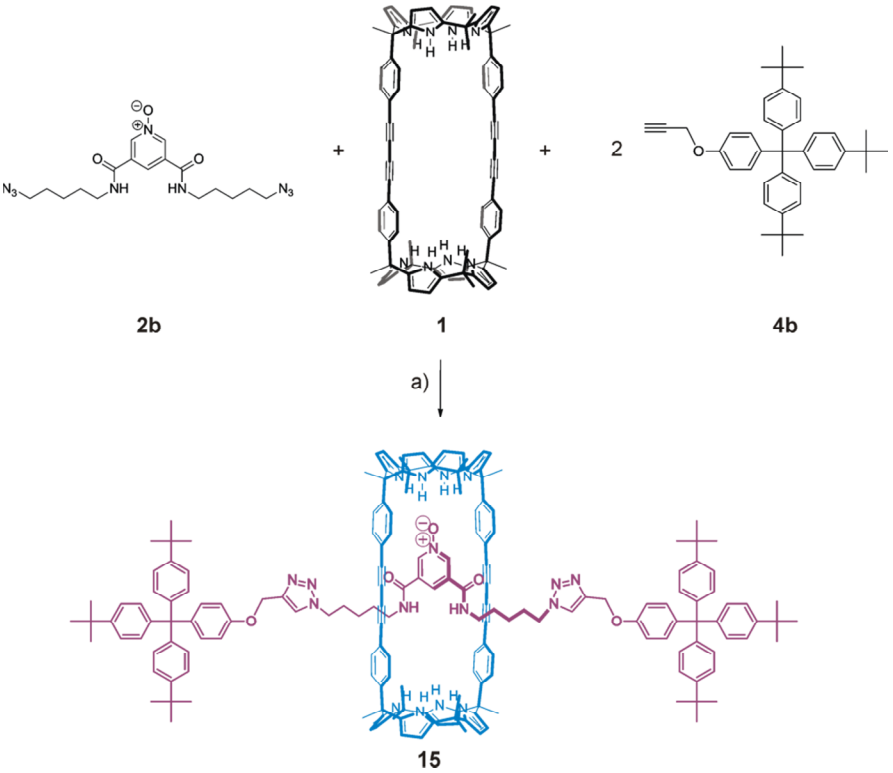

Scheme 4. 1. Synthetic scheme for the synthesis of [2]rotaxane **15**. Macrocycle **1**[50] and stopper **4a**[51] were synthetized following a reported procedure. a) Reaction conditions: $[Cu[(CH_3CN)_4PF_6]$, TBTA, DIPEA, DCM.

Purification of the reaction crude by column chromatography using 10% THF/DCM led to the isolation of two fractions corresponding to the macrocycle **1** (~90% of the starting

macrocycle) and the linear component capped with two terminal stoppers **11** (85% yield). In addition to these two fractions, we also collected a third fraction in a very reduced extent that produced a white solid upon solvent evaporation (~ 1 mg). The obtained solid was characterized using a combination of spectroscopic techniques and HRMS spectrometry. A careful analysis of the obtained spectral data suggested that the small isolated fraction corresponded to a [3]rotaxane structure instead of the desired [2]rotaxane. The complete characterization data, as well as the structure assigned to the [3]rotaxane are described in section 4.2 of this chapter.

We were really surprised with the obtained result. On the one hand, using very similar reaction conditions and the larger stopper unit **4a** we could isolate the [2]rotaxane **5** in a moderate 27% yield. However, the use of the smaller terphenyl unit **4b** as blocking group did not produce the expected [2]rotaxane at a level that was high enough to allow its isolation. On the other hand, simple molecular modelling suggested that stoppers **4b** were bulky enough to avoid dethreading of the linear component and locked the rotaxane structure with an efficient mechanical bond (Figure 4. 2).

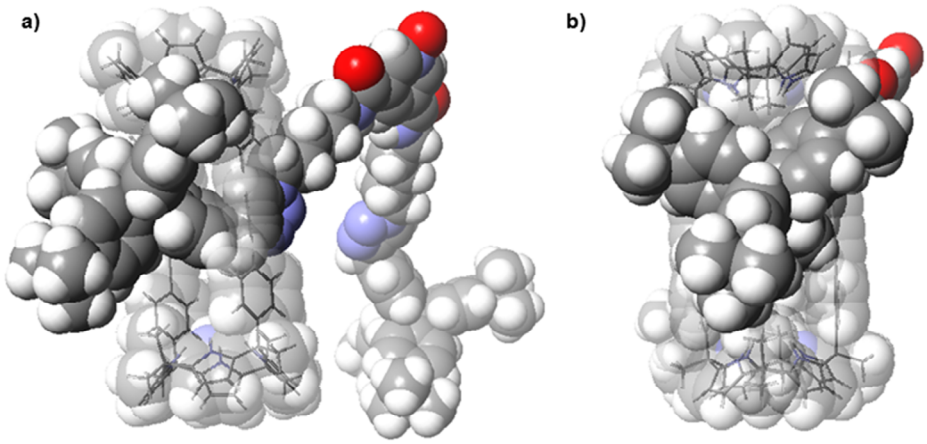

Figure 4. 2. Energy minimized structure (MM3) of the proposed [2]rotaxane **15**. The molecule is displayed in CPK representation. Macrocycle unit **1** is depicted as shadow for clarity. Linear component **11** is slightly removed from inside of the cavity for a better perspective to show the relative size between stopper **4b** and macrocycle´s cavity, side view a) front view b).

We hypothesized two different scenarios in order to explain why in the case at hand the free components (**1** and **11**) of the [2]rotaxane **15** were mainly isolated and not the desired interlocked structure. The first scenario is based on the possibility that the

monostoppered axle **13** produced an interweaved structure (**1●13**) with significantly reduced thermodynamic stability compared to the [2]pseudorotaxane (**1●2b**) used as synthetic precursor. Unknown effects may induce and reduce thermodynamic stability for the [2]-semirotaxane and force the dethreading of the axle from the macrocycle. Consequently, the second click reaction of the axle would take place in a non-threaded state yielding the two components of the [2]rotaxane free in solution instead of the interlocked structure (see Scheme 4. 2 A). Alternatively, we surmised that stoppers **4b** might not be large enough to avoid dethreading and thus the resulting [2]rotaxane **15** was not locked. Based on this second hypothesis, even if rotaxane **15** was formed, the dethreading of its interlocked components would take place, most likely, during the work-up that involved purification using silica column chromatography (see Scheme 4. 2 B).

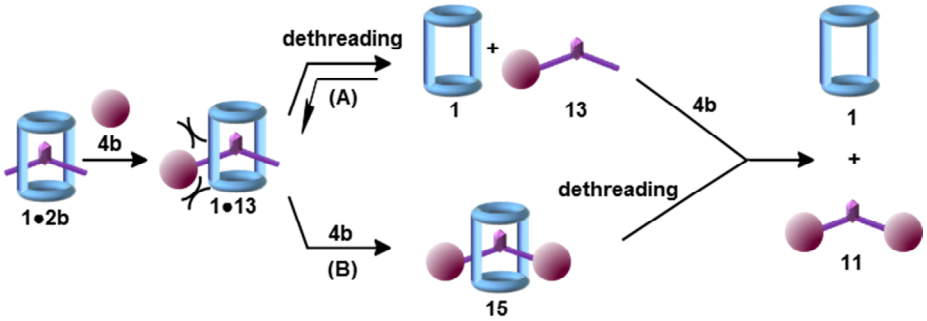

Scheme 4. 2. Schematic representation of the proposed hypothesis: first click reaction forces dethreading followed by second reaction outside of the cavity or product **15** can dethread because stoppers **4b** are not large enough to block the complex **15**.

To test our first hypothesis, (Scheme 4. 2 A) we synthesized the mono-substituted axle components, **12** and **13**, by clicking a single blocking group in the linear component precursor. Our aim, was the assessment of the thermodynamic stability constants for the [2]semirotaxanes **1●12** and **1●13** in chloroform solution (Scheme 4. 3).

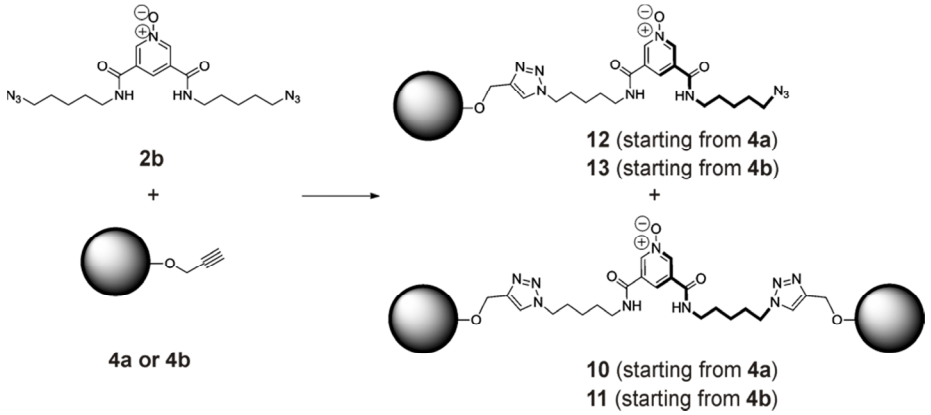

Scheme 4. 3. Synthesis of mono-click products **12** and **13**. Reaction conditions: **2b** (1 equiv.), **4a-4b** (1 equiv.),[Cu[$(CH_3CN)_4PF_6$] (0.25 equiv.), TBTA (0.25 equiv.), DIPEA (4 equiv.), DCM.

The mono-substitution reaction of the linear bis-azide **2b** was performed using a 1:1 molar ratio of either large **4a** or small **4b** alkyne functionalized stoppers (Scheme 4. 3). The "click" reaction was performed using diluted conditions (3.5 mM) in an effort to favor the mono-substitution. The isolation of the mono-functionalized derivatives **12** and **13** was not free of complications. The separation of the monosubstituted axles, **12** and **13** from the disubstituted counterparts **10** and **11**, required the use of semi-preparative HPLC (Chiralpack IA, eluent 20% THF/CH_2Cl_2).[52]

With mono-click axles **12** and **13** in our hands, we aimed to compare the thermodynamic stabilities of their interwoven assemblies with macrocycle **1** (semirotaxanes **1●12** and **1●13**) with respect to their analogue based on the axle without blocking groups (**1●2b**). Addition of incremental amounts of **12** or **13** to a millimolar dichloromethane solution of **1** produced broadening for many of the proton signals registered in the ^{1}H NMR spectra of the mixtures. This broadening was provoked, most likely, by the pirouetting process of the lineal component occurring at an intermediate rate on the ^{1}H NMR timescale. Moreover, the broadening of the signals and the disappearance of some of them beyond detection did not allow the fit of the titration data to the theoretical binding model. Consequently, the direct comparison of association constant values derived from the ^{1}H NMR titrations was not possible. These results prompted us to compare the stabilities of the interwoven structures assisted by addition of OCNTBA **3a**. We expected that the addition of the salt would produce

kinetically stable assemblies producing sharp proton signals in the ^{1}H NMR spectra of the interwoven complexes.

Previously, we reported that the addition of 1 equiv. of OCNTBA **3a** to an equimolar millimolar mixture of **1** and **2b** in $CDCl_3$ produced a dramatic change in the ^{1}H NMR spectrum of the mixture. All proton signals corresponding to **1** and **2b** become sharp and well-defined and they can easily be assigned to the quantitative formation of the pseudorotaxane complex **3a**⊂**1**•**2b** with an association constant higher than 10^4 M^{-1}.[50] The addition of 1 equiv of OCNTBA to an equimolar mixture of macrocycle **1** and monostoppered axle **12** also produced the diagnostic and sharp proton signals expected for the quantitative and exclusive formation of the semirotaxane complex **3a**⊂**1**•**12**, for which we also estimated an association constant higher than 10^4 M^{-1}, Figure 4. 3a.

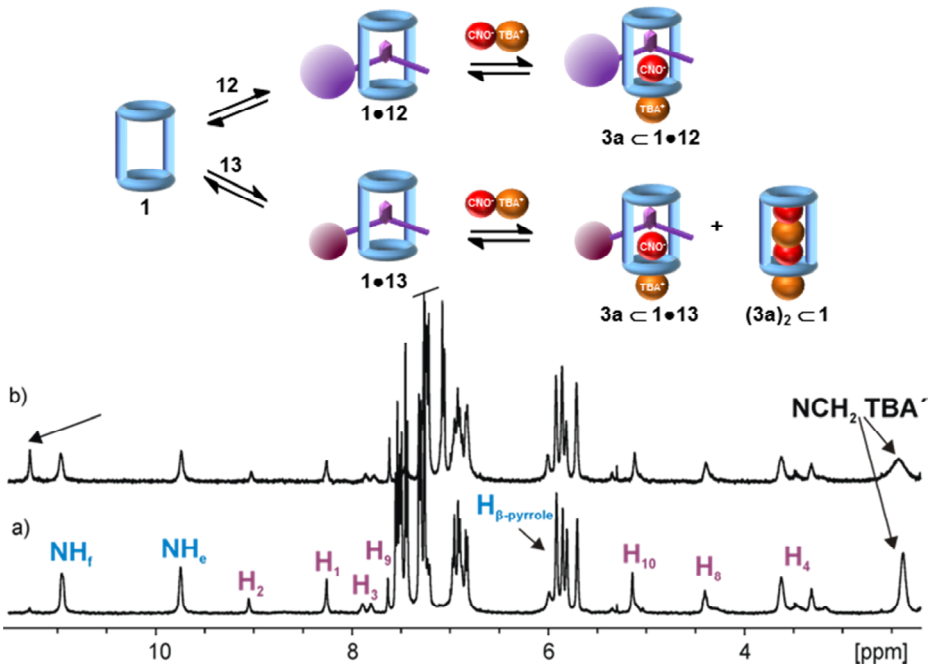

Figure 4. 3. a) Schematic representation of the solution equilibria established upon the addition of OCNTBA to separated mixture of monostoppered axles **12** and **13** with macrocycle **1**. b) ^{1}H NMR spectra ($CDCl_3$, 500 MHz, 298 K) of solutions containing equimolar amounts of **3a**, **1** and **12** a) and **3a, 1** and **13** b).

Surprisingly, the addition of 1 equiv of **3a** to an equimolar mixture of macrocycle **1** and monostoppered axle **13** produced 2 different sets of proton signals in the ^{1}H NMR

spectrum of the mixture. A careful analysis of the number of proton signals and their chemical shift values, allowed us to assign one set of signals to the semirotaxane complex **3a**⊂**1**•**13** and the other set of proton signals to the formation of the 2:1 complex (**3a**)$_2$⊂**1** (see Figure 4. 3b).[53]

This result indicated that the size of the stopper had a significant effect on the relative thermodynamic stability exhibited by the semirotaxane and the cascade complex. The non-stoppered axle **2b** and the monostoppered axle **12** featured a similar behavior in solution under the described conditions. Both of them, in an equimolar mixture of **1** and **3a** assembled exclusively and quantitatively in [2]pseudorotaxane and [2]semirotaxane complexes, **3a**⊂**1**•**2b** and **3a**⊂**1**•**12**, respectively. Conversely, monostoppered axle **13** equipped with a single and small stopper under identical conditions, produced a mixture of two assemblies with macrocycle **1**, the [2]semirotaxane **3a**⊂**1**•**13** and the 2:1 cascade complex (**3a**)$_2$⊂**1**. The effect of the stopper size in the assembly of the [2]semirotaxene is notable. However, for the monofunctionalized axle **13**, containing the small stopper **4b**, the [2]semirotaxane is still assembled to a significant extent. This finding rules out the possibility that the synthesis and subsequent isolation of the [2]rotaxane **15** is a direct consequence of the lack of assembly of the corresponding synthetic precursor with [2]semirotaxane topology.

Taking advantage of the synthesized monostoppered lineal components **12** and **13**, we decided to explore the synthesis of [2]rotaxanes using [2]semirotaxane assemblies derived from them as synthetic precursors. We applied the same reaction conditions used in the synthesis of [2]rotaxane **5** but the lineal unfunctionalized component **2b** was substituted by a monostoppered counterpart, **12** and **13**.(see Figure 4. 4 and Figure 4. 5).

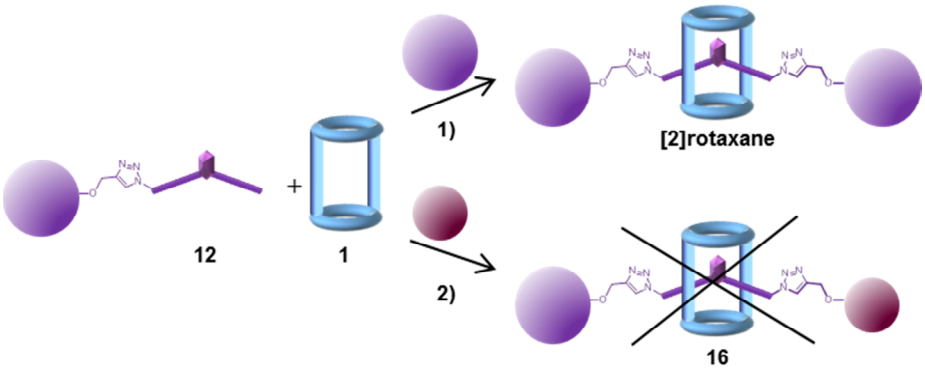

Figure 4. 4. Schematic representation for the preparation of [2]rotaxanes using monosubstituted axle **12** and large **4a** or small **4b** unit as second blocking group. Reaction conditions: **12** (1 equiv.), **4a-4b** (1 equiv.), $[Cu[(CH_3CN)_4PF_6]$ (0.05 equiv.), TBTA (0.05 equiv.), DIPEA (4 equiv.), DCM. Free lineal components **10** and **14** are also formed in reaction 1) and 2) respectively.

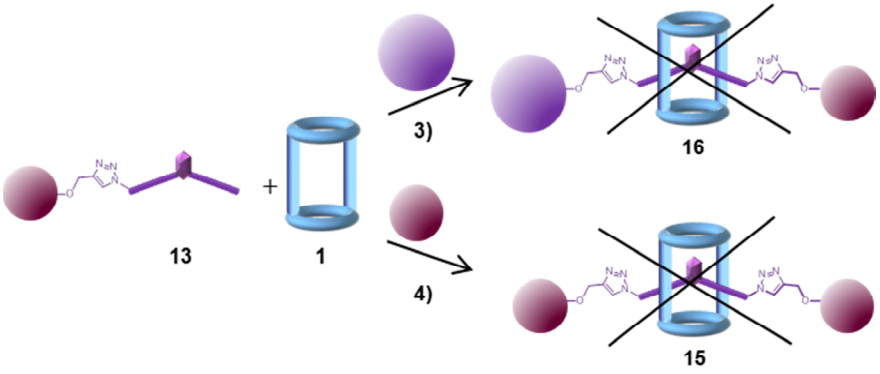

Figure 4. 5. Schematic representation for the preparation of [2]rotaxanes using monosubstituted axle **13** and large **4a** and small **4b** units as second blocking groups. Reaction conditions: **13** (1 equiv.), **4a-4b** (1 equiv.), $[Cu[(CH_3CN)_4PF_6]$ (0.05 equiv.), TBTA (0.05 equiv.), DIPEA (4 equiv.), DCM. Free lineal components **14** and **11** are also formed in reaction 3) and 4) respectively.

To a 12 mM equimolar mixture of macrocycle **1** and one of the monostoppered axles, **12** or **13**, in dichloromethane solution was added 1 equiv. of one of the alkyne-functionalized terphenyl stoppers, **4a** or **4b**, 4 equiv. of diisopropyl ethyl amine (DIPEA), a catalytic amount of $[Cu(CH_3CN)_2]PF_6$ (5%) and tris(benzyltriazoylmethyl)amine (TBTA) (5%) as ligand. The results obtained from these reactions are summarized in Table 4. 1. We concluded that the assembly with [2]rotaxane structure could only be isolated when the large **4a** units were used as

blocking groups at both ends of the linear component, (Table 4. 1, entry 1). It is worthy to note that [2]rotaxane **5** was isolated in a slightly higher yield (30%) compared to the one obtained in the previous synthesis (27%) using the lineal unsubstituted axle **2b** under more concentrated conditions. This result is in agreement with a reduction of the number of cycloaddition reactions required for the synthesis of **5** in the former synthetic strategy.

Table 4. 1. Yields of isolated macrocycle **1**, linear component (LC, **10**, **11**, **14**) and [2]rotaxane. [a] Concentrations (mM) of the axle and the blocking group used in each experiment. The concentration of the cyclic component [**1**] =12 mM in all cases. See Figure 4. 4 (exp. 1-2) and Figure 4. 5 (Exp. 3-4) for reaction schemes .[b]Isolated yields based on macrocycle **1**.

Exp.[a]	[12]	[13]	[4a]	[4b]	Recovery 1	Yield LC[b]	[2]rotaxane[b]
1	12	_	12	_	40%	59%	30%
2	12	_	_	12	96%	90%	0
3	_	12	12	_	91%	91%	0
4	_	12	_	12	87%	81%	0

The use of the smaller stopper **4b**, did not lead in any of its combinations to the isolation of the corresponding [2]rotaxane structure (neither starting from monostoppered **13** and adding stopper **4a** or **4b** nor starting from monostoppered **12** and adding **4b,** entries 2-4 from Table 4. 1). In all the attempts, almost quantitative amounts of the free components of the putative [2]rotaxane were recovered after column chromatography purification of the reaction crude (from 87-96 % of macrocycle **1** is recovered).

We have evidenced the assembly of the [2]semirotaxane in solution using axle **13**. Therefore, considering the results summarized in the Table 4. 1, we concluded that, most likely the stopper unit **4b** was not large enough to prevent de disassembly of the assembly **15** and the interwoven assembly with two different terminal blocking units, **4a** and **4b**, in its lineal component. Most likely, the complete dethreading of the interlocked components takes place during the work-up of the reaction, especially in the column chromatography purification.

Nevertheless, the dethreading hypothesis requires additional results in order to be substantiated beyond any reasonable doubt. For example, slipping experiments

performed using the doubly stoppered lineal component **11** with small blocking units **4b** and macrocycle **1** are expected to produce the corresponding [2]psedorotaxane assembly in the presence of **1** equiv. of a suitable salt (i.e **3a**). The slipping approach is a synthetic strategy used for the synthesis of rotaxanes. In this methodology the macrocycle slips over one of the axle stoppers.[54] This strategy usually requires heating the mixture of macrocycle and axle components at high temperatures in order to overcome the energy barrier to afford the interlocked structure. Upon cooling the solution to room temperature the interlocked structure is kinetically trapped as a result of the high energy required for the deslipping (Figure 4.6).[6] In addition, the favorable interactions stablished between the macrocycle and axle components in the interlocked structure, compared to the free components, stabilize the interlocked assembly and increases de energy required for its dissociation.

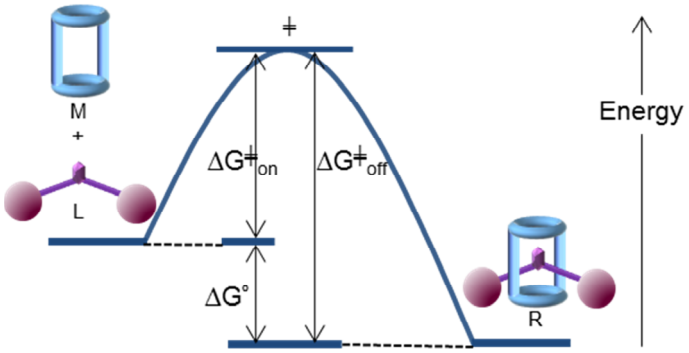

Figure 4. 6. Schematic representation of the slipping approach for rotaxanes formation. M, L and R denote Macrocycle, Linear component and Rotaxane respectively. $\Delta G^{\ddagger}_{on}$ is overcome by heating a solution of M and L. To obtain a stable rotaxane $\Delta G^{\ddagger}_{off} > \Delta G^{\ddagger}_{on}$ ($\Delta G^{o} = \Delta G^{\ddagger}_{off} - \Delta G^{\ddagger}_{on}$).

Unfortunately, under the conditions tested, we have no evidence of the functioning of the slipping process in the assembly of **1** and **11** assisted by **3a**. We hypothesize that the mixture may be trapped in a kinetic minimum or that the interwoven structure is not the thermodynamic energy minimum in this case.

4.2.2 Characterization of a new species

As mentioned in the first part of this chapter, during the purification of the multiple reaction attempts performed to synthesize rotaxane **15** using the small stopper units **4b**,

we detected the presence of a new species in a very small amount. This unknown compound had an Rf very similar to the one corresponding to rotaxane **5**. Luckily, we were able to isolate few fractions containing this species **17** as a pure compound when performing a silica column chromatography purification of the reaction crude using 10% THF/DCM as eluent. Solvent evaporation of the combined fractions produced a white solid that was characterized by a set of high-resolution spectra (NMR spectroscopy and MS spectrometry.

The ^{1}H NMR spectrum of the white solid in $CDCl_3$ solution displayed both sharp and broad signals corresponding to the protons of the macrocycle as well as those in the lineal axle (Figure 4. 7). The β-pyrrole protons appeared as two separate signals resonating at 5.9 and 5.6 ppm. These signals were upfield shifted in comparison to those of the free macrocycle and to [2]rotaxane **5**. The pyrrole NHs appeared as a broad band centered at ~9 ppm. This signal was significantly downfield shifted with respect to the chemical shift value determined for the same protons in the free macrocycle. The aromatic protons of the macrocycle walls and the proton signals corresponding to the terphenyl stoppers overlapped. The triazole proton of the axle component resonated as a singlet at 7.5 ppm.

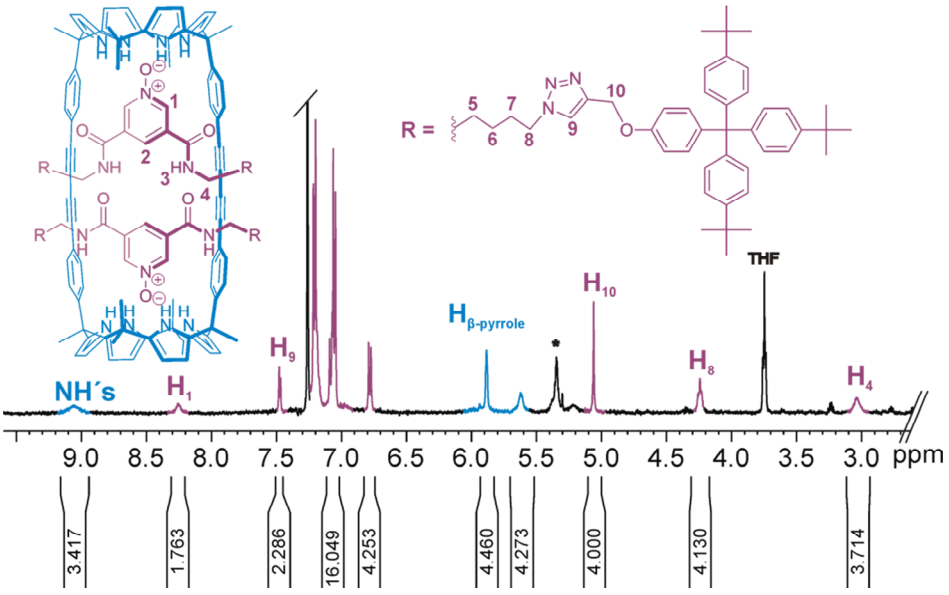

Figure 4. 7. ^{1}H NMR spectrum of [3]rotaxane **17** ($CDCl_3$, 500 MHz, 298 K). Bottom part is indicated the integral values for each signal. (*) Impurity.

Surprisingly, the relative integral values of the signals corresponding to the β-pyrrole protons of the macrocycle and the ones corresponding to the axle were not in accordance with the 1:1 molar ratio expected for a [2]rotaxane complex. This observation prompted us to discard the assignment of [2]rotaxane topology to this new species. Conversely, the relative integral values for axle-to-ring protons were in agreement with a 2:1 axle:macrocycle ratio. This finding strongly suggested that two axle units were present in the assembly with one macrocycle.

Increasing the temperature to 328 K produced the sharpening of some signals and allowed the observation of the signal for the H_2 protons in the lineal axle that was broadened at room temperature. The signal of the amide protons overlapped with those of the aromatic protons corresponding to the terphenyl stoppers at ~7.1 ppm. By lowering the temperature, we observed both sharpening of some of the signals and broadening of others that did not provided any additional information for the structural assignment. 2D NMR experiments were useful for the assignment of some proton signals. A COSY experiment (Figure 4. 8) revealed the existence of cross peaks due to scalar coupling between the two chemically unequivalent β-pyrrole protons. We also observed cross peaks that related the triazole protons H_9 with the protons H_{10} of the axle component.

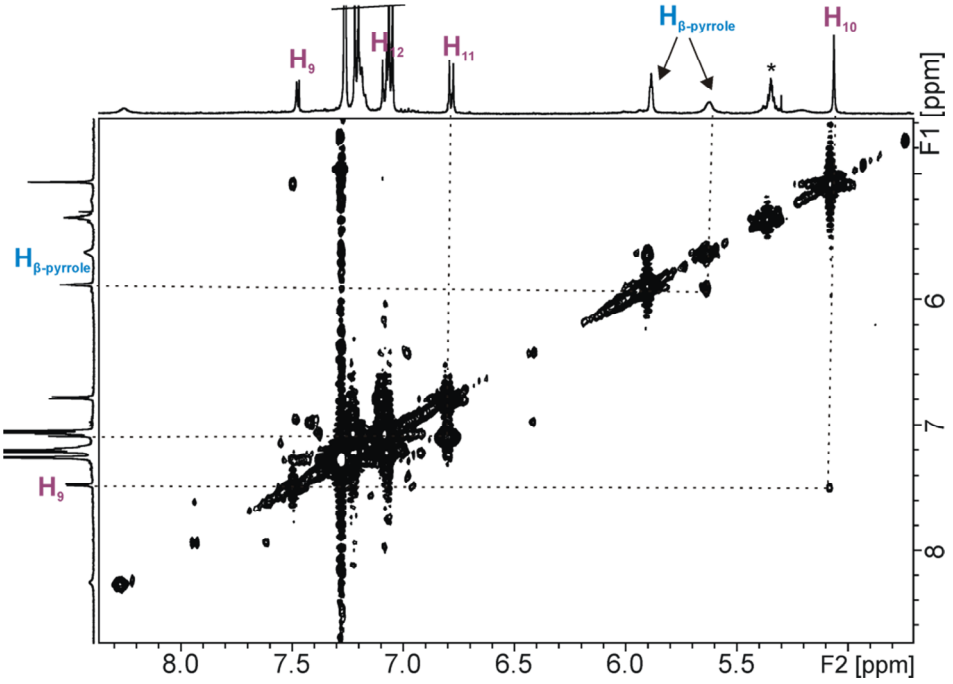

Figure 4. 8. Selected downfield region of the COSY experiment ($CDCl_3$, 500 MHz, 298 K) of a millimolar solution of [3]rotaxane showing the assignment of some relevant cross-peaks. (*) Impurity.

Interestingly, a ROESY NMR experiment (Figure 4. 9) showed through space close contact cross peaks between the β-pyrrole protons and the proton H_1 of the *N*-oxide moiety in the axle. This observation is in accordance with the inclusion of the *N*-oxide unit of the axle inside of the macrocycle´s cavity by hydrogen bonding to the calix[4]pyrrole core.

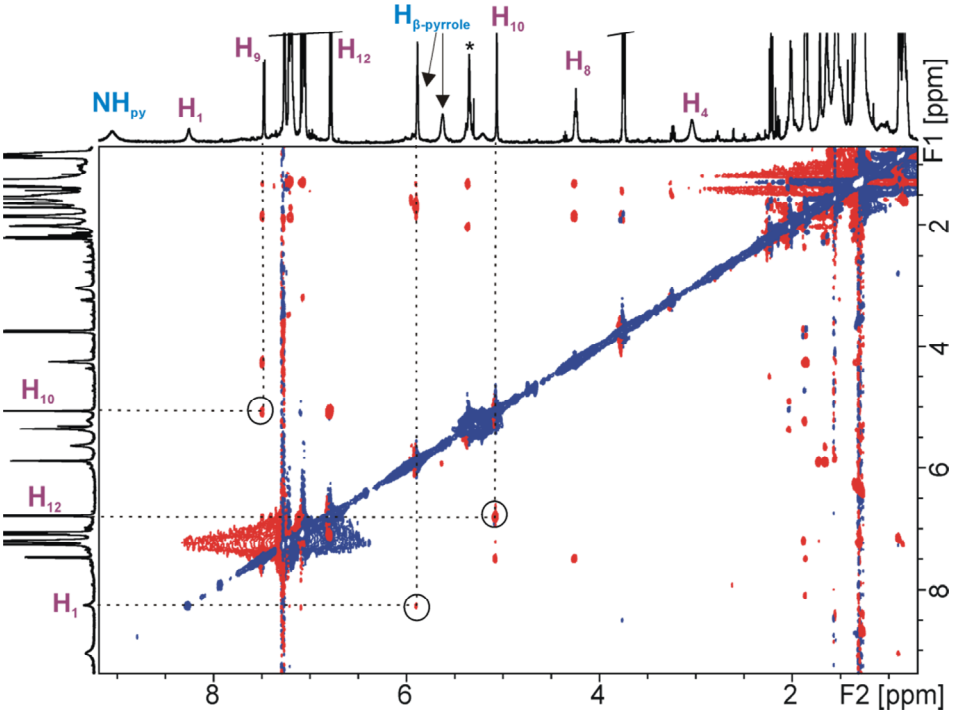

Figure 4. 9. Selected region of the ROESY experiment ($CDCl_3$, 500 MHz, 298 K) of a millimolar solution of [3]rotaxane showing the assignment of some relevant cross-peaks. (*) Impurity.

Finally, we performed a Diffusion Ordered Spectroscopy (DOSY) NMR experiments of a millimollar solution of **17** in $CDCl_3$, (Figure 4. 10). The DOSY NMR showed that the diffusion constant values calculated for the decay of the proton signals´ intensities corresponding to the linear axle and to the macrocycle were identical. Considering the difference in the size of the two molecular components, this result indicated that both were involved in the formation of a unique species. We determined a diffusion constant value of 3.89×10^{-10} m^2/s. Remarkably, this value is smaller than the diffusion constant obtained for the free macrocycle (6.74×10^{-10} m^2/s) or even slightly smaller than the one determined for [2]rotaxane **5** (4.29×10^{-10} m^2/s) in the same solvent. Taken together, these results indicated that the new isolated species had a larger hydrodynamic radius than the previous described [2]rotaxane **5**.

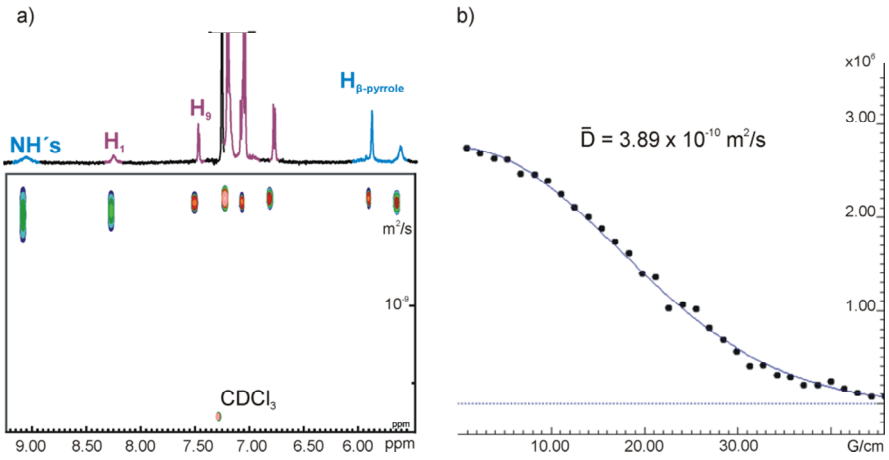

Figure 4. 10. ^{1}H pseudo-2D DOSY ($CDCl_3$, 500 MHz, 298 K) of a millimolar solution of [3]rotaxane **16** (a) and fit of the decay in the peak height at 5.88 ppm to a monoexponential function (b).

Based on the NMR spectroscopy results and simple molecular modeling studies, we propose that the new isolated species corresponds to a molecule with [3]rotaxane topology, **17**. Compound **17** features two axles threading the macrocycle´s cavity. (Figure 4. 11).

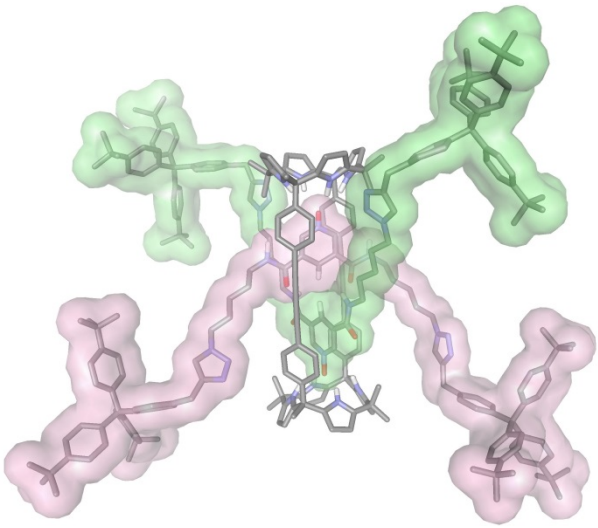

Figure 4. 11. Energy minimized structure (MM3) of the putative double-threaded [3]rotaxane **17**. The double-thread is depicted with van der waals surface. Non-polar hydrogens were removed for clarity.

It is worthy to note that we did not isolate any compound with [3]rotaxane topology when using the bigger stopper units **4a**. Most likely, the use of the smaller stopper units **4b** allows the interwoven assembly of two axles minimizing steric clashes between them.

In the proposed energy minimized structure of the putative [3]rotaxane **17,** macrocycle **1** contains one hydrogen-bonded *N*-oxide unit of an axle in each of its two hemispheres without noticeable distortion of its cyclic structure compared to the unthreaded or monothreaded states. Each *N*-oxide pyridyl residue in **17** establishes four hydrogen bond interactions with the calix[4]pyrrole core in one hemisphere of the macrocycle. Moreover, amide groups of one lineal axle can also establish hydrogen bond interactions with the amide group of the adjacent *N*-oxide unit bound on the opposite hemisphere.[55] Two possible conformations of the lineal threads in **17** stablishing hydrogen bonds interactions are depicted in Figure 4. 12.

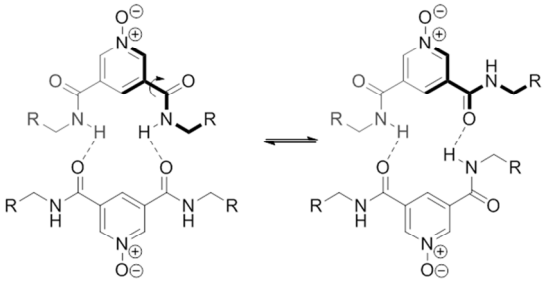

Figure 4. 12. Possible conformations by hydrogen bond interactions between two pyridine *N*-oxide units inside of the macrocycle cavity.

Analysis of the crude reaction mixture by HPLC provided further evidence for the formation of this new species. The comparison of the HPLC traces of the reaction crudes obtained in the synthesis of [2]rotaxane **5** and the putative [3]rotaxane **17** assigned a higher retention time for the new species **17** compared to **5** (7% THF/DCM) (Figure 4. 13). This result is in agreement with the expected higher polarity of **17** provided by the presence of two *N*-oxide axles in its structure.

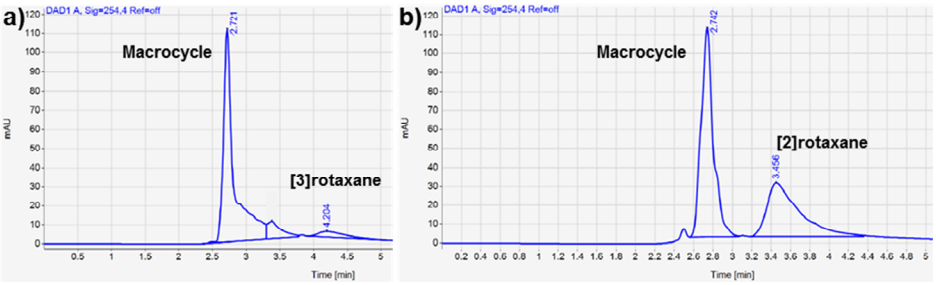

Figure 4. 13. HPLC traces of a millimolar aliquot[56] from crude reaction for [3]rotaxane synthesis a) and from crude reaction of [2]rotaxane synthesis b). [3]rotaxane retention time (4.2 min) is higher than for [2]rotaxane (3.4 min) under the same chromatographic conditions (7% THF/CH_2Cl_2). Both rotaxane signals appear as broad peak.

Previously, we observed that the UV-vis spectrum of [2]rotaxane **5** featured a red shift (~2 nm) of the bands assigned to the macrocyclic unit (maxima at 300, 320 and 343 nm) in comparison to the free compound **1** (maxima at 298, 318 and 341 nm).

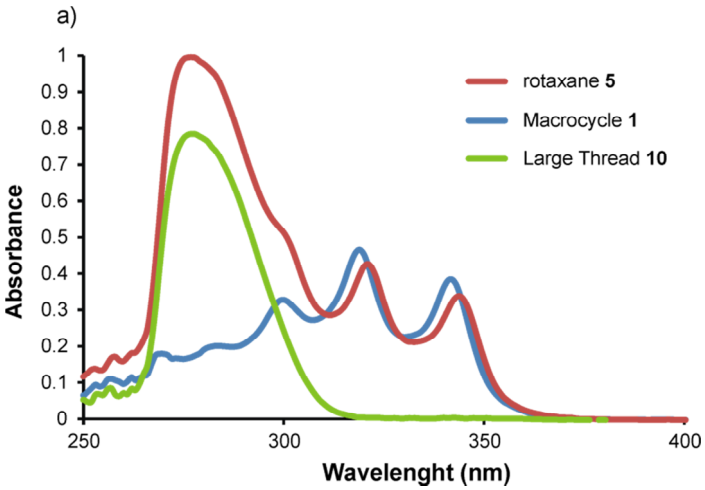

Figure 4. 14. UV-visible spectra of micromolar CH_2Cl_2 solutions of: a) free macrocycle **1** (blue line), linear component **10** (green line) and [2]rotaxane **5** (red line).

Identical spectroscopic changes were observed in the UV-vis spectrum of the putative [3]rotaxane **17**, which provide additional evidence to its interwoven topology (maxima at 300, 320 and 343 nm), Figure 4. 15 b.

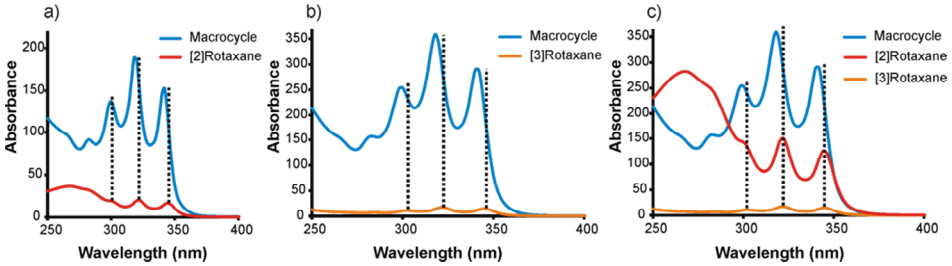

Figure 4. 15. Comparison of the UV-visible spectra of macrocycle **1** (blue line), [2]rotaxane **5** (red line) and new species **17** (orange line). The spectra were selected from the UV-vis of the peaks obtained in the HPLC analysis of crude reactions obtained in the synthesis of rotaxanes with large and small stoppers. Reaction conditions Scheme 4. 2.

Finally, we were able to identify an ion-peak with the exact mass and isotopic patterns expected for the molecular formula of the double-threaded [3]rotaxane **17** using ESI-HRMS$^+$ spectrometry.

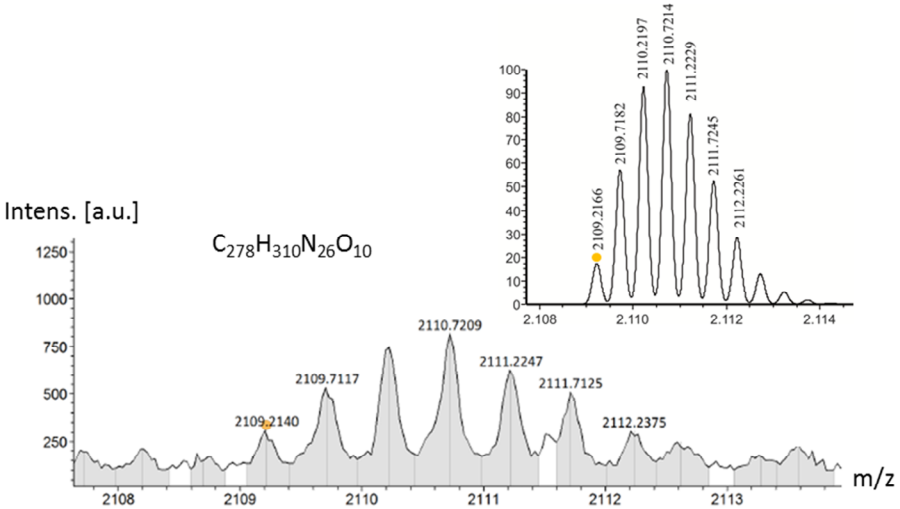

Figure 4. 16. Simulated and experimental HR-MS (ESI-TOF ES+) of [3]rotaxane. m/z calculated for $C_{278}H_{310}N_{26}O_{10}Na_2$ ([M+2Na])$^{2+}$ 2109.2166, found ([M+2Na])$^{2+}$ 2109.2140.

It is worthy to note that the putative [3]rotaxane **17** was isolated in very low yields (< 5%). Modification of the reaction conditions in order to favor its formation (2 equiv. of **2b**, 12 mM) did not result in any yield improvement. Moreover, a careful analysis of all the column chromatography fractions isolated during the synthesis of rotaxane **5** using the same eluting conditions than the ones used to isolate **17** did not evidence the presence of species featuring [3]rotaxane topology when using the big stopper units **4a**.

Scheme 4. 4 shows a schematic representation of the plausible equilibria that are involved in the production of **5** and **17**. When large stopper units **4a** are used, only the compound with [2]rotaxane topology was isolated (steps a and b from Scheme 4. 4). Most likely, the larger size of the stopper units hinders the accommodation of two threads within the macrocyclic unit and prevents the formation of [3]pseudorotaxane assemblies as precursor intermediates in the synthesis of the [3]rotaxane (steps d-g, Scheme 4. 4).

On the other hand, when small stopper units **4b** are used, the free components and a compound with putative [3]rotaxane topology are isolated. Most probably, the size of the stopper unit **4b** is not large enough to prevent the deslipping process (step c, Scheme 4. 1) yielding the free components in solution. In addition, the reduced size of the stoppers would allow the presence of two lineal axles within the macrocycle cavity (steps d-g, Scheme 4. 4) yielding the [3]rotaxane species. The inclusion of two threads in the macrocycle cavity driven by hydrogen bonding interactions must overcome the steric clashes that may be present in the crowded environment of the assembly. This interpretation explains the poor yield obtained for [3]rotaxane **17**.

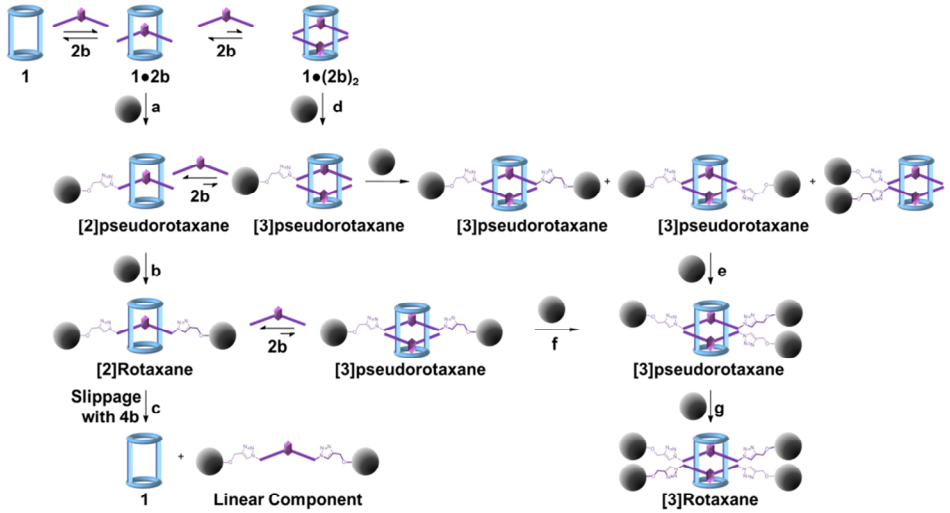

Scheme 4. 4. Schematic representation of the plausible equilibria and possible intermediate species involved in the formation of the [2]rotaxane **5** and [3]rotaxane **17**.

We are working in optimizing the structures of molecular components that would increase the formation of related compounds with [3]rotaxane topology. We consider

that favorable components would involve the use of longer chains. A larger chain[19,20] in the substituted pyridine *N*-oxide would diminish steric clashes between the stoppers. These suggestions would be directed to stabilize the **1●(11-13)** species, the intermediate previous to [3]rotaxane formation. Other factors must be taken into account such as stoichiometry (excess of axle component) and concentration.

4.3 Conclusions

In summary, we concluded that the size of the stopper (tris(biphenyl) stopper **4a** or terphenyl stoppers **4b**) used for the stoppering reaction in the formation of the interlocked structure involving bis(calix[4]pyrrole) macrocycle **1** and 3,5-bis-amidepyridyl-*N*-oxide derivative axle have a strong effect on the final structure isolated. While the use of large stoppers **4a** yields the final interlocked structure **5** described in Chapter 2, the use of small stoppers **4b** mainly led to the recovery of free macrocycle **1** (~90% of the starting macrocycle) and the free linear component **11** from the reaction mixture. We hypothesized that most likely stoppers **4b** might not be large enough to lock the [2]rotaxane **15** assembly and dethreading of the interlocked components can take place during the work-up. However, so far, we have not been able to demonstrate the opposite process, the slippage of the lineal component **11** through the macrocycle **1**. Moreover, we identified the formation of a new species in a very reduced amount when using the small stopper unit **4b**. We assigned a doubly threaded structure to this compound, that is a [3]rotaxane. We characterized structurally [3]rotaxane **17** through a combination of HPLC analysis, NMR spectroscopy and ESI-HRMS$^+$ spectrometry.

4.4 Experimental section

4.4.1 General information and instrumentation

All reagents were obtained from commercial suppliers and used without further purification. Anhydrous solvents were obtained from a solvent purification system SPS-400-6 from Innovative Technologies, Inc. All solvents were of HPLC grade quality, commercially obtained and used without further purification. Routine ^{1}H NMR spectra were recorded on a Bruker Avance II 400 Ultrashield NMR spectrometer. Variable

temperature experiments and 2D NMR spectra were performed on a Bruker Avance 500 (500.1 MHz for ^{1}H NMR) Ultrashield spectrometer. $CDCl_3$ from Sigma Aldrich was used for NMR studies. Chemical shifts are given in ppm, relative to TMS. Analytical HPLC experiments were performed using a HPLC1100 Agilent instrument.[57] UV-Vis measurements were carried out on a Shimadzu UV-2401PC spectrophotometer equipped with a photomultiplier detector, double beam optics and D2 and W light sources.

4.4.2 Synthetic procedures

3-(4-(Tris(4'-tert-butylbiphen-4-yl)methyl)phenoxy)propyne **4a**,[51] and 1-(prop-3-ynoxy)-4-(tris-(4-tert-butyl-phenyl)-methyl)-benzene **4b**,[58] were synthesized according to reported procedures.

*General procedure for the synthesis of half-threads **12** and **13**:*

A mixture of **2b** (150 mg, 0.372 mmol), **4a** (272 mg, 0.353 mmol), $Cu(CH_3CN)_4PF_6$ (39.6 mg, 0.100 mmol) and TBTA (49.3, 0.100 mmol) were dissolved in dry CH_2Cl_2 (50 mL) in a two necked round bottom flask (100 mL). Finally, *N*-ethyl-*N*-isopropylpropan-2-amine (260µL, 1.487 mmol) was added to the reaction mixture. The reaction was stirred at room temperature under argon. After 3 hours, the crude was washed with water (2x40 mL). The organic layer was dried over anhydrous Na_2SO_4 and concentrated *in vacuo*. The residue was redisolved in CH_2Cl_2 and precipitated with acetonitrile. The mixture was filtered and the resulting solid containing half-thread and linear component was purified by chiral semi-preparative HPLC column chromatography.[52] Eluent 20% THF/CH_2Cl_2 for large half-thread **12** purification and 17% THF/CH_2Cl_2 for small half-thread **13** purification. We obtain the desired product as a white solid (85 mg, 54%).

^{1}H NMR (400 MHz, Chloroform-*d*) of **12**, δ 8.78 (s, 2H, H_1), 8.28 (t, J = 5.5 Hz, 1H, $H_{3'}$), 8.13 (s, 1H, H_2), 7.65 (s, 1H, H_9), 7.54 (d, J = 8.5 Hz, 6H, H_{15}), 7.50 (d, J = 8.5 Hz, 6H, H_{14}), 7.44 (d, J = 8.5 Hz, 6H, H_{16}), 7.30 (d, J = 8.5 Hz, 7H, H_{13}-H_3), 7.24 (d, J = 9.0 Hz, 2H, H_{12}), 6.85 (d, J = 9.0 Hz, 2H, H_{11}), 5.09 (s, 2H, H_{10}), 4.44 (t, J = 6.3 Hz, 2H,

$H_{8'}$), 3.44 (m, 4H, H_4, $H_{4'}$), 3.19 (t, J = 6.8 Hz, 2H, H_8), 1.96 (m, 2H, $H_{7'}$), 1.59 (m, 8H, H_5, $H_{5'}$, H_7, H_6), 1.40 (m, 2H, $H_{6'}$), 1.35(s, 27H, CH_3-*t*But).

$^{13}C\{^1H\}$ NMR (101 MHz, $CDCl_3$) of **12**, δ 162.76, 156.30, 150.43, 145.84, 140.56, 140.23, 138.65, 137.80, 134.31, 133.82, 132.60, 131.60, 126.77, 126.16, 125.90, 123.54, 122.80, 116.56, 113.64, 63.87, 61.76, 51.42, 49.89, 40.29, 39.91, 34.73, 31.56, 29.24, 29.05, 28.66, 27.52, 24.29, 22.76.

HR-MS (ESI-TOF ES+) of **12**, m/z calculated for $C_{75}H_{83}N_9O_4Na$ $([M+Na])^+$ 1196.6456, found $([M+Na])^+$ 1196.6421

^1H NMR (400 MHz, Chloroform-*d*) of **13** δ 8.80 (s, 2H, H_1), 8.44 (m, 1H, $H_{3'}$), 8.09 (s, 1H, H_2), 7.67 (s, 1H, H_9), 7.23 (d, J = 8.6 Hz, 6H, H_{14}), 7.09 (d, J = 8.9 Hz, 2H, H_{12}), 7.12 (d, J = 8.6 Hz, 6H, H_{13}), 6.98 (m, 1H, H_3) 6.78 (d, J = 8.9 Hz, 2H, H_{11}), 5.07 (s, 2H, H_{10}), 4.48 (t, J = 6 Hz, 2H, $H_{8'}$)3.47 (m, 4H, H_4, , $H_{4'}$), 3.18 (t, J = 6.7 Hz, 2H), 1.98 (m, 2H, $H_{7'}$), 1.70 (m, 2H, H_5), 1.60 (m, 2H, $H_{5'}$), 1.54 (m, 2H, H_7), 1.37 (m, 4H, H_6, $H_{6'}$), 1.29(s, 27H, CH_3-*t*But).

^{13}C NMR (101 MHz, $CDCl_3$) of **13** δ 162.69, 156.02, 154.46, 152.79, 148.67, 144.16, 140.83, 138.71, 132.69, 130.90, 124.31, 121.60, 113.23, 63.29, 61.60, 51.43, 40.24, 39.86, 34.53, 31.60, 29.93, 29.13, 29.02, 28.68, 27.15, 25.79, 24.31.

HR-MS (ESI-TOF ES+) of **13**, m/z calculated for $C_{57}H_{71}N_9O_4Na$ $([M+Na])^+$ 968.5521, found $([M+Na])^+$ 968.5503.

General procedure for the synthesis of [2]rotaxane and [3]rotaxane:

Conditions a (starting from large half-thread **12**): Macrocycle **1** (39.80 mg, 0.033 mmol), large half-thread **12** (39.00 mg, 0.033 mmol), **4a** (25.6 mg, 0.033 mmol), TBTA (1.42 mg, 2.68×10^{-3} mmol) and the catalyst $Cu[(CH_3CN)_4PF_6]$ (1.00 mg, 2.68×10^{-3} mmol) were placed in a two necked round bottom flask (25 mL) and dissolved in dry DCM (2.7 mL). Finally, the Hünig's base (0.023 ml, 0.133 mmol) was added to the reaction mixture and was stirred at room temperature under Ar for 5 hours. The reaction could be monitored by TLC (2% MeOH/DCM, Rf rotaxane=0.36; Rf macrocycle=1; Rf linear component=0). The reaction mixture was washed with water (2×40 mL). The organic phase was dried over anhydrous Na_2SO_4 and the solvent was removed *in vacuo*.

The residue was purified by column chromatography (30% AcOEt/DCM) to give the desired product as a white solid (31 mg, 30%). Upon changing the eluent to 5% MeOH/DCM we could isolate the free linear component. Reaction between **12** with small stopper **4b** did not afford the product. Recovery unreacted macrocycle and linear component **14** (Table 4. 1).

^{1}H NMR (400 MHz, Chloroform-*d*) of **14** δ 8.76 (s, 1H, H_1), 8.11 (m, 2H, H_3), 7.65 (s, 2H, H_1), 7.54 (d, *J* = 8.5 Hz, 8H, H_{15}, H_9), 7.50 (d, *J* = 8.5 Hz, 6H, H_{14}), 7.47 (d, *J* = 8.5 Hz, 6H, H_{16}), 7.30 (d, *J* = 8.5 Hz, 8H, $H_{13,}$ H_{12}), 7.22 (d, *J* = 8.5 Hz, 6H, $H_{14'}$), 7.10 (d, *J* = 8.8 Hz, 2H, $H_{12'}$), 7.06 (d, *J* = 8.5 Hz, 6H, $H_{13'}$), 6.83 (d, *J* = 8.8 Hz, 2H, H_{11}), 6.75 (d, *J* = 8.8 Hz, 2H, $H_{11'}$), 5.49 (s, 2H, H_{10}), 5.03 (m, 2H, $H_{10'}$), 4.35 (m, 4H, H_8), 3.45 (s, 4H, H_4), 1.85 (s, 4H, H_5), 1.63 (br, 8H, H_6, H_7), 1.35 (s, 27H, H_{17}), 1.29 (s, 27H, $H_{17'}$).

HR-MS (ESI-TOF ES+) of **14**, m/z calculated for $C_{115}H_{129}N_9O_5Na$ $([M+Na])^+$ 1739.0009, found $([M+Na])^+$ 1739.0009.

Conditions b (starting from small half-thread **13**): Macrocycle **1** (25.30 mg, 0.021 mmol), half-thread **13** (20.00 mg, 0.021 mmol), **4b** (16.30 mg, 0.021 mmol), TBTA (0.60 mg, 1.05×10^{-3} mmol) and the catalyst $Cu[(CH_3CN)_4PF_6]$ (0.40 mg, 1.05×10^{-3} mmol) were placed in a two necked round bottom flask (25 mL) and dissolved in dry DCM (1.7 mL). Finally, the Hünig's base (0.015 mL, 0.085 mmol) was added to the reaction mixture and was stirred at room temperature under Ar for 5 hours. The reaction could be monitored by TLC (2% MeOH/DCM, Rf rotaxane=0.36; Rf macrocycle=1; Rf linear component=0). The reaction mixture was washed with water (2×40 mL). The organic phase was dried over anhydrous Na_2SO_4 and the solvent was removed *in vacuo*. The residue was purified by column chromatography (10% THF/DCM) followed by 5% MeOH/DCM to isolate the free linear component (**11** or **14**). The reaction did not afford the desired product. The reaction between small half-thread **13** with **4a** or **4b** did not form any rotaxane product.

^{1}H NMR (400 MHz, Chloroform-*d*) of **11** δ 8.78 (s, 2H, H_1), 8.16 (m, 3H, H_2, H_3), 7.54 (s, 2H, H_9), 7.22 (d, *J* = 8.6 Hz, 12H, H_{14}), 7.10 (d, *J* = 8.8 Hz, 4H, H_{12}), 7.06 (d, *J* = 8.6 Hz, 12H, H_{13}), 6.76 (d, *J* = 8.8 Hz, 4H, H_{11}), 5.03 (s, 4H, H_{10}), 4.36 (t, *J* = 6.5 Hz, 4H, H_8), 3.44 (m, 4H, H_4), 1.87 (m, 4H), 1.67 (m, 2H), 1.34 (m, 2H)1.29(s, 27H, CH_3-*t*But).

^{13}C NMR (101 MHz, $CDCl_3$) of **11** δ 163.02, 156.14, 148.62, 144.19, 140.70, 132.62, 130.90, 124.29, 113.29, 63.28, 61.73, 60.61, 49.88, 39.74, 34.51, 31.60, 29.40, 27.77, 22.89, 14.42.

HR-MS (ESI-TOF ES+) of **11**, m/z calculated for $C_{97}H_{117}N_9O_5Na_2$ $([M+2Na])^{2+}$ 766.9481, found $([M+2Na])^{2+}$ 766.9465.

4.4.3 Experimental section: Figures

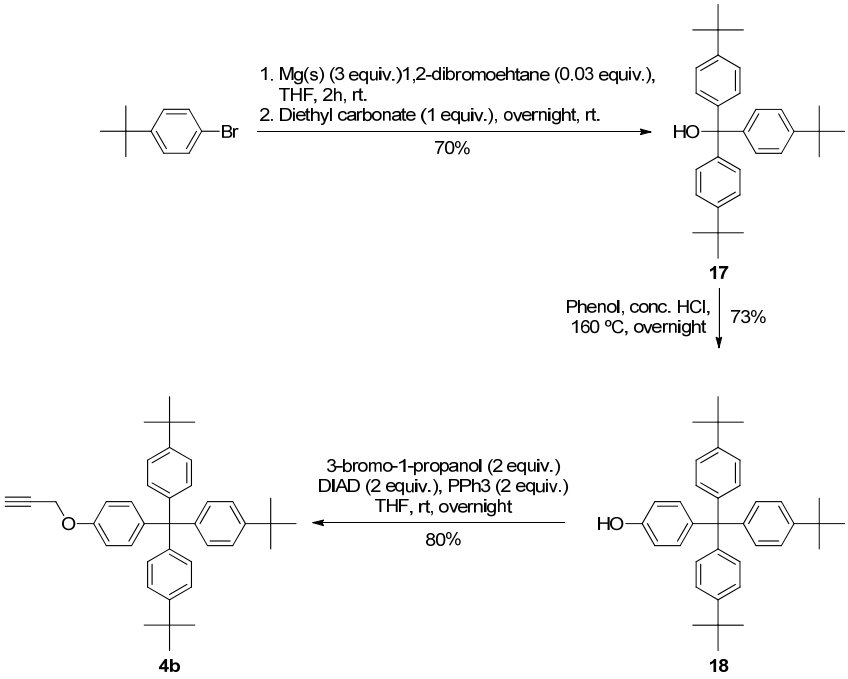

Figure 4. 17. Schematic synthesis of small stopper **4b**.[58]

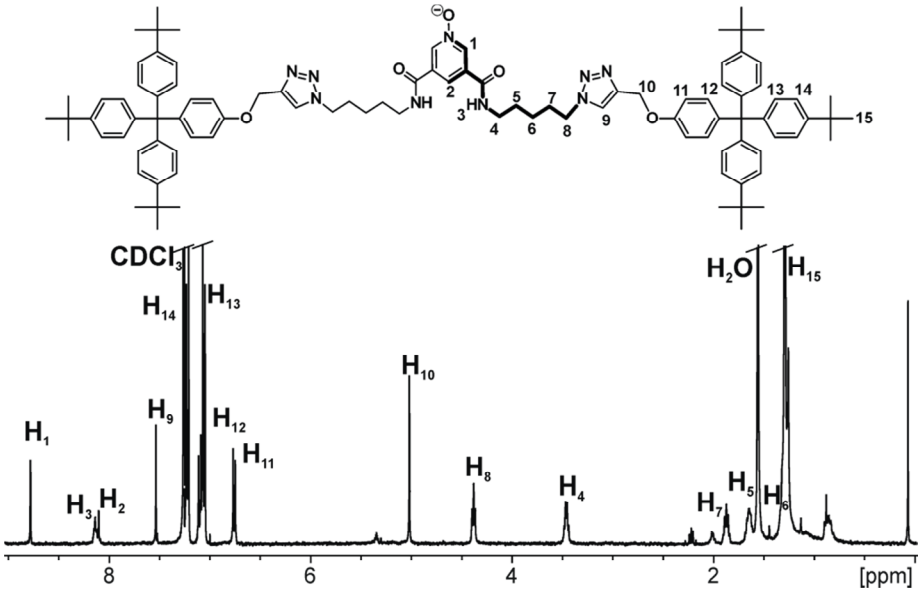

Figure 4. 18. ^{1}H NMR spectrum of linear component **11** ($CDCl_3$, 400 MHz, 298K).

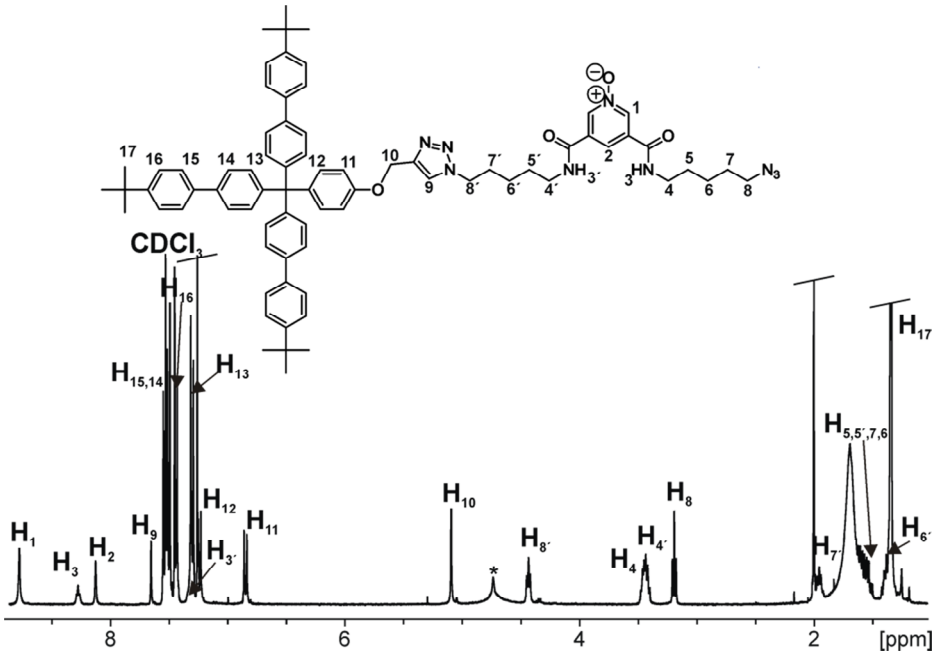

Figure 4. 19. ^{1}H NMR spectrum of linear component **12** ($CDCl_3$, 400 MHz, 298K).

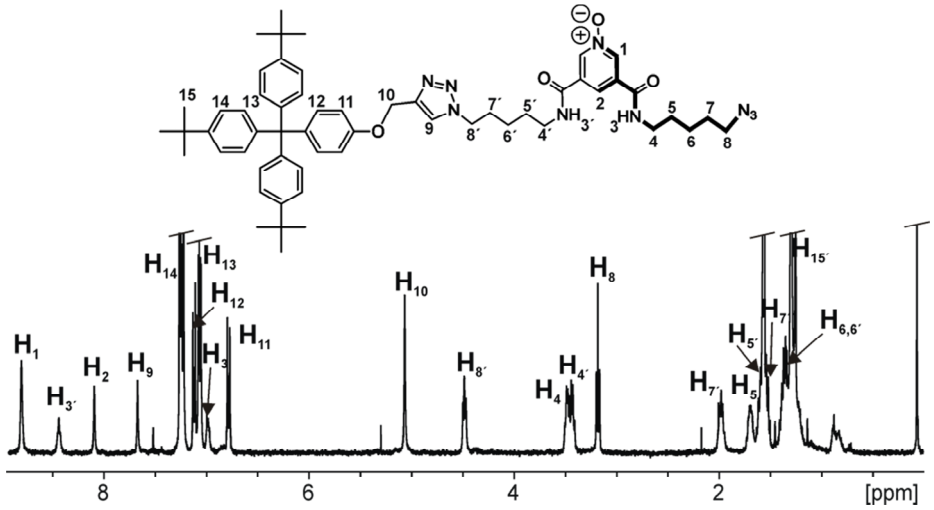

Figure 4. 20. ^{1}H NMR spectrum of **13** ($CDCl_3$, 400 MHz, 298K).

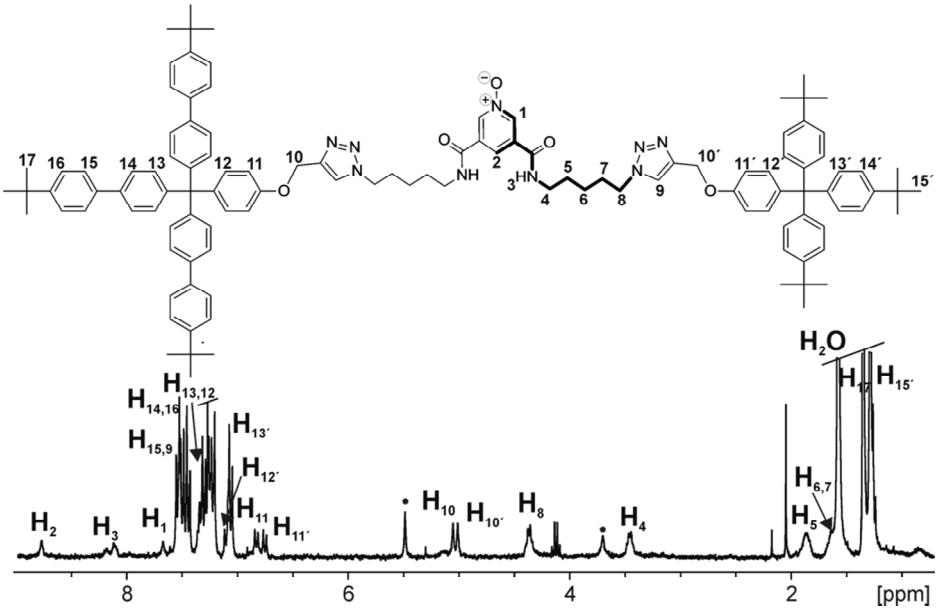

Figure 4. 21. ^{1}H NMR spectrum of linear component **14** ($CDCl_3$, 400 MHz, 298K).

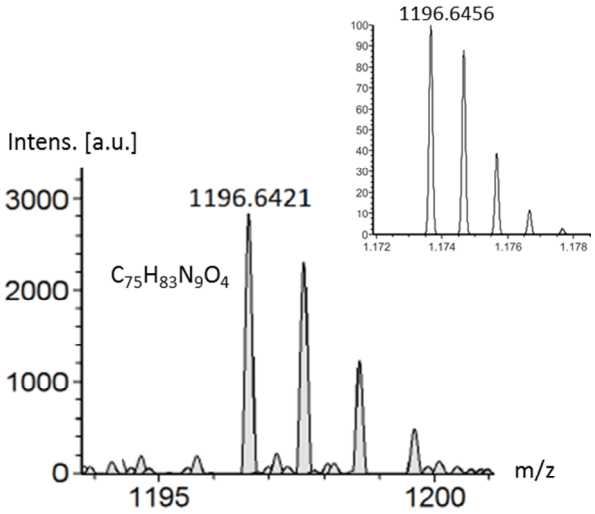

Figure 4. 22. Simulated and experimental HR-MS (ESI-TOF ES+) of **12**. m/z calculated for $C_{75}H_{83}N_9O_4Na$ $([M+Na])^+$ 1196.6456, found $([M+Na])^+$ 1196.6421.

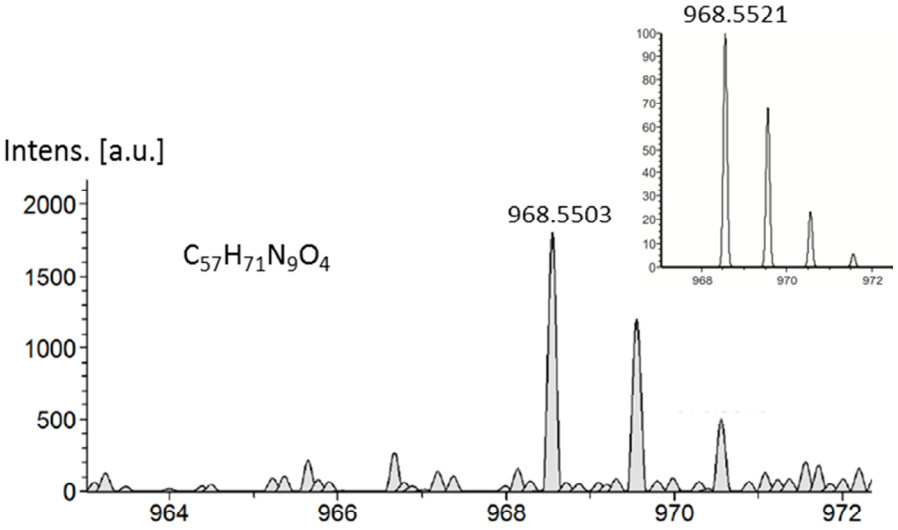

Figure 4. 23. Simulated and experimental HR-MS (ESI-TOF ES+) of **13**. m/z calculated for $C_{57}H_{71}N_9O_4Na$ $([M+Na])^+$ 968.5521, found $([M+Na])^+$ 968.5503.

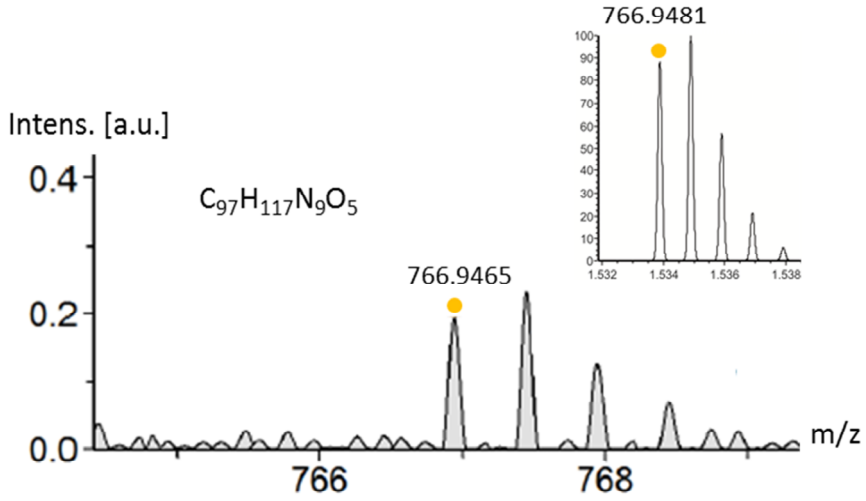

Figure 4. 24. Simulated and experimental HR-MS (ESI-TOF ES+) of **11**. m/z calculated for $C_{97}H_{117}N_9O_5Na_2$ $([M+2Na])^{2+}$ 766.9481, found $([M+2Na])^{2+}$ 766.9465.

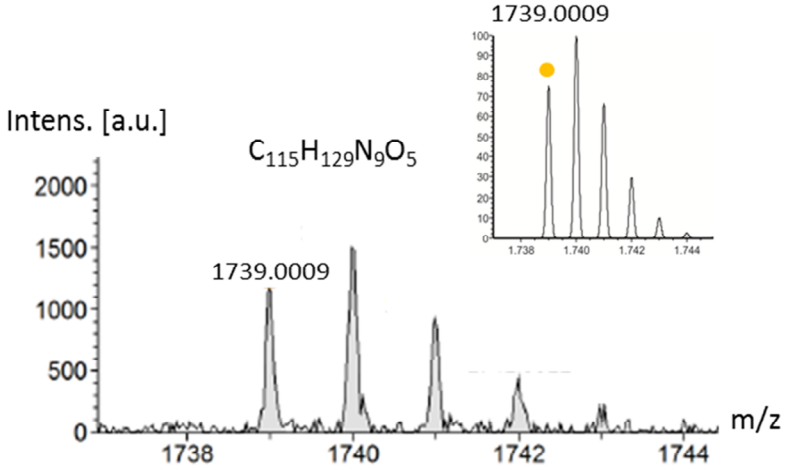

Figure 4. 25. Simulated and experimental HR-MS (ESI-TOF ES+) of **14**. m/z calculated for $C_{115}H_{129}N_9O_5Na$ $([M+Na])^{+}$ 1739.0009, found $([M+Na])^{+}$ 1739.0009.

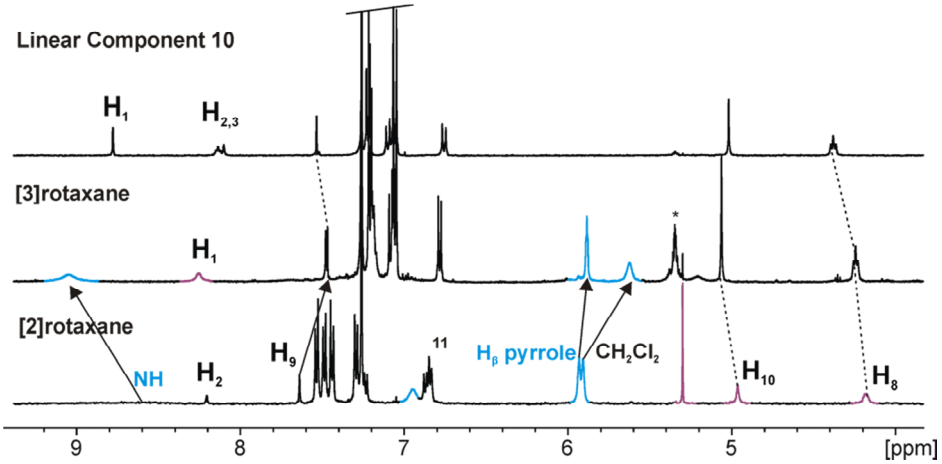

Figure 4. 26. Selected downfield region of the ^{1}H NMR spectra ($CDCl_3$, 400 MHz, 298K) of [2]rotaxane, **5** [3]rotaxane **17** and small linear component **11**. Comparison between different spectrums since [3]rotaxane share common signals and shifting behavior similar to [2]rotaxane and free **11**. Blue color for macrocycle protons and purple color for axle protons.

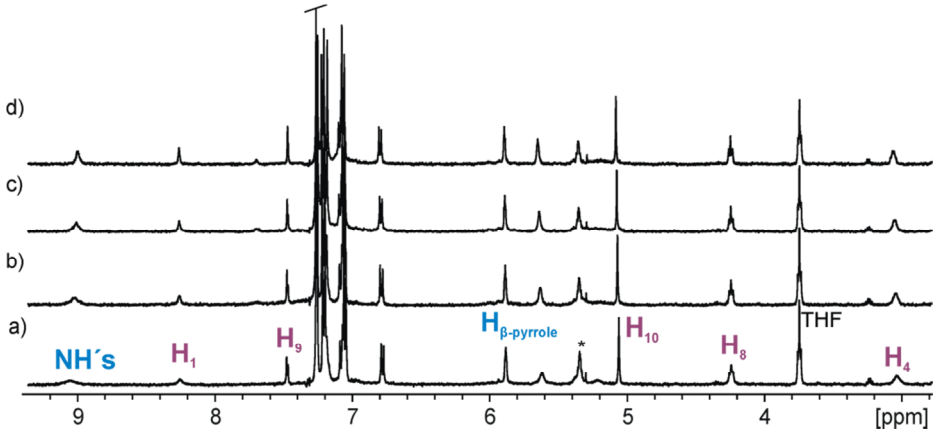

Figure 4. 27. Selected region of the variable temperature ^{1}H NMR experiments ($CDCl_3$, 500 MHz) of a millimolar solution of [3]rotaxane **17** at 298 K a) 308 K b) 318 K c) 328 k d).

Table 4. 2. Relation of initial and final amounts in milligrams of starting material and isolated products during the cross reactions performed between half-threads **12** and **13** with large **4a** and small **4b** stoppers in the presence of macrocycle **1**. [a]Large mono-stopper **12**. [b]Small mono-stopper **13**. [c]Linear component **10**. [d]Linear component **11**. [e]Linear component **14**.

	Initial Reagents		**Final isolated products**			
	1	**Monostopper**	**1**	**Linear Comp.**	**[2]Rotaxane yield**	**Linear comp. yield**
1)	39.8	39[a]	16	38[c]	30%	59%
2)	28.6	27.98[a]	27.4	37[e]	_	90%
3)	25.3	20[b]	23	33[d]	_	91%
4)	25.3	20[b]	22	25.4[e]	_	81%

4.5 References and notes

[1] Frisch, H. L.; Wasserman, E., *J. Am. Chem. Soc.* **1961,** *83* (18), 3789-3795.
[2] Harrison, I. T.; Harrison, S., *J. Am. Chem. Soc.* **1967,** *89* (22), 5723-5724.
[3] Harrison, I. T., *J. Chem. Soc., Chem. Commun.* **1972,** (4), 231-232.
[4] Harrison, I. T., *J. Chem. Soc., Perkin Trans. 1* **1974,** (2), 301-304.
[5] Gibson, H. W.; Lee, S. H.; Engen, P. T.; Lecavalier, P.; Sze, J.; Shen, Y. X.; Bheda, M., *J. Org. Chem.* **1993,** *58* (14), 3748-3756.
[6] Asakawa, M.; Ashton, P. R.; Ballardini, R.; Balzani, V.; Belohradsky, M.; Gandolfi, M. T.; Kocian, O.; Prodi, L.; Raymo, F. M.; Stoddart, J. F.; Venturi, M., *J. Am. Chem. Soc.* **1997,** *119* (2), 302-310.
[7] Ashton, P. R.; Baxter, I.; Fyfe, M. C. T.; Raymo, F. M.; Spencer, N.; Stoddart, J. F.; White, A. J. P.; Williams, D. J., *J. Am. Chem. Soc.* **1998,** *120* (10), 2297-2307.
[8] Raymo, F. M.; Houk, K. N.; Stoddart, J. F., *J. Am. Chem. Soc.* **1998,** *120* (36), 9318-9322.
[9] Heim, C.; Affeld, A.; Nieger, M.; Vogtle, F., *Helv. Chim. Acta* **1999,** *82* (5), 746-759.
[10] Hubner, G. M.; Nachtsheim, G.; Li, Q. Y.; Seel, C.; Vogtle, F., *Angew. Chem., Int. Ed.* **2000,** *39* (7), 1269-1272.
[11] Affeld, A.; Hubner, G. M.; Seel, C.; Schalley, C. A., *Eur. J. Org. Chem.* **2001,** (15), 2877-2890.
[12] Felder, T.; Schalley, C. A., *Angew. Chem., Int. Ed.* **2003,** *42* (20), 2258-2260.
[13] Tachibana, Y.; Kihara, N.; Furusho, Y.; Takata, T., *Org. Lett.* **2004,** *6* (24), 4507-4509.
[14] Tokunaga, Y.; Akasaka, K.; Hashimoto, N.; Yamanaka, S.; Hisada, K.; Shimomura, Y.; Kakuchi, S., *J. Org. Chem.* **2009,** *74* (6), 2374-2379.
[15] Tokunaga, Y.; Wakamatsu, N.; Ohiwa, N.; Kimizuka, O.; Ohbayashi, A.; Akasaka, K.; Saeki, S.; Hisada, K.; Goda, T.; Shimomura, Y., *J. Org. Chem.* **2010,** *75* (15), 4950-4956.
[16] Lahlali, H.; Jobe, K.; Watkinson, M.; Goldup, S. M., *Angew. Chem., Int. Ed.* **2011,** *50* (18), 4151-4155.
[17] Saito, S.; Nakazono, K.; Takahashi, E., *J. Org. Chem.* **2006,** *71* (24), 9252-9252.
[18] Saito, S.; Takahashi, E.; Wakatsuki, K.; Inoue, K.; Orikasa, T.; Sakai, K.; Yamasaki, R.; Mutoh, Y.; Kasama, T., *J. Org. Chem.* **2013,** *78* (11), 5816-5816.
[19] Hayashi, R.; Mutoh, Y.; Kasama, T.; Saito, S., *J. Org. Chem.* **2015,** *80* (15), 7536-7546.
[20] Yamashita, Y.; Mutoh, Y.; Yamasaki, R.; Kasama, T.; Saito, S., *Chem. Eur. J.* **2015,** *21* (5), 2139-2145.
[21] Elizarov, A. M.; Chiu, S. H.; Glink, P. T.; Stoddart, J. F., *Org. Lett.* **2002,** *4* (5), 679-682.
[22] Kim, S. Y.; Ko, Y. H.; Lee, J. W.; Sakamoto, S.; Yamaguchi, K.; Kim, K., *Chem. Asian J.* **2007,** *2* (6), 747-754.
[23] Leung, K. C. F.; Lau, K. N., *Polymer Chemistry* **2010,** *1* (7), 988-1000.
[24] Gunter, M. J.; Merican, Z., *Supramol. Chem.* **2005,** *17* (7), 521-528.
[25] Mullen, K. M.; Johnstone, K. D.; Webb, M.; Bampos, N.; Sanders, J. K. M.; Gunter, M. J., *Org. Biomol. Chem.* **2008,** *6* (2), 278-286.
[26] Langton, M. J.; Matichak, J. D.; Thompson, A. L.; Anderson, H. L., *Chem. Sci.* **2011,** *2* (10), 1897-1901.
[27] Brown, A.; Beer, P. D., *Dalton Trans.* **2012,** *41* (1), 118-129.
[28] Fathalla, M.; Strutt, N. L.; Barnes, J. C.; Stern, C. L.; Ke, C. F.; Stoddart, J. F., *Eur. J. Org. Chem.* **2014,** *2014* (14), 2873-2877.
[29] Sakamoto, K.; Takashima, Y.; Yamaguchi, H.; Harada, A., *J. Org. Chem.* **2007,** *72* (2), 459-465.
[30] Langton, M. J.; Robinson, S. W.; Marques, I.; Felix, V.; Beer, P. D., *Nature Chem.* **2014,** *6* (12), 1039-1043.
[31] Terao, J.; Konoshima, Y.; Matono, A.; Masai, H.; Fujihara, T.; Tsuji, Y., *Beilstein J. Org. Chem.* **2014,** *10*, 2800-2808.

[32] Yu, S. L.; Yuan, J. T.; Shi, J. H.; Ruan, X. J.; Wang, Y. L.; Gao, S. F.; Du, Y., *J. Mater. Chem. B* **2015,** *3* (26), 5277-5283.
[33] Zhang, Z. J.; Zhang, H. Y.; Wang, H.; Liu, Y., *Angew. Chem., Int. Ed.* **2011,** *50* (46), 10834-10838.
[34] Neal, E. A.; Goldup, S. M., *Chem. Sci.* **2015,** *6* (4), 2398-2404.
[35] Yang, Y. D.; Fan, C. C.; Rambo, B. M.; Gong, H. Y.; Xu, L. J.; Xiang, J. F.; Sessler, J. L., *J. Am. Chem. Soc.* **2015,** *137* (40), 12966-12976.
[36] Akae, Y.; Koyama, Y.; Sogawa, H.; Hayashi, Y.; Kawauchi, S.; Kuwata, S.; Takata, T., *Chem. Eur. J.* **2016,** *22* (15), 5335-5341.
[37] Barendt, T. A.; Docker, A.; Marques, I.; Félix, V.; Beer, P. D., *Angew. Chem., Int. Ed.* **2016,** *55* (37), 11069-11076.
[38] Inouye, M.; Yoshizawa, A.; Shibata, M.; Yonenaga, Y.; Fujimoto, K.; Sakata, T.; Matsumoto, S.; Shiro, M., *Org. Lett.* **2016,** *18* (9), 1960-1963.
[39] Ueno, A.; Takahashi, K.; Osa, T., *J. Chem. Soc., Chem. Commun.* **1980,** (19), 921-922.
[40] Kim, J.; Jung, I. S.; Kim, S. Y.; Lee, E.; Kang, J. K.; Sakamoto, S.; Yamaguchi, K.; Kim, K., *J. Am. Chem. Soc.* **2000,** *122* (3), 540-541.
[41] Kim, H. J.; Heo, J.; Jeon, W. S.; Lee, E.; Kim, J.; Sakamoto, S.; Yamaguchi, K.; Kim, K., *Angew. Chem., Int. Ed.* **2001,** *40* (8), 1526-1529.
[42] Klotz, E. J. F.; Claridge, T. D. W.; Anderson, H. L., *J. Am. Chem. Soc.* **2006,** *128* (48), 15374-15375.
[43] Prikhod'ko, A. I.; Durola, F.; Sauvage, J. P., *J. Am. Chem. Soc.* **2008,** *130* (2), 448-449.
[44] Prikhod'ko, A. I.; Sauvage, J. P., *J. Am. Chem. Soc.* **2009,** *131* (19), 6794-6807.
[45] Cheng, H. M.; Leigh, D. A.; Maffei, F.; McGonigal, P. R.; Slawin, A. M. Z.; Wu, J., *J. Am. Chem. Soc.* **2011,** *133* (31), 12298-12303.
[46] Hayashi, R.; Wakatsuki, K.; Yamasaki, R.; Mutoh, Y.; Kasama, T.; Saito, S., *Chem. Commun.* **2014,** *50* (2), 204-206.
[47] Danon, J. J.; Leigh, D. A.; McGonigal, P. R.; Ward, J. W.; Wu, J., *J. Am. Chem. Soc.* **2016,** *138* (38), 12643-12647.
[48] Movsisyan, L. D.; Franz, M.; Hampel, F.; Thompson, A. L.; Tykwinski, R. R.; Anderson, H. L., *J. Am. Chem. Soc.* **2016,** *138* (4), 1366-1376.
[49] Romero, J. R.; Aragay, G.; Ballester, P., *Chem. Sci.* **2016**.
[50] Valderrey, V.; Escudero-Adan, E. C.; Ballester, P., *J. Am. Chem. Soc.* **2012,** *134* (26), 10733-10736.
[51] Clever, G. H.; Shionoya, M., *Chem. Eur. J.* **2010,** *16* (39), 11792-11796.
[52] Chromatographic parameters: Chiralpack IA, 5µ silica 10 mm x 250 mm column; mobile phase: 20% THF/DCM for **12** purification and 17% THF/DCM for **13**; flow rate 5 mL/min, T = 25 ºC, injection volume: 500 µL for **12** and 700 µL for **13**. Instrument details: waters pump 2545; waters UV detector 2489; waters injector sample manager 2767.
[53] Valderrey, V.; Escudero-Adan, E. C.; Ballester, P., *Angew. Chem., Int. Ed.* **2013,** *52* (27), 6898-6902.
[54] Ashton, P. R.; Belohradsky, M.; Philp, D.; Stoddart, J. F., *J. Chem. Soc., Chem. Commun.* **1993,** (16), 1269-1274.
[55] Hunter, C. A., *J. Am. Chem. Soc.* **1992,** *114* (13), 5303-5311.
[56] Crude aliquots of 100 µL were washed with a portion of water. The organic phase dried over Na_2SO_4 anhydrous and the solvent removed. The solid residue was redisolved in 200 µL of CH_2Cl_2 prior to injection on HPLC instrument.
[57] Chromatographic parameters: waters spherisorb 5µ silica 4.6 mm x 250 mm column, 7% THF/DCM for **12** and 8% THF/DCM for **13** as mobile phase, flow rate 1 mL/min, T = 25 ºC, injection volume 1µL.
[58] Hoekman, S.; Kitching, M. O.; Leigh, D. A.; Papmeyer, M.; Roke, D., *J. Am. Chem. Soc.* **2015,** *137* (24), 7656-7659.

UNIVERSITAT ROVIRA I VIRGILI
INTERLOCKED ARCHITECTURES BASED ON A BIS-CALIX[4]PYRROLE MACROCYCLE FOR ION-PAIR RECOGNITION
Jose Ramon Romero Lopez

General Conclusions

In summary, the work presented herein describes a series of studies related to the synthesis and binding properties of unprecedented [2]rotaxane architectures that function as ion-pair receptors. The reported molecules are based on a biscalix[4]pyrrole macrocycle and a linear component containing a 3,5-*bis*-aminopyridil-*N*-oxide unit.

In particular, we describe the synthetic approach employed for the synthesis of a [2]rotaxane in a remarkable 50% yield through an optimized "*in situ*" stoppering strategy using the copper(I)- catalyzed azide-alkyne cycloaddition reaction. During the synthetic optimization studies we concluded that the use of anion templation was detrimental not only for the isolation of the pure [2]rotaxane but also for the good performance of the catalytic reaction. The synthesized [2]rotaxane architecture **5** comprises the first example of a mechanically locked molecule that incorporates calix[4]pyrrole units in its scaffold.

We demonstrated that rotaxane **5** is a good heteroditopic receptor for ion-pairs showing higher affinity for polyatomic anions (cyanate, nitrate) than for monoatomic counterparts (chloride) in non-polar solvents (chloroform). Conversely, we found that in polar non-protic solvents (acetone) the binding selectivity was reversed. The interlocked receptor showed higher binding constants for chloride than cyanate or nitrate as tetralkylammonium salts. These results were attributed to the superior solvation of the cation in acetone solution, which significantly reduces the competition for anion binding. This allows the engagement of the dissociated chloride anion in stronger hydrogen bonding interactions with the receptor owing to its reduced size in comparison to the polyatomic counterparts.

Additionally, we could identify that [2]rotaxane **5** forms complexes of different binding stoichiometries with the ion-pairs. Under strict stoichiometric control, a complex with 1:1 binding stoichiometry was assembled in both solvents (chloroform and acetone). However, the formation of complexes with higher stoichiometry, 2:1 complexes, was detected for the chloride and cyanate ion-pairs upon increasing their concentrations. The formation of the 2:1 complexes became more evident when working in acetone solution.

The hydrogen-bonding acceptor nature of the solvent competes with the *N*-oxide unit for the complexation with the calix[4]pyrrole core. In addition, it also promotes the ion-pair dissociation by preferential solvation of the cation.

Finally, we were confronted with the important role played by the size of the stopper in the formation of [2]rotaxane architecture. We demonstrated that the use of the large and bulky tris(biphenyl) stopper afforded the desired [2]rotaxane structure. Conversely, the use of the smaller terphenyl substituents as blocking groups produced the isolation, during the column chromatography purification of the reaction crude, of the macrocycle and the doubly functionalized axle in separated fractions. Remarkably, we also isolated a third compound in trace quantities. We assigned a putative [3]rotaxane structure to this compound, in which the bis(calix[4]pyrrole) macrocycle is threaded by two doubly stoppered axle units.

With all these results in our hands, we envisage, as future perspectives of this work, the transfer of the synthesized interlocked structures to aqueous media. Indeed, the thermodynamic features measured for the binding of the [2]rotaxane **5** with ion-pairs augur well for the application of these type of receptors in the recognition of anions in aqueous media. The synthesis of a water-soluble version of these structures requires e.g. the incorporation of stoppers featuring water-solubilizing groups. The complexation of anions and other biologically relevant polar guests in water is still a challenging aspect for supramolecular chemists.

Another field of application of the type of interlocked structures described here lies in the area of molecular switches. The design of a lineal component with two different recognition moieties (different stations) could end up with the development of a molecular shuttle that can operate in response to anion/ion-pair recognition.

List of abbreviations

COSY	–	Correlation spectroscopy
CPK	–	Corey-Pauling-Koltun model
CuAAC	–	Copper(I)-catalyzed azide-alkyne cycloaddition
DIPEA	–	*N*,*N*-Diisopropylethylamine
DOSY	–	Difusion Ordered Spectroscopy
equiv.	–	equivalent
ESI	–	Electrospray ionization
HMBC	–	Heteronuclear multiple-bond correlation spectroscopy
HPLC	–	High performance liquid chromatography
HRMS	–	High resolution mass spectrometry
HSQC	–	Heteronuclear single-quantum correlation spectroscopy
ITC	–	Isothermal titration calorimetry
K	–	Kelvin
Kcal	–	Kilocalorie
LC	–	Lineal component
MHz	–	Megahertz
MM3	–	Molecular mechanics force field
MS	–	Mass spectrometry
MTOA	–	Methyltrioctylammonium
NMR	–	Nuclear magnetic resonance
Oxone®	–	Potassium peroxymonosulfate
ROESY	–	Rotating frame overhauser effect Spectroscopy
TBA	–	Tetrabutylammonium
TBTA	–	Tris(benzyltriazolylmethyl)amine
TLC	–	Thin Layer Chromatography
TMS	–	Tetramethylsilane
TOF	–	Time-of-flight
T-ROESY	–	Transverse Rotating frame overhauser effect spectroscopy
UV	–	Ultraviolet

UNIVERSITAT ROVIRA I VIRGILI
INTERLOCKED ARCHITECTURES BASED ON A BIS-CALIX[4]PYRROLE MACROCYCLE FOR ION-PAIR RECOGNITION
Jose Ramon Romero Lopez

UNIVERSITAT ROVIRA I VIRGILI
INTERLOCKED ARCHITECTURES BASED ON A BIS-CALIX[4]PYRROLE MACROCYCLE FOR ION-PAIR RECOGNITION
Jose Ramon Romero Lopez

UNIVERSITAT ROVIRA I VIRGILI
INTERLOCKED ARCHITECTURES BASED ON A BIS-CALIX[4]PYRROLE MACROCYCLE FOR ION-PAIR RECOGNITION
Jose Ramon Romero Lopez

UNIVERSITAT ROVIRA I VIRGILI
INTERLOCKED ARCHITECTURES BASED ON A BIS-CALIX[4]PYRROLE MACROCYCLE FOR ION-PAIR RECOGNITION
Jose Ramon Romero Lopez

UNIVERSITAT ROVIRA I VIRGILI
INTERLOCKED ARCHITECTURES BASED ON A BIS-CALIX[4]PYRROLE MACROCYCLE FOR ION-PAIR RECOGNITION
Jose Ramon Romero Lopez

UNIVERSITAT
ROVIRA i VIRGILI